Antidiabetic effect of the intrapancreatic application of mesenchymal stem cells through β-cell regeneration

Inaugural-Dissertation

submitted to the

Faculty of Medicine

in partial fulfilment of the requirements

for the PhD-degree

of the Faculties of Veterinary Medicine and Medicine

of the Justus Liebig University Giessen

by

Rahul Khatri

of

New Delhi, India

Giessen 2019

From the

Clinical Research Unit,

Head: Univ.-Prof. Dr. med. Thomas Linn

Affiliated to Medical Clinic and Policlinic 3

Director: Prof. Dr. med. Andreas Schäffler

Universitätsklinikum Giessen und Marburg GmbH, Standort Giessen

Justus Liebig University

First Supervisor and Committee Member: Univ.-Prof. Dr. med. Thomas Linn

Second Supervisor and Committee Member: Prof. Dr. Sybille Mazurek

Chairman of Committee Member: Prof. Dr. Ralph Schermuly

External Examiner: Prof. Dr.-Ing. Peter Czermak

Date of Doctoral Defense: 12-05-2020

TABLE OF CONTENTS

ABBREVIATIONS

DM	Diabetes mellitus
T1D	Type 1 diabetes
T2D	Type 2 diabetes
T3D	Type 3 diabetes
β-cell	Beta cell
STZ	Streptozotocin
NMRI	Naval Medical Research Institute
IVR	Intravenous route
IPR	Intrapancreatic route
EGF	Epidermal growth factor
IGF-1	Insulin like growth factor-1
Ins1	Preproinsulin 1
Ins2	Preproinsulin 2
TGF-β	Transforming growth factor beta
TNF-α	Tumor necrosis factor alpha
IL-10	Interleukin-10
BAX	BCL2-associated X protein
BCL-2	B-cell lymphoma 2
ERK	Extracellular signal regulated kinases
DLK1	Delta like non canonical notch ligand 1
FoxO1	Forkhead box 1
BrdU	Bromodeoxyuridine
AKT	Protein kinase B
FOXA2	Forkhead box A2
PDX-1	Pancreatic and duodenal homeobox1
GLUT-2	Glucose transporter 2
PI3K	Phosphatidylinositol-4, 5-bisphosphate 3-kinase
MSC	Mesenchymal stem cells
ESC	Embryonic stem cells

iPSC	Induced pluripotent stem cells
IL-12	Interleukin-12
IDO1	Indoleamine 2,3-dioxygenase 1
TIMP-1	Metallopeptidase inhibitor 1
VEGF	Vascular endothelial growth factor
CXCR4	C-X-C chemokine receptor type 4
SDF-1	Stromal cell derived factor-1
TMB	3,3',5-5'-tetramethylbenzidine
ml	Millilitre
min	Minute
mM	Millimolar
APS	Ammonium persulfate
BSA	Bovine serum albumin
EDTA	Ethylene diamine tetra acetic acid
FACS	Fluorescence activated cell sorting
IHC	Immunohistochemistry
°C	Degree Celsius
HRP	Horseradish peroxidase
FCS	Fetal calf serum
cDNA	Complementary DNA
DNA	Deoxyribonucleic acid
DNase	Deoxyribonuclease
DTT	Dithiothreitol
dNTPs	2'-deoxynucleoside-5'-triphosphate
g	Gram
Kg	Kilogram
NaCl	Sodium chloride
PCR	Polymerase chain reaction
RNase	Ribonuclease
RT	Room temperature

DMSO	Dimethyl sulfoxide
DC	Direct co-culture
IDC	Indirect co-culture
ELISA	Enzyme-linked immunosorbent assay
MIN6	Mouse insulinoma, 6th subclone
ADMSC	Adipose derived mesenchymal stem cells
hTERT-MSC	Human telomerase reverse transcriptase mesenchymal stem cells
NF-kB	Nuclear factor-kappa B
IFN- γ	Interferon-gamma
IL-1β	Interleukin 1 beta
SDS-PAGE	Sodium dodecyl sulfate polyacrylamide gel electrophoresis
Th1	Type 1 helper cells
Th2	Type 2 helper cells
NOD	Non-obese diabetic (NOD)
Px	Partial pancreatectomy
α	Alpha cell
γ	Gamma cell
δ	Delta cell
GABA	Gamma-aminobutyric acid
CFU-F	Colony forming unit-fibroblasts
NGN3	Neurogenin 3
PARP	Poly (ADP-ribose) polymerase
ATP	Adenosine triphosphate
NAD	Nicotinamide adenine dinucleotide

Summary

Type 1 diabetes (T1D) is an autoimmune disease due to β-cell destruction and leads to hyperglycemia and lifelong insulin dependency. Mesenchymal stem cell (MSC) infusion was reported to control hyperglycemia and preserve pancreatic β-cell function. Most studies employed MSC through the systemic route (intravenous route) of transplantation in T1D animal models. However, the systemic route subjected MSC to the lungs, resulting in microvasculature entrapment and decreased therapeutic outcome. In this study, we investigated β-cell regeneration after hTERT-MSC infusion in partially pancreatectomized mice and the antidiabetic effect of ADMSC through two different routes; intravenous (IVR) and intrapancreatic route (IPR) in streptozotocin-induced diabetic NMRI nude mice.

Both hTERT-MSC and ADMSC were characterized by specific cell surface markers (CD90, CD44, CD105, CD73) using a flow cytometer. Further, possible tumor formation was ruled out by transplanting 0.5×10^6 ADMSC, hTERT-MSC and PANC1 into the flank of NMRI nude mice. No tumor was observed with ADMSC and hTERT-MSC.

IPR-hTERT-MSC-administration increased the frequency of newly formed insulin producing β-cells (labelled with BrdU) along with the number of islets per section and insulin content in the residual pancreas than IVR and control after partial pancreatectomy. However, IPR also exhibited greater retention of MSC after eight days of transplantation compared to IVR. In the presence of MSC, murine EGF was enhanced and inflammatory molecules such as IFN-γ and TNF-α were decreased. MSC induced higher expression of FOXA2, PDX-1, P-AKT and downregulated FoxO1. Therefore, present work confirmed the superior effect of IPR over IVR in proliferating β-cells through AKT/ PDX-1/ FOXA2/ FoxO1 signaling pathway in partially pancreatectomized mice.

Further, IPR-ADMSC-administration in STZ-induced diabetic NMRI nude mice ameliorated hyperglycemia as compared to IVR, STZ and control groups. In the IPR group, replicating β-cells, the number of islets per section and the islet area was enhanced. ADMSC rescued the diabetic pancreas by stimulating the secreting of growth factor (EGF) and maintaining Th1/ Th2 balance by downregulation of IL-1β, TNF-α and upregulation of IL-10. Physical contact of MSC with the damaged MIN6 cells provided higher protection than the paracrine effect in *in-vitro* studies. In

summary, this study reveals the higher antidiabetic effect of ADMSC through DLK1/ EGF/ ERK/ FoxO1 signaling cascade in the IPR group compared to the IVR group.

Zusammenfassung

Diabetes mellitus Typ 1 (T1D) ist eine Autoimmunerkrankung, welche auf dem Untergang von β-Zellen beruht und zu Hyperglykämie sowie lebenslanger Insulinabhängigkeit führt. Durch den Einsatz mesenchymaler Stammzellen (MSC) konnte die Hyperglykämie kontrolliert und die Funktion der pankreatischen β-Zellen erhalten werden. Die meisten bisherigen Studien transplantierten die MSC über den systemischen Weg (intravenös) in das T1D-Modell. Auf diesem Weg gelangten die MSC in die Lungen, wo sie mikrovaskulär gefangen waren und das therapeutische Ergebnis verringerten. In der vorliegenden Studie wurde die Regeneration von β-Zellen untersucht, nachdem hTERT-MSC in Mäuse mit partieller Pankreatektomie infundiert wurden, sowie die antidiabetische Wirkung von ADMSC. Deren Infusion erfolgte auf zwei unterschiedliche Wege in Streptozotocin-induzierte, diabetische NMRI-nude-Mäuse: intravenös und intrapankreatisch.

Die spezifischen Oberflächenmarker (CD90, CD44, CD105, CD73) der hTERT-MSC und der ADMSC wurden mittels Durchflusszytometrie charakterisiert. Die Bildung von Tumoren wurde ausgeschlossen, indem 0.5×10^6 ADMSC, hTERT-MSC and PANC1 in die Flanke der NMRI-nude-Mäuse transplantiert wurden. Bei ADMSC und hTERT-MSC kam es zu keiner Tumorbildung.

Im Gegensatz zu IVR und der Kontrolle konnte die Gabe von IPR-hTERT-MSC sowohl das Auftreten von neu gebildeten, insulinproduzierenden β-Zellen (gekennzeichnet durch BrdU) steigern, als auch die Anzahl von Inseln pro Ausschnitt und den Insulingehalt im Restpankreas. IPR zeigte, im Vergleich zu IVR, acht Tage nach der Transplantation eine stärkere Persistenz von MSC. In Anwesenheit von MSC stieg die Expression von murinem EGF an; inflammatorische Moleküle, wie z.B. IFN-γ und TNF-α, nahmen ab. MSC induzierten die stärkere Expression von FOXA2, PDX-1, P-AKT und regelten FoxO1 herunter. Daher untermauert die vorliegende Arbeit die Überlegenheit von IPR über IVR für proliferierende β-Zellen durch die Signalwege AKT/PDX-1/FOXA2/FoxO1 in Mäusen mit unvollständiger Pankreatektomie.

Außerdem verbesserte die Gabe von IPR-ADMSC, im Vergleich zu IVR, STZ und Kontrollen, den Blutzucker zusammen mit gesteigertem Pankreas- und Gesamtgewicht. Sich replizierende β-Zellen, die Anzahl von Inseln pro Ausschnitt und Fläche der Inseln waren in der IPR –Gruppe höher im Vergleich mit den anderen Gruppen. ADMSC retteten das diabetische Pankreas indem

sie Wachstumsfaktoren (EGF) sezernierten und die Th1/Th2-Balance aufrecht erhielten, durch die Senkung von IL-1β, TNF-α, sowie die Zunahme von IL-10. Direkter Kontakt von MSC zu geschädigten MIN6-Zellen lieferte stärkeren Schutz als der parakrine Effekt von MSC in-vitro. Diese Untersuchung zeigt, dass der antidiabetische Effekt von ADMSC durch die DLK1/ EGF/ ERK/ FoxO1-Signalwege in IPR stärker war, verglichen mit dem systemischen Weg.

1. INTRODUCTION

1.1 Diabetes mellitus

Diabetes mellitus (DM) is characterized by the chronic hyperglycemic state as a cause for long-term organ complications ranging from the eye to kidney disease, followed by vessel occlusion in the heart or peripheral arteries. A chronic hyperglycemic state is the consequence of the destruction of pancreatic β-cells. According to World Health Organization and international guidelines, diabetes mellitus is classified as type 1 (T1D), type 2 (T2D), gestational diabetes, and type 3 diabetes mellitus (T3D) with the latter including monogenic and cystic fibrosis-related diabetes. The most prevalent is T2D, manifested by insulin resistance and inadequate secretion [1]. T1D results in complete insulin deficiency by autoimmune destruction of the pancreatic β-cells.

In 1500 B.C.E an Egyptian first noticed the symptoms of diabetes (loss in weight and urination) and later Aretaeus (80 to 138 C.E; Greek physician) discovered the sweetness of the urine. Interestingly, Matthew Dobson measured the glucose concentration in the urine of diabetic patients at that time [2, 3]. Later, Joseph von Mering and Oskar Minkowski (1889) observed the severe symptoms of diabetes, after the removal of a dog pancreas which revealed its major role in glucose metabolism. Insulin was first discovered by Frederick Banting and Charles H. Best in 1992. They also treated diabetic dog by transplanting pancreatic islets isolated from a healthy dog. Along with James Collip and John Macleod, further purified insulin and used for the treatment [2, 4, 5].

Other forms of diabetes (T3D) may develop due to a genetic defect in insulin secretion or abnormality in the function of pancreatic β-cells [6-8]. Acute metabolic complications of hyperglycemia are polyuria, polydipsia, ketoacidosis or nonketotic coma, fatigue and body weight loss. DM also elevates the level of hepatic gluconeogenesis, intravascular lipolysis and plasma level of free fatty acids and ketone bodies which are the reasons for diabetic ketoacidosis. Persisting hyperglycemic state for a year could cause diabetic retinopathy, foot ulcer, polyneuropathy, coronary heart disease and kidney failure [6, 9-11]

1.1.1 Prevalence of DM

According to the International Diabetes Federation, the prevalence of DM will increase from 415 million (2015) to 642 million (2040). In 2012 itself, 2.2 million deaths were reported (47% of individuals were above 70 years). As per Diabetes Atlas, frequency among the age of 20-79 years will increase from 8.8% (2015) to 10.4% (2040) [12]. 75% of DM people are from developing or underdeveloped countries and serve as a huge financial global burden of 673 billion US dollars

(2015). Total adult population (8.8%) has DM out of which 10-15% are suffering from T1D especially children below the age of 15 years. More than 0.5 million children are battling with T1D worldwide and each year more than 90,000 children's diagnosed [13]. The prevalence of DM in Germany is low as compared to Scandinavian countries, but an accelerating trend was recognized from 8.9% in 2009 to 9.8% in 2015. The majority of cases were from T2D. However, T1D cases marginally declined from 0.33% in 2009 to 0.28% in 2015 [14].

1.1.2 Type 1 diabetes (T1D)

Type 1 diabetes (juvenile diabetes/ insulin-dependent diabetes mellitus) is an immune-mediated disease. It is more prevalent in the adolescent age but may also influence later stages of life. Its aetiology is still elusive, but genetic and environmental factors are assumed to contribute to its pathogenesis [15]. T1D occurs due to the autoimmune destruction of pancreatic β-cells. This destruction is attributed by the T-cells response [T helper 1 (Th1) cells]. Moreover, in some T1D patients, immune system and autoantibodies does not play any role which is referred to as idiopathic diabetes or type 1b diabetes [16, 17].

T1D contributes to 10-15% of total diabetes prevalence. There is a peak of manifestation at an adolescent age, but children and even babies less than two years of age may also acquire this condition [17]. Prior to the onset of T1D, autoantibodies appear against insulin, glutamate decarboxylase 2 (GAD65), zinc transporter 8 (ZNT8) or insulinoma-associated protein 2 (IA2) [17, 18]. There are various stages during the pathogenesis of T1D based on the autoantibodies, dysglycemia and the symptoms.

Stage 1: β-cell autoantibodies are present, but dysglycemia and diabetic symptoms are absent. At this stage, genetic and environmental factors play a crucial role.

Stage 2: β-cell autoimmunity leads to β-cell loss. Dysglycemia occurs without diabetic symptoms. Dysglycemia is the major transition factor between stage 1 and stage 2 which is detected by the oral or intravenous glucose tolerance test.

Stage 3: β-cell autoimmunity results in further β-cell loss. Hyperglycemia and diabetic symptoms become prominent [17].

1.1.3 Role of immune cells in T1D

During the progression of T1D, first, the immune system will attack putative insulin producing β-cell antigens, accompanied by strong pro-inflammatory action against β-cell and subsequent failure over the regulation of the autoreactive immune response. All the immune cells such as B-cells, T-helper 1 cells (T-cells), dendritic cells, macrophages, natural killer cells play a vital role in the onset of T1D [19, 20]. CD8+ T-cells, CD4+ T-cells, CD20+ B-cells and CD68+ macrophages were detected in the pancreas of T1D patients [19, 21]. In distinct ways, T-cells can damage islets. CD8+ T-cells damage β-cells in direct contact via MHC class 1 mediated cytotoxicity. CD4+ and CD8+ T-cells activate CD90 (FAS, death receptor) and different chemokines by releasing interferon-γ (IFN-γ). IFN-γ in response stimulates macrophages and enhances β-cell destruction by releasing tumor necrosis factor-α (TNF-α) and interleukin-1β (IL-1β).

Indeed, dendritic cells and macrophages are also responsible for triggering the immune response against β-cells. Resident dendritic cells in islets of healthy individuals process β-cell antigens and display them to T-cells [22, 23]. Moreover, nuclear factor-kappa B (NF-kB) activation in dendritic cells of non-obese diabetic (NOD) mice, stimulates IL-12 release which attracts macrophages. TNF producing macrophages were identified in the islets of T1D patients. Additionally, macrophages removed dead cells in NOD mice, which is an established mouse model of T1D. They even permit the priming of B- and T-cells [19, 24]. The infiltration of natural killer cells was also observed in the pancreas [25, 26].

1.1.4 Type 2 diabetes (T2D)

Type 2 diabetes is a chronic metabolic disorder linked to obesity, characterized by insulin resistance and imbalance or high blood glucose level. It is the most frequent form of diabetes and mainly appears at a higher age. T2D is a leading cause of morbidity and mortality. Its prevalence has recently increased in young adults also [27].

1.1.5 Animal models in the regeneration of pancreas and T1D

In T1D, there is an autoimmune destruction of β-cells. This situation can be achieved in the mouse model by several mechanisms. It mainly includes chemically induced diabetes, an autoimmune model of T1D (NOD mice, BB rats, LEW.1AR1/-iddm rats), genetically induced insulin-dependent diabetes (AKITA mice), virus-induced models of diabetes and non-rodent model of

T1D (pancreatectomy and chemical ablation of β-cells in larger animals) [28, 29]. Chemically induced T1D can be achieved by streptozotocin (STZ) or alloxan. Both molecules carry a glucose moiety which allows them to target pancreatic β-cells via the GLUT-2 transporter. STZ [2-deoxy-2-(3-methyl-3-nitrosoureido)-D glucopyranose] is injected intraperitoneally (i.p.) or intravenously (i.v.), induce DNA alkylation, followed by PARP induction (NAD+ reduction), loss of ATP and inhibition of insulin synthesis, whereas alloxan generates the excessive quantity of free radicals to damage the β-cells [28, 30, 31]. STZ is administrated as a single dose (200 mg/ kg body weight) or multiple low doses (40 mg/ kg body weight) for up to five consecutive days [32]. Multiple low doses induce a slow rise of blood glucose level within fourteen days rather than hyperglycemia next day after injection and rapid destruction of the β-cells [32]. The low dosage of STZ will not damage all the β-cells so that the remaining cells form a pool for potential regenerative processes [33].

1.1.6 NMRI nude mice (NMRI Foxn1 nu/ Foxn1 nu)

NMRI nu/ nu mice were first developed by Lynch. Afterwards, the stock was transferred to Poiley at NIH in 1937, followed by the Naval Medical Research Institute (NMRI) to Zentralinstitut für Versuchstierzucht, Germany and kept as an outbred stock. NMRI is an immunodeficient homozygous nude mouse, possessing the recessive nude gene and genetic mutation in the Foxn1 gene on chromosome 11 (earlier known as Whn or Hfh11). This leads to the defective thymus and lack of body hairs which gain them as a nickname "nude mice". NMRI nude mice lack proliferation and differentiation of thymic epithelial cells (TECs; help in the maturation of T-lymphocyte) as well as the precursor for T-lymphocyte. This model is not absolutely immunodeficient as small populations of T-cells are functional and antibody action is restricted to IgM class. As a result, there is a compensatory mechanism, an increase in the natural killer cells was observed, which could elicit the gradual rejection of transplanted organs [34]. These mice showed a lower growth rate, no vibrissae at birth, less fertility and confined life span (live up to one year in the normal condition and up to two years in germ-free housing condition). T-cell activity increases with age, therefore, younger mice with the age of six to twelve weeks are preferred. This is also a subcutaneous heterotopic type of tumor model which allows seeing the tumor growth with naked eyes. Once transplanted subcutaneously, tumor appeared within two to six weeks. It's a preferred model for tumor and stem cell engraftment studies. This model was applied to investigate the islets engraftment in T1D therapy and pancreas regeneration after partial pancreatectomy [35].

1.2 Pancreas

The pancreas in the Greek expression means 'all flesh' and is also referred to as "two organs in one" as it operates the endocrine and exocrine vital functions. The human pancreas is divided into three parts, head embedded into the duodenal loop, the body stretched close to the splenic vein, and tail located at the level of the hilus of the spleen. The dimensions are length (14-18 cm), width (2-9 cm), thickness (2-3 cm) and weight (50-100 g) [36]. Exocrine cells secrete digestive enzymes and through the ductal network, they reach the intestine. It is mainly composed of the acinar, duct, and centroacinar cells covering 95% of the pancreatic mass. Endocrine cells maintain normal blood glucose and are present in the pancreatic islets. They were discovered by the German pathologist, Paul Langerhans in 1869. He defined them as nets of the cell cluster distributed in the pancreas with great significance in endocrine metabolism [37]. Islets composed of 1-2% of the entire pancreatic mass. In healthy adults, one million islets are present and each islet contains 3,000 to 4,000 cells.

Five different types of cells are present in each islet. In the central core of rodent islets, β-cells are responsible for glucose uptake and corresponding insulin secretion. They also synthesize amylin which inhibits lipolysis. Insulin producing β-cells are surrounded by alpha cells (α-cells; they secrete glucagon and control glycogenolysis), gamma cells (γ-cells; secrete pancreatic polypeptide), delta cells (δ-cells; secrete somatostatin and control polypeptide) and epsilon cells (Ɛ-cells; secrete ghrelin) as illustrated in figure 1.2 [38].

1.2.1 Development of pancreas

In order to construct an appropriate structure or architecture of a mature pancreas, it is helpful to consider embryologic steps occurring in a series. The primary morphological transformation in the embryological development commences with the condensation of mesenchyme. After the condensation event, on 9.5 days (E9.5) of the gestation period in mice and 26 days of gestation in human, endoderm starts to evaginate from the mesenchyme [39-41]. After a few hours, an evagination of the dorsal bud continues to lengthen with a wide opening and the reduction in the cell division [42]. The process of dorsal bud formation occurs prior to the loss of contact between notochord and the dorsal bud. The paired dorsal aorta intervenes into the middle of the notochord and dorsal bud. During this time, coelomic epithelium which is only responsible for the mesenchyme formation around the pancreas starts to move dorsally and divides into the discrete

section of the pancreas. Gut moves from the dorsal aorta and constructs another dorsal non-gut architecture [43].
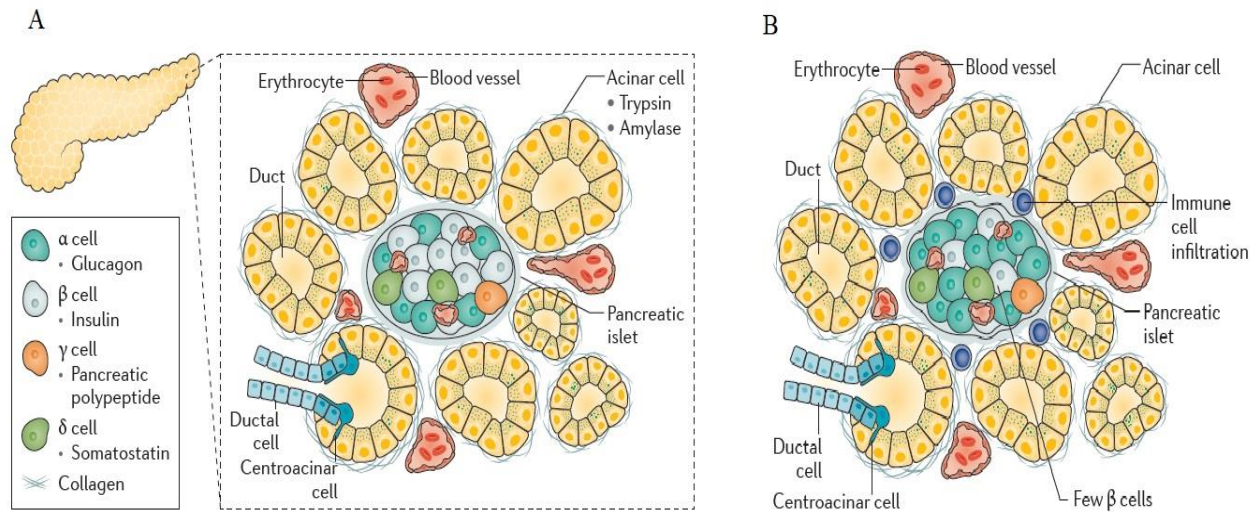
Figure 1.2: The unique cell types within the islets of Langerhans (A) normal, healthy pancreatic islets (B) during the progression of type 1 diabetes. Adapted and modified image from C. Ellis et al. [44].

At this time, the proliferation of mesenchyme cells was observed between the pancreatic and coelomic epithelium. Afterwards, ventral bud started to emerge in mouse (after twelve hours of dorsal bud evagination) and human (after six days of dorsal bud evagination) from the hepatic/ biliary bud. Formation of dorsal and ventral bud had similar morphology but different in their molecular control. However, this process followed by the development in the stalk region of the pancreatic bud which started to elongate and formed branching morphogenesis of the bud (apical region) and followed a distinctive pattern. Different from kidney, lung and salivary gland branching morphogenesis (usual 90º outgrowth), pancreas showed a definite angle branching to avoid the intervening mesenchyme and persisted in the proximity of newly formed adjacent branches [43].

This elimination of mesenchyme-initiated lineage selection and epithelial-mesenchymal interaction leads to the visible endocrine formation. At this point, the combinational effect of gut rotation and the dorsal bud elongation, specifically ventral stalk developed pancreatic ducts. Therefore, duodenal anlage C-loop formed due to the fusion of the ventral and the dorsal bud. In mice contact and fusion occurred on E12 to E13 and E37 to E42 in humans. This fused length persists throughout the pancreas length, known as the duct of Wirsung (further appear from distal

dorsal bud epithelium and ventral bud epithelium) and proximal portion remained smaller to dorsal bud known as the duct of Santorini which further emerges from dorsal bud epithelium (proximal portion) [43].

During the secondary transition, the amplification of glucagon-positive cells and β-cells occurred. Just after this event instant branching morphogenesis and differentiation of acinar cells (exponential increase in the gene expression) were also observed accompanied by the formation of rough endoplasmic reticulum and zymogen granules [45]. Due to many zymogen granules, pancreas appears opaque from naked eyes. Similarly, the insulin level undergoes a massive increase at this point.

1.2.2 Pancreatectomy and the regeneration of the pancreas

Pancreatectomy is the oldest method to study the proliferation and regenerative potential of the pancreas. It was first studied and examined by Johann C. Brunner on the dog in 1683 [46]. Later, in 1890 it was reported to disturb glucose metabolism [47]. Adult pancreas posed restricted regenerative ability which further declined with increasing age [48, 49]. Pancreatectomy model has been studied extensively for pancreatic β-cell proliferation and regeneration in mice and rat model [50-52]. However, partial pancreatectomy (Px) which is a 50% removal of the pancreas represents another injury model which is not associated with diabetes and indeed provides a paradigm to study the regeneration potential and proliferation capacity of the pancreas. Post-surgical resection of the pancreas showed constrain regenerative growth and not fully recovered in its original shape or volume [53, 54]. Pancreatic β-cells regenerate either by the proliferation of pre-existing β-cells or pancreatic progenitor cells derived from ductal epithelium, also known as neogenesis [55]. However, the partial pancreatectomy method is reported to increase in pancreatic and duodenal homeobox 1 (PDX-1) expression via the IGF/ PI3K pathway in ductal cells [48, 56, 57]. Indeed, subtotal pancreatectomy also induced ductal cell proliferation in rats, which confirmed the role of ductal cells in elevated islet mass after pancreatectomy whereas other studies contradict its existence [58-60]. No evidence of β-cell neogenesis was observed in lineage tracking studies followed by partial pancreatectomy [59, 61]. Similarly, no NGN3 expression was observed in NGN3-GFP transgenic mice after partial pancreatectomy [59, 62]. The role of ductal cells and other related cells cannot be neglected, but existing literature and experiments strongly support the concept that the pancreatic β-cells regenerate via pre-existing β-cells [58, 59, 61, 63]. However,

two groups independently reported increased replication along with neogenesis [60, 64]. Thus, the exact origin of replicating β-cells is still debatable and further needs to be elucidated [53].

1.2.3 Epidermal growth factor (EGF)

EGF is a 53 amino acid single chain peptide derived from mouse submandibular glands. It's also present in the gastrointestinal tract, Brunner's gland, salivary gland, pancreas, pancreatic juices and initiated the proliferation of pancreatic and gastrointestinal tissues [65, 66]. The exogenous administration of EGF and gastrin combination improved the blood glucose level in rodents via increasing β-cell mass but failed when injected individually [67]. In the past, it was proposed that EGF acts via both β-cell regeneration and neogenesis (progenitor cells) but a definite mechanism is still debatable [68]. Recent evidence failed to support the conversion of ductal progenitor cells into insulin producing β-cells [69].

1.2.4 Delta like non canonical notch ligand 1 (DLK1)

DLK1 also known as a preadipocyte factor 1 (Pref-1) or fetal antigen 1 (FA1) is a member of the EGF protein family, primarily formed as a transmembrane protein having six tendons with EGF-like repeats [70]. However, it is also considered as a key regulator in mesenchymal stem cells differentiation towards adipocyte and osteoblasts [71]. DLK1 or Pref-1 participated in the differentiation and proliferation of several precursor cells and considered as an adult stem cell marker [72]. During early embryonic development, DLK1 is displayed throughout the pancreas until postnatal stage. At birth, its expression increased five-fold and four days onwards decreased rapidly [73]. DLK1 was also reported differentiating pancreatic ductal cells into insulin producing cells via ERK-FoxO1-PDX-1 intracellular signaling cascade [74].

1.2.5 Forkhead box A2 (FOXA2)

FOXA2 also known as hepatocyte nuclear factor-3 beta (HNF-3B) is a transcription factor expressed during initial pancreatic development which tightly regulates and controls the expression of PDX-1 [75]. FOXA2 is one of the target genes for SOX17 and pioneer factor for endodermal tissue generation and gut formation [76]. Both FOXA2 and SOX17 are considered crucial regulators for definitive endoderm required for pancreas development and successful differentiation of any kind of stem cells (MSC, iPSC, ESC) into insulin producing like cells *in-vitro*. Ablation of FOXA2 gene in knockout mice resulted in reduced expression of PDX-1 within the islets, both on mRNA and protein level [75].

1.2.6 Pancreatic and duodenal homeobox 1 (PDX-1)

PDX-1 also known as insulin promoter factor 1 (IPF1) is a transcription factor and plays an important role throughout the pancreas development ranging from the initial step (foregut) to the mature β-cells. Over the last 15 years, PDX-1 is the most studied transcription factor for pancreatic specification. During early development of the pancreas, PDX-1 was expressed in the epithelium and later repressed in the committed endocrine cells [77]. Afterwards, PDX-1 reappeared when committed endocrine cells started differentiating into insulin producing cells [78]. In 1994, PDX-1 null mice were created by Edlund lab and reported having pancreatic agenesis [43, 79]. However, pancreatic agenesis was also reported in man upon PDX-1 mutation in homozygous and lack of insulin in heterozygous condition [80, 81].

1.2.7 Forkhead box 1 (FoxO1)

The transcription factor FoxO1 plays an evident role in glucose metabolism and β-cell function. FoxO1 can act through protein kinase B to modulate the cell cycle of the β-cell [82]. In humans, FoxO1 variants lead to a higher risk of diabetes, glucose intolerance and impaired β-cell function [83]. Ablation of embryonic FoxO1 was reported in degranulation of β-cell and deteriorated glucose-stimulated insulin secretion (GSIS) [84]. However, in the case of the MIN6 cell line, FoxO1 facilitated PDX-1 nuclear-export-switch which diminish PDX-1 activity and inhibit insulin synthesis [85]. In 60% partial pancreatectomy C56BL/6 mice model, FoxO1 dependent β-cell proliferation and cell growth were observed [55]. FoxO1 has the potential to regulate PDX-1 and thus modulate β-cell proliferation and cell survival [86]. Nonetheless, FoxO1 downregulation was mediated and reported through the phosphorylation of AKT [87].

Four isoforms of FoxO1 are present in the mammalian cells; FoxO1, FoxO3, FoxO4, FoxO6 among which FoxO1 is present abundantly in adipose tissue, liver and pancreatic β-cells [86, 88]. However, enhanced FoxO1 mRNA expression was detected in the islets of T2D patient [89]. In PDX-1 promotor, both FoxO1 and FOXA2 compete for DNA binding site. In the case of FoxO1 binding, suppressed PDX-1 and decreased pancreatic β-cell proliferation was observed. On the contrary, FOXA2 binding leads to increase in β-cell survival and proliferation [86, 90]. Transcriptome analysis revealed the suppression of FoxO1 gene in low doses of streptozotocin-induced diabetic mice [91].

1.2.8 β-cell mass turnover

In the prediabetic/ diabetic condition, ample of β-cells are present which act as a new source of insulin producing β-cells. Four major factors were identified to control the regeneration process; neogenesis i.e. the formation of novel β-cells from non-β precursors, initial cell mass, rate of proliferation and apoptosis. In theory, subtracting the rate of β-cell apoptosis from proliferating rate could provide an estimation of the net turnover which could reflect the status of β-cell growth more exactly. Based on these considerations, the β-cell mass would expand several times due to replication in an individual life span. However, its reversible expansion was also observed during pregnancy and weight gain via different canonical and non-canonical signaling pathways [92, 93]. Non-β-cells have the potential to transdifferentiate into β-cell. Both α- and δ-cells were shown to rescue β-cell loss [94, 95]. It was reported that the expression of a paired box gene 4 (PAX4) alone was adequate to transdifferentiate α- into β-cells. Although, aristaless related homeobox gene (ARX) and PAX4 have an opposite and convertible function, mice with diminished expression of ARX in α-cells show a similar phenotype as mice over-expressing PAX4. Moreover, treatment with γ-aminobutyric acid (GABA) and the anti-malarial drug artemisinin inhibited ARX expression and enhanced PAX4 function which further confirmed conversion into β-cells from α-cells [44, 96].

1.3 Transplantation therapy for T1D

In the case of T1D and T2D, there is a loss of β-cell mass and insufficient compensation leads to the elevation of blood glucose level. This condition requires subcutaneous insulin injections or oral antidiabetic drugs to control and regulate the blood glucose level. Theoretically, insulin administration is intended to precisely substitute for lack of insulin secretion. Still, patients remain at the risk of hypoglycemia. Moreover, they will take four to five insulin injections per day and as many for blood glucose tests. This means a given subject takes more than 0.2 million injections till the age of 70 years, which exerts extra psychological pressure on T1D patients.

1.3.1 Pancreas transplantation

Pancreas transplantation is yet another interesting approach to restore hyperglycemia. In conformity with the International Pancreas Transplant Registry, at least 35 thousand pancreas transplantations were performed till 2010. But due to mandatory immunosuppression as well as

complications such as graft rejection, technical or surgical failure and metabolic or infectious sequelae to therapy, restrict its widespread use for T1D [97].

1.3.2 Pancreatic islet transplantation

Islet transplantation is also a potential approach to treat T1D [98]. In 1983, a sheep pancreatic fragment was first transferred into a diabetic patient by Watson Williams. Afterwards, a series of clinical islet transplantation programs were conducted with the Edmonton protocol [99]. While various sites such as kidney capsule, bone marrow, spleen, gastric mucosal surface and omental pouch were investigated in preclinical studies, the portal venous system was recognized as the most effective and convenient site for islet transplantation in the clinical programs [100-103]. Islet transplantation restored the normal glucose level for about one year on average. Accordingly, a combined attack from thrombotic reaction, allogenic and autoimmune rejection required more than one infusion. Normalization of blood glucose without concomitant hypoglycemic events improved life quality and prevented from diabetic complications. Taking into consideration the lack of donor pancreases qualified for collagenase digestion, continuous immunosuppression and graft rejection, the use of islet transplantation seems to be limited. In a healthy individual, there would be 100% β-cell mass, in the prediabetic condition it reduces to 50%, a further 25% reduction leads to insulin therapy. However, donor islet mass is considered as 100%. After the collagenase-mediated isolation procedure, 60 to 80% of pancreatic islets remain functional, a further 10% reduction is observed in culture and in intraportal islets transfer. Therefore, expected islet replacement would clearly require more than one donor pancreas which could mean a long way if any to reach the patient's insulin demand [102].

1.3.3 Stem cells

Stem cells provide an alternative road to restore glycemic control in T1D patients. Stem cells are unspecialized cells having self-renewal capacity via cell division and are assumed to replace injured tissue. They can be induced or differentiated into tissue/ organ specialized cells or progenitor cells. Progenitors have limited self-renewal ability, but the capacity to transform into precursors of tissue-specific fully functional cells. Thus, they may be defined as per their ability to differentiate into a specific cell type. Pluripotent stem cells have the potential to differentiate into the endoderm, ectoderm and mesoderm lineages whereas multipotent progenitor cells can differentiate into multiple but restricted lineages. There are several types of stem cells such as

embryonic stem cells (ESC), induced pluripotent stem cells (iPSC) and mesenchymal stem cells (MSC). They were discussed to potentially differentiate into β-cell-like-cells in tissue culture [104].

1.3.3.1 Embryonic stem cells (ESC)

Embryonic stem cells (ESC) are derived from blastocysts and differentiate in all three lineages. ESC differentiated into β-cell-like-cells, which were capable of controlling blood glucose level in diabetic mice [105, 106]. Protocols were developed to drive ESC into β-cell-like-cells by stage-specific differentiation [107]. Definitive endoderm (DE) was the primary stage at which SOX17, CXCR4 and FOXA2 markers were expressed. Pancreatic endoderm was characterized by PDX-1, HNF2 and PAX6. In the next stage, the generation of pancreatic progenitor cells was aimed at, which induced the expression of NGN3, NEURO D, MAFA B and NKX2.2 and finally insulin in the cells [104, 108, 109]. In an ongoing trial with pancreatic progenitor cells derived from ESC (ViaCyte Inc. clinical trials identifier: NCT02239354), the formation of a tumor-like lesion was seen at the engrafted site [110]. Therefore, due to ethical issues and the possibility of tumor formation, their use in clinical trials is limited.

1.3.3.2 Induced pluripotent stem cells (iPSC)

Discovery of induced pluripotent stem cells (iPSC) provided new hope for cell-based therapy and an alternative to ESC [111, 112]. iPSC potentially differentiates into several types of cells and can be maintained in the form of a cell line [113]. Human and mouse somatic cells were used to generate iPSC by induced expression of OCT3/ 4, SOX2 along with KlF4, c-MYC, NANOG and lin28. iPSC derived from mouse skin fibroblast were reported to differentiate into β-cell-like-cells and correct the blood glucose level in diabetic mice. Human iPSC were also reported to differentiate into β-cell-like-cells and release insulin and C-peptide upon glucose stimulation [114]. In the past, iPSC derived from T1D and T2D patients were used to differentiate into β-cell-like-cells *in-vitro* [115, 116]. Compared to ESC, iPSC are considered at lower risk of tumor development and there is less ethical concern. In addition, the rejection of transplanted β-cell-like-cells generated from iPSC is a major issue. Moreover, fibroblasts are transduced to express specific transcription factors by viral transfection. Virus DNA may facilitate mutations in the host genome and puts the recipient at risk of teratoma formation [117].

1.3.3.3 Mesenchymal stem cells (MSC)

Within the bone marrow, a small population of spindle-shaped cells were first identified by Friedenstein and termed colony forming unit-fibroblasts (CFU-F) [118, 119]. These CFU-F had self-renewal potential and differentiation capacity into several lineages. In the 1980s, CFU-F was renamed as mesenchymal stem cells and recently the International Society for Cellular Therapy (ISCT) denoted them as multipotent mesenchymal stromal cells (MSC) [120, 121].

However, after their discovery, MSC were isolated from several organs such as bone marrow, adipose tissue, dental pulp, Wharton's jelly, umbilical cord matrix/ umbilical cord blood, placenta, pancreas, skeletal muscle, fetal lung, fetal liver, salivary gland, amniotic membrane/ amniotic fluid and endometrium [122]. MSC have the potential to differentiate into osteoblast, cardiomyocyte, adipocyte, myoblasts, tenocytes, chondrocyte, renal cells, hematopoietic cells, neural cells and pancreatic lineage cells under *in-vitro* condition [122-124].

MSC have a substantial advantage over other stem cells due to their immunomodulatory properties after transplantation, reproducible recovery from different tissues, multipotential differentiation, *in-vitro* expansion, safe usage without tumor formation and potential for tissue repair. The release of growth factors at the sites of injury makes them important for cell replacement therapy, such as diabetes mellitus, renal dysfunction, myocardial infarction and neurodegenerative diseases.

MSC participate in wound healing and tissue repair. In a diabetic scenario, the reduction in the proliferation and enhancement in senescence was demonstrated. In fact, the hyperglycemic condition promotes differentiation into adipocytes over osteogenic and angiogenic potential [125, 126]. Alterations of specific cell surface markers on MSC retrieved from diabetic subjects were observed but still wound healing, tissue repair and immunomodulatory properties were preserved as shown in figure 1.3.3.3 [127, 128].

1.3.3.4 Characterization of MSC

According to the norms of the International Society for Cellular Therapy (ISCT), MSC should have fibroblast-like appearance and plastic adherence property. First, >95% of MSC should express CD90, CD73 and CD105 cell surface markers and should be negative for CD45, CD11b, CD14, CD19, CD34, HLA-II. Second, it is required that a committed cell line differentiates into the mesoderm lineage under specific culture conditions. Moreover, MSC should display

hypoimmunogenic phenotype by low expression of MHC class 1 molecule and no expression of Fas ligand, MHC class II and co-stimulatory molecules B7 and CD40 [129].
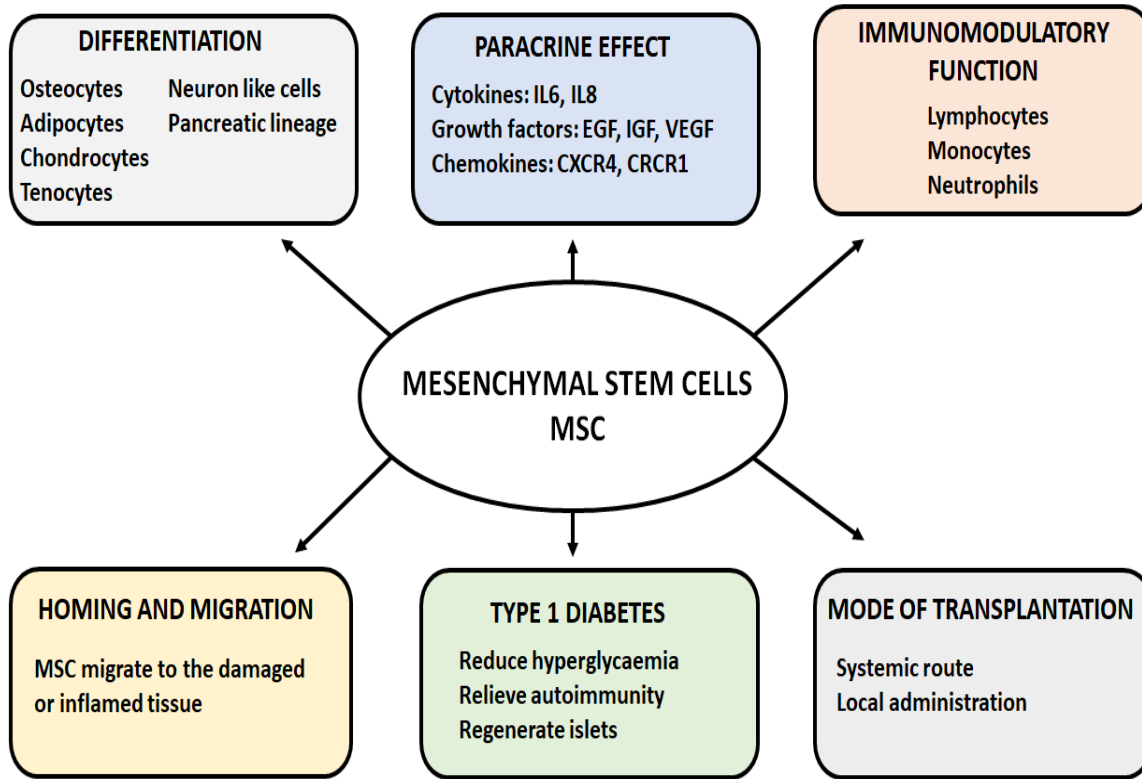
Figure 1.3.3.3: Systematic representation of the biological function of mesenchymal stem cells in injured tissue. Adapted and modified image from Squillaro. T (2018) and Wu. H (2014) [130, 131]. Interleukin 6 (IL6), interleukin 8 (IL8), epidermal growth factor (EGF), insulin-like growth factor-1 (IGF-1), vascular endothelial growth factor (VEGF), C-X-C chemokine receptor type 4 (CXCR4), C-X-C chemokine receptor type 1 (CXCR1).

1.3.3.5 Adipose derived mesenchymal stem cells (ADMSC)

ADMSC can be harvested from human lipoaspirates and cultured in large quantity. The lean individual carries three to four kg of adipose tissue whereas an obese individual can have >40 kg extra fat. An adequate amount of ADMSC can be obtained from one to two kg of fat [132]. ADMSC possess similar differential and secretory properties like BM-MSC. Obtaining ADMSC is less invasive in the human and a more practical approach due to its availability, autologous tissue and abundance as well. In the presence of fibroblast growth factor in culture, they showed Isl1 expression which is presumed mandatory for regeneration of nerve cells and pancreatic β-cells. Dang LT et al. reported the strength of ADMSC to differentiate into β-cell-like-cells expressing

C-peptide, insulin, PDX-1, NGN3, Neuro D and other pancreatic progenitor markers *in-vitro* [133]. Combination therapy of ADMSC along with pancreatic islets resulted in a better outcome in islet transplantation compared to islets alone [134].

1.3.3.6 hTERT-MSC

Bone marrow-derived human telomerase reverse transcriptase mesenchymal stem cells (hTERT-MSC) is an immortalized line, produced by transfecting bone marrow-derived MSC with a retrovirus containing hTERT gene. Due to replicative senescence, primary MSC have a limited proliferative capability. However, to get rid of the limited life span of primary MSC, the human telomerase reverse transcriptase gene was introduced for unlimited *in-vitro* expansion [135]. hTERT-MSC could be used for trilineage differentiation into adipocyte, osteocyte and chondrocyte along with endocrine lineage cells. These cells act through a paracrine effect, having anti-inflammatory and migratory properties. They maintain the telomerase length during successive passages [136].

1.3.4 Interaction of MSC and damaged tissues

The capacity of self-renewal, multipotent differentiation ability, beneficial outcomes from preclinical and clinical trials altogether emphasize the important role of MSC in repairing tissue damage and wound healing. At the tissue injury site, immune cells such as macrophages, neutrophils, B-cells, CD4+ T-cells and CD8+ T-cells are associated with the inflammation and produced in the response of necrotic cells, apoptotic cells and damaged microvasculature. Damaged cells produce inflammatory factors such as TNF-α, IL-1β, reactive oxygen species and other chemokines by phagocytosis [137]. As a result, immune cells along with inflammatory factors alter the microenvironment of the tissue which initiates the mobilization and differentiation of MSC into the stroma and helps in repairing the tissue [138]. MSC initiate migration from bone marrow or can be tissue resident. But after penetrating into the damaged tissue, they were reported to release certain factors such as vascular endothelial growth factor (VEGF), epidermal growth factor (EGF), transforming growth factor-β (TGF-β), platelet-derived growth factor (PDGF), insulin growth factor-1 (IGF-1), hepatocyte growth factor (HGF), stromal cell-derived factor-1 (SDF-1), keratinocyte growth factor (KGF) and angiopoietin-1 (Ang-1) [139, 140]. These factors modulate the microenvironment of the damaged tissue by enhancing the development and formation of fibroblasts, endothelial cells in wound healing and tissue repair [138].

1.3.5 MSC and its immunomodulatory properties

Apart from the tissue repair and wound healing, MSC have an immunomodulatory function which can inhibit the host immune response such as MSC can stop the maturation of DC by inhibiting MHC class II and other related factors [141]. Indeed, they can stimulate IL-10 secreting macrophages and inhibit IL-2 and IL-5 recruited natural killer cell maturation in inflamed and damaged tissue [142]. Moreover, the immunomodulatory properties of MSC are initiated by the inflammatory niche within the tissue. IFN-γ along with other cytokines such as TNF-α and IL-1β, stimulates the secretion of chemokines and adhesion factors such as vascular cell adhesion molecule-1 (VCAM-1), CCR5 ligands, CXCR3 ligand and cellular adhesion molecule-1 (ICAM-1) [143].

Interestingly, MSC mediated immunosuppression varies across the species. In the murine system, MSC-mediated immunosuppression via nitric oxide synthase (iNOS) leads to increased nitric oxide (NO) production [143]. However, in human it is mediated by the enzyme indoleamine 2,3-dioxygenase (IDO). IDO degrades tryptophan and locally accumulates tryptophan metabolites. Apart from IDO, tumor necrosis factor-inducible gene-6 (TSG6), can be activated by TNF-α in human MSC to exert its immune modulatory properties. TSG6 initiates zymosan-induced mouse peritonitis in resident macrophage via toll-like receptor 2 (TLR2)/ nuclear factor-kappa B (NF-kB) signaling pathway [144]. Additionally, human leukocyte antigen G (HLA-G) and leukemia inhibitory factor (LIF) also mediate immunosuppression through human MSC under *in-vitro* condition. But several molecules could mediate immunosuppression in the murine model as well as in humans, such as programmed cell death-ligand 1 (PD-L1), IL-6, hemeoxygenase-1 (HO-1), IL-10 and prostaglandin E2 (PGE2) [142, 145].

1.3.6 Migration of MSC

The outcome of the preclinical and clinical studies depends upon the migration and engraftment of MSC to desired sites after systemic transplantation. MSC follows an identical pattern like leukocyte migration [146]. The homing of the MSC after systemic injection is still a major issue in transplantation experiments. Most of the cells are entrapped in the lungs. However, a smaller fraction of MSC cross the endothelial barrier and migrate to the inflamed site [147]. This migration is mediated by integrin and adhesion molecules with respect to several chemotactic stimuli. In mice with acute pancreatitis (AP), a high level of stromal cell-derived factor-1 (SDF-1) expression

was measured up to seven days. The migration of BM-MSC towards damaged pancreas was mediated via SDF-1/ CXCR4 interaction. However, this effect was diminished after the pretreatment of transplanted BM-MSC with anti-CXCR4 antibody [148]. In another study, BM-MSC migrated in response to CX3CL1, CXCL16, CXCL12, CCL3, CCL19 and CCL2 with respect to CX3CR1, CXCR6, CXCR4, CCR1 and CCR7. Moreover, pancreatic islets initiated the migration of BM-MSC via CX3CL1-CX3CR1 and CXCL12-CXCR4 [149].

1.3.7 Route of transplantation

The therapeutic effectiveness of MSC depends upon its route of administration [150]. After infusion, MSC migrated towards inflamed tissue to repair damaged cells and provide a beneficial effect to the organs. In diabetic condition, MSC showed control over hyperglycemia and preserved pancreatic β-cell function [151]. However, most of the studies in MSC administration employed the systemic route of transplantation in the mice model (intravenous route/ intra-arterial) and clinical trials [152-154]. Systemic route of transplantation exposed MSC to the lungs where they entrapped into the microvasculature and had restricted access to the damaged tissue [155]. The diameter of the MSC (15-19 micron) is bigger than the average size of pulmonary capillaries (6 microns) [156]. MSC after entrapping into the lung capillary could induce an incident of tachypnea and apnea, cessation/ decreased blood flow and even death up to 40% in MSC administered mice [155-157]. Indeed, after entrapment, they could penetrate lung parenchyma and cause osteosarcoma (tumor-like nodules) [158]. Therefore, the local administration of MSC could be the desired procedure.

In mixed meal tolerance test of T1D patient up to one year, intravenously administered hBM-MSC improved C-peptide blood levels as a measure of residual insulin synthesis but failed to reduce glycosylated haemoglobin [152]. In different disease models, MSC were tested for local and intra-arterial injections which could bypass the lung [159-161]. After intra-arterial injections in rats suffering from traumatic brain injury, MSC showed superior engraftment over intravenous administration [159]. Moreover, the local injection of hBM-MSC provided better relief from pain due to arthritic joints as compared to the intravenous route [160]. In the diabetic mouse model, intrasplenic and intrapancreatic route of allogenic MSC administration was applied. Intrasplenic route of MSC administration reversed blood glucose level of 70% diabetic mice, as opposed to 42% with intrapancreatic route [162]. In another study intravenous administration of human

umbilical cord-derived MSC provided better protection with intravenous than intrapancreatic injection [163]. Recently, Norimtsu Murai et al. conducted an elegant study, showing the superior effect of hBM-MSC via intrapancreatic infusion over the intravenous route [164]. The beneficial effect of MSC is still debatable which needs to be further elucidated for its better therapeutic efficacy.

1.3.8 Direct and indirect contact of MSC with β-cells

The protective effect of local and systemic administration of MSC could be different in direct (physical contact) and indirect (paracrine effect) contact with pancreatic β-cells [164]. Co-culture of MSC with pancreatic islets proved to be beneficial in terms of islet viability and function. However, it is still debatable whether MSC secreting growth factors are adequate to enhance islet function or whether physical contact is required *in-vivo* [165, 166]. Studies demonstrated higher islets survival rate when co-cultured with MSC, both in direct and indirect co-culture approach. In indirect co-culture, MSC were separated from islets with a semipermeable membrane which granted the exchange of soluble factors through transwell. In this indirect system, MSC preserved the islet viability and function through the activation of P-AKT and P-ERK signaling pathway [167]. In direct co-culture system, MSC were in physical contact with islets. This approach was proposed to provide additional support to isolated islets and have a great advantage in clinical islet transplantation [168]. Moreover, direct contact modulated the islet function to secrete insulin and reduce apoptosis [169]. Further, Lin et al. demonstrated conserved islets viability and function using a co-culture system of bone marrow MSC with pancreatic islets on the microfluidic chip. Pancreatic islets and MSC were cultured into two different micro-compartments, connected through passage allowing the exchange of soluble factors [170]. Direct co-culture system firstly preserved the structural integrity, maintained favourable anti-inflammatory environment, secondly reduction in TNF-α, MCP-1 secretion and induction of TIMP-1, VEGF and thirdly superior insulin secretion after glucose challenge over indirect co-culture system [171].

1.4 Aims of the study

1) Characterization and *in-vivo* safety of bone marrow-derived hTERT-MSC cell line and primary adipose derived MSC.

2) Regeneration potential of pancreatic β-cells after MSC administration in the partially pancreatectomized mouse.

3) Antidiabetic effect and sustainability of administered MSC in STZ-induced diabetic NMRI nu/ nu mice through the intravenous route (IVR) and intrapancreatic route (IPR).

2. MATERIAL AND METHODS

2.1 Materials

2.1.1 Chemicals

Chemicals	Company
Agarose (LM-MP)	Sigma
Acetic acid	Roth
Ammonium persulfate (APS)	Bio-Rad
Acetic acid n-butyl ester (EBE)	ROTH
β-mercaptoethanol	Life Technologies
BSA (protein standard)	Sigma
Bovine serum albumin (BSA)	Sigma
3,3'-diaminobenzidine tetra HCl	Sigma
DNase I	Qiagen
Dimethyl sulfoxide (DMSO)	Fluka
Donkey serum	Jackson ImmunoResearch
Dithiothreitol (DTT)	Invitrogen
Ethanol absolute	Sigma
Ethylenediaminetetraacetic acid (EDTA)	Fluka
ECL Western blotting substrate	Thermo Scientific Pierce
Fetal calf serum (FCS)	Biowest
Formaldehyde solution 3.5-3.7%	Fischar
Glutamine	Invitrogen
Gentamycin	Invitrogen
Glucose	Sigma
Bisbenzimide H 33342 Fluorochrome Trihydrochloride	Calbiochem
Hank's buffered salt solution (HBSS)	Invitrogen
Hydrochloric acid (1M HCl)	Merck
HEPES buffer	Sigma
Isopropanol	Baxter
Isoflurane	Baxter
Methanol	Merck

Magnesium sulfate (MgSO$_4$)	Merck
Magnesium chloride (MgCl$_2$)	Merck
N, N, N', N'-Tetra-methyl-ethylenediamine (TEMED)	Bio-Rad
Oligo (dT) 20	Invitrogen
Penicillin/ Streptomycin	Invitrogen
Paraformaldehyde	Merck
Phosphate buffered saline (PBS 1X)	Lonza
Dulbecco's phosphate buffered saline (DPBS 10 X)	Lonza
Prolong Gold	Invitrogen
Protease and phosphatase inhibitor cocktail	Thermo Scientific
RNase-free water	Invitrogen
Sodium chloride (NaCl)	Roth
Sodium hydroxide (NaOH)	Fluka
Sodium dodecyl sulfate (SDS)	Bio-Rad
Glycerol	Merck
Skim milk powder	Merck
Streptozotocin (STZ)	Invitrogen
SYBR Green	Invitrogen
Strept AB Complex	DAKO
Tris-HCl	Sigma
Trypan Blue	Sigma
Trizol	Invitrogen
Tris-base	Sigma
Triton X-100	Sigma
Trypsin/ EDTA	Invitrogen
Thymidine	Sigma
Tween 20	Merck
Roti-load (4X)	Carl Roth
Tissue PE-LB	G-Bioscience
Protease Arrest	Protease Arrest

Goat serum	Bio west
Tris-wash buffer, TBS (20X)	Zytomed Systems GmbH
Paraffin 46-48	Merck
Medium Plast 58 ℃	Medium Histotechnologie
Objektträger SuperFrost Utra Plus	R. Langenbrinck GmbH

2.1.2 Kits

Kits	Company
BCA Protein Assay Kit	Thermo Scientific Pierce
Mouse Insulin ELISA Kit	DRG Instruments
RNeasy Mini Kit	Qiagen
RNeasy Micro Kit	Qiagen
SuperScript® III Reverse Transcriptase	Invitrogen
Human MSC Analysis Kit	BD
VECTOR Blue Alkaline Phosphatase (Blue AP) Substrate Kit	VECTOR Laboratory
ImmPACT™ AMEC Red Substrate	VECTOR Laboratory
Mouse-on-mouse HRP Polymer Bundle	Biocare Medical
Fuchsin + Substrate Chromogen System	Dako

2.1.3 Instruments

Instrument	Company
Centrifuge Biofuge 13	Heraeus
Centrifuge Universal 320R	Hettich
ELISA Plate Reader	Berthold Technologies-Mithra LB940
Fluorescence microscope LB30T Leica	Leica
Gel Doc	Vilber Lourmat
Incubator	Heraeus
Magnetic stirrer	Ika
Microplate Reader Mithra LB940	Berthold
Light Microscope camera DFC 420	Leica

NanoDrop 1000 Spectrophotometer	Thermo Scientific
OneTouch Glucometer	LifeScan
StepOne Plus Real-Time PCR	Applied Biosystems
Shaker	Keutz
BD FACSCANTO II	BD Bioscience
Vortex	Cenco
Microwave	Bosch
Water Bath 1052	GFL

2.1.4 Softwares

Software	Company
Bio 1D	Vilber Lourmat
EndNote X8	Thomson Reuters
Image J	National Institutes of Health
Leica Application Suite	Leica
BD FACS DIVA	BD Bioscience
Statistical Analysis	GraphPad Prism
Western blot	PEQLAB

2.1.5 Primary antibodies

Primary Antibody	Dilution	Company
Rabbit Beta-tubulin, Polyclonal antibody	1:10000 (WB)	Abcam
Guinea Pig Anti-Insulin, Polyclonal antibody	1:100 (IHC)	DAKO
Mouse Anti-BrdU, Monoclonal antibody	1:100 (IHC)	DAKO
Rabbit AKT Antibody, Polyclonal antibody	1:1000 (WB)	Cell signaling
Rabbit Phospho-AKT (Ser473), Polyclonal antibody	1:1000 (WB)	Cell signaling
Rabbit ERK Antibody, Polyclonal antibody	1:1000 (WB)	Cell signaling
Rabbit Phospho-p44/42 MAPK (Erk1/2), Polyclonal antibody	1:1000 (WB)	Cell signaling

Rabbit Anti-FoxO1 antibody, Monoclonal antibody	1:100 (IHC) 1:1000 (WB)	Abcam
Rabbit EGF, Polyclonal antibody	1:500 (WB)	Bioss
Rabbit Anti-FOXA2, Monoclonal antibody	1:10000 (WB)	Abcam
Rabbit Anti PDX-1, Polyclonal antibody	1:10000 (WB)	Merck

2.1.6 Secondary antibodies

Secondary Antibody	Dilution	Company
Polyclonal Goat Anti-Rabbit Immunoglobul -ins/ HRP	1:3000 (WB)	DAKO
Antibody Alkaline Phosphatase Conjugated Goat Anti-Rabbit IgG	1:200 (IHC)	Dianova
Anti-GUINEA PIG IgG (H&L) (GOAT) Antibody Alkaline Phosphatase Conjugated	1:40 (IHC)	Biomol

2.1.7 Human Primers

Human Primers	Sequences
h RPL13 fw	5'-CCTGGAGGAGAAGAGGAAAGAGA-3'
h RPL13 rev	5'-TTGAGGACCTCTGTGTATTTGTCAA-3'
h TIMP1 fw	5'-TTGTGGACGGACCAGCTCCT-3'
h TIMP1 rev	5'-GGTGGACACTGTGCAGGCTT-3'
h VEGF fw	5'-5'-CTACCTCCACCATGCCAAGT-3'
h VEGF rev	5'- AGCTGCGCTGATAGACATCC-3'
h IDO1 fw	5'-AGTGGGCTTTGCTCTGCCAA-3'
h IDO1 rev	5'-GGCGCTGTGACTTGTGGTCT-3'
h CXCR4 fw	5'-GACTGGCATAGTCGGCAATG-3'
h CXCR4 rev	5'-AGAAGGGGAGTGTGATGACAAA-3'
Human Alu seq fw	5'-CAT GGT GAA ACC CCG TCT CTA-3'
Human Alu seq rev	5'-GCC TCA GCC TCC CGA GTA G-3'

2.1.8 Mouse primers

Mouse Primers	Sequences
m RPL32 fw	5'-GGAGAAGGTTCAAGGGCCAG-3'
m RPL32 rev	5'-GCGTTGGGATTGGTGACTCT-3'
m EGF fw	5'-TCTCGGATTGACCCAGAT-3'
m EGF rev	5'-CCCAGACACCTTCCTCTCT-3'
m IGF-1 fw	5'-TGGATGCTCTTCAGTTCGT-3'
m IGF-1 rev	5'-GTCTTGGGCATGTCAGTGT-3'
m BAX fw	5'-TGAAGACAGGGGCCTTTTTG-3'
m BAX rev	5'-AATTCGCCGGAGACACTCG-3'
m BCL-2 fw	5'-ATGCCTTTGTGGAACTATATGGC-3'
m BCL-2 rev	5'-GGTATGCACCCAGAGTGATGC-3'
m GLUT-2 fw	5'-TGTGCTGCTGGATAAATTCGCCTG-3'
m GLUT-2 rev	5'-AACCATGAACCAAGGGATTGGACC-3'
m Ins1 fw	5'-TAT AAA GCT GGT GGG CAT CC-3'
m Ins1 rev	5'-GGG ACC ACA AAG ATG CTG TT-3'
m Ins2 fw	5'-GGCTTCTTCTACACACCCATGT-3'
m Ins2 rev	5'-AAGGTCTGAAGGTCACCTGCTC-3'
m IL-1β fw	5'-AGGTCGCTCAGGGTCACAAG-3'
m IL-1β rev	5'-GTGCTGCCTAATGTCCCCTTGAATC-3'
m TNF-α fw	5'-CATCTTCTCAAAATTCGAGTGACAA-3'
m TNF-α rev	5'-TGGGAGTAGACAAGGTACAACCC-3'
m IL-10 fw	5'-TAAGGCTGGCCACACTTGAG-3'
m IL-10 rev	5'-GTTTTCAGGGATGAAGCGGC-3'
m PI3K fw	5'-CTCTCCTGTGCTGGCTACTGT-3'
m PI3K rev	5'-GCTCTCGGTTGATTCCAAAC-3'
m AKT fw	5'-ATCCCCTCAACAACTTCTCAGT-3'
m AKT rev	5'-CTTCCGTCCACTCTTCTCTTTC-3'
m FoxO1 fw	5'-TTCAATTCGCCACAATCTGTCC-3'
m FoxO1 rev	5'-GGGTGATTTTCCGCTCTTGC-3'

m DLK1 fw	5'-AGTGCGAAACCTGGGTGTC-3'
m DLK1 rev	5'-GCCTCCTTGTTGAAAGTGGTCA-3'
m PDX-1 fw	5'-GAACCCGAGGAAAACAAGAGG-3'
m PDX-1 rev	5'-GTTCAACATCACTGCCAGCTC-3'
m FOXA2 fw	5'-GACATACCGACGCAGCTACA-3'
m FOXA2 rev	5'-TAGATCTCGCTCAGCGTCAG-3'
m ERK fw	5'-TCAGTTTGTCCCCTTCCATTG-3'
m ERK rev	5'-TCCACTCCCACAATGCACAC-3'
m IFN-γ fw	5'-CGGCACAGTCATTGAAAGCC-3'
m IFN-γ rev	5'-TGCATCCTTTTTCGCCTTGC-3'
m SDF-1 fw	5'-AACCAGTCAGCCTGAGCTAC-3'
m SDF-1 rev	5'-GGGTCAATGCACACTTGTCTG-3'

2.1.9 Animals

Ten to twelve weeks old athymic male NMRI nu/ nu mice were purchased from Janvier laboratory (France). Animals were maintained at 14:12 hour (light: dark cycle) with standard food (ad libitum, Altromin), water, humidity and temperature as per German Animal Welfare Law. All surgical procedures were approved by the ethical committee and implemented according to the German Animal Welfare Law and Guidelines under the code 31/2017.

2.2 Methods

2.2.1 Animal experimental design

Ten to twelve weeks old athymic male NMRI nu/ nu mice were utilized in three experimental designs: tumor, pancreatectomy and diabetes experiment as detailed below. They were provided with standard laboratory food and water. All mice were anaesthetized and sacrificed by intraperitoneal injection of xylazine (20 mg/ kg body weight) and ketamine (100 mg/ kg body weight). Prior to organ retrieval, mice were weighed and samples prepared according to the requirement of the different experimental setup. Organs were inspected and weights of lung, liver, spleen, kidney, heart and pancreas were measured to exclude severe organ damage as a consequence of the experimental procedures.

2.2.1.1 Tumor experiment

Group 1: 0.5 X 10^6 hTERT-MSC transplanted subcutaneously in the flank of NRMI mice.
Group 2: 0.5 X 10^6 Primary ADMSC transplanted subcutaneously in the flank of NRMI mice.
Group 3: 0.5 X 10^6 PANC1 (positive control) transplanted subcutaneously in the flank of NMRI mice.

0

Measurement of tumor diameter thrice
a week with Vernier caliper

42 days

Days

When the tumor size exceeds 15mm,
mice were sacrificed

Figure 2.2.1.1: Systematic representation of tumor experiment. Mice were administered with 0.5 x 10^6 hTERT-MSC, ADMSC and PANC1 in the flank of NMRI nude mice.

2.2.1.2 Regeneration experiment

IVR   IPR

Bromodeoxyuridine
(BrdU)

PK   Px   0.5 X 10^6
hTERT-MSC   PK   PK

Group 1 : 0.5 X 10^6 hTERT-MSC transplanted by intravenous route (IVR)
Group 2 : 0.5 X 10^6 hTERT-MSC transplanted by intrapancreatic route (IPR)
Group 3 : MEM media injected by intravenous route

-1   0   2   6   7   8

Days

PK: Pain killer
Px: Partial Pancreatectomy

Figure 2.2.1.2: Experimental model of regeneration study. After partial pancreatectomy, 0.5 x 10^6 hTERT-MSC were administered through intravenous route (IVR) or intrapancreatic route (IPR). Pain killer (PK), partial pancreatectomy (Px), bromodeoxyuridine (BrdU).

2.2.1.3 Diabetes experiment

Figure 2.2.1.3: Experimental set-up of the diabetes experiment. 0.5×10^6 ADMSC were administered from two distant routes: intravenous route (IVR) and intrapancreatic route (IPR) in STZ-induced NMRI nude mice on day seven after the first of three STZ injections.

2.2.1.4 Post-operative pain management

One day before to two postoperative days, mice were treated with tramadol (2.5 mg = 0.25 ml/ 100 ml) in drinking water. Additionally, metacam (1mg/ kg) was injected subcutaneously for post-operative pain management.

2.2.2 Partial pancreatectomy

Ten to twelve weeks old athymic male NMRI nu/ nu mice were utilized for 50% partial pancreatectomy. Mice were anaesthetized with xylazine (20 mg/ kg body weight) and ketamine (100 mg/ kg body weight) by intraperitoneal injection. A midline incision was executed to expose the pancreas. The pancreas was identified as a fragile and pink color organ near the spleen. Afterwards, blood vessels near splenic hilum and the head region near duodenum were blocked with absorbable silk suture. Further, 50 to 60% of the spleen portion of the pancreas was resected with scissors. Abdominal wall and upper skin were closed with absorbable silk suture. All animals were sacrificed eight days later.

2.2.3 Streptozotocin (STZ) and bromodeoxyuridine (BrdU) injection

2.2.3.1 STZ injection

A total dose of 120 mg/ kg body weight of STZ was injected intraperitoneally in the course of three consecutive days by applying a stopper. Multiple low-dose injections of STZ induced a

gradual rise of blood glucose over a period of ten days accompanied by inflammatory symptoms of pancreatic islets as opposed to a single injection of full dosage [172]. The latter results in blood glucose level at maximum one or two days after the injection of STZ.

2.2.3.2 BrdU injection

Prior to the organ retrieval, BrdU (100 mg/ kg body weight) was injected intraperitoneally for three consecutive days to label proliferating cells within the islets of the pancreas. On the third day, organs were retrieved two hours following the last BrdU injection.

2.2.4 Blood glucose measurement

Glucose was measured thrice a week pin-pricking the tail vein with a 26G needle (0.45 mm x 13 mm) by hand-held glucose meter One Touch® Ultra®2 (LifeScan) using a volume of 1-3 µl blood. The meter was calibrated using standard solutions; control solution 1 (ranging from 25 to 50 mg/ dl) and control solution 2 (ranging from 255 to 345 mg/ dl). Applied control solution 1 and control solution 2, if the glucometer readings appeared in the above-mentioned range of the respective solution, glucometer showed OK sign otherwise ERROR sign will appear on the screen.

2.2.5 Cell culture

2.2.5.1 PANC1 cells

PANC1 cells (human tumor-cell line, ATCC®) were cultured in DMEM medium (high glucose with L-glutamine, ATTCC) along with the supplements 10% FCS (Biowest, S1810-500) and 1% penicillin-streptomycin (Gibco, 15140-122) in the culture flask. Every second-day medium was changed. Cells were cultured for four consecutive passages after reviving from frozen stock. At 80% confluency, cells were detached with trypsin-EDTA. The reaction was stopped by adding DMEM containing 10% FCS. Cells were centrifuged (1000 rpm, 5 min at 4 °C) and resuspended in 5 ml DMEM media. Cells were counted with trypan blue and resuspended in 0.5×10^6 cells/ 100 µl/ injection in DMEM media (without supplements) for transplantation into the flank of NMRI mice.

2.2.5.2 hTERT-MSC

hTERT-MSC were grown at a density of 5×10^4 cells/ cm^2 in MEM media (Gibco) with 10% FCS (Biowest, S1810-500), 1% L-glutamine, 1% penicillin-streptomycin and incubated at 37 °C with 5% CO_2 in T-75 culture flask. Media was changed every second day. After 70-80% confluency,

cells were detached with trypsin-EDTA. The reaction was stopped by adding MEM media containing 10% FCS. Cells were centrifuged (1000 rpm, 5 min at 4 °C) and resuspended in 5 ml MEM media. Cells were counted with trypan blue and 0.5×10^6 viable cells were resuspended in 100 µl MEM medium without supplements for injection into the flank of NMRI mice for the tumor experiment.

In pancreatectomy experiment, hTERT-MSC (0.5×10^6 cells/ 100 µl/ injection) were transplanted by the intravenous route (IVR) and directly into the residual pancreas (intrapancreatic route, IPR) immediately after removal of the splenic portion of the pancreas. In the pancreas, 0.5×10^6 hTERT-MSC/ 100 µl were administered slowly (within in ten sec) in the deep middle part resulted in a bulge or depot (figure 2.2.1.2) and slowly withdraw the needle to avoid the leakage. After transplantation of the cells, the injection site was observed for fifteen seconds. No further bleeding or leakage of the injected fluid was observed. In the control group, the same amount of MEM 100 µl/ injection was injected by the intravenous route (IVR) and directly into the pancreas (IPR).

2.2.5.3 ADMSC

ADMSC retrieval was approved by the institutional review board (Ethikkommission) of the Faculty of Medicine, Justus Liebig University (JLU), Giessen under Reg.– No 141/04. Adipose tissue was surgically removed in Dept. of Oral and Maxillofacial Surgery, (Head: Prof. Dr Hans-Peter Howaldt) and stromal cells were isolated from the tissue by Prof. Dr Heinrich Sauer from the Department of Physiology, JLU, Giessen. Adipose tissue or fat was divided into smaller parts and washed with PBS containing 0.075% Liberase™ (Roche, Mannheim, Germany) for 2 hr. Afterwards, cells were grown into 75 cm^2 culture flask in Ham´s F10 medium (10% FCS, 0.1 mM β-mercaptoethanol, 2 mM glutamine, 2 mM minimal essential medium, penicillin (100 IU/ ml) and streptomycin (100 µg/ ml) with 5% CO_2 in an incubator. After ten days, cells acquired fibroblast-like appearance and ADMSC stocks were prepared.

For the experiment, cells seeded at a density of 5×10^4 cells/ cm^2 in DMEM media (D5671, Sigma with 4500 mg/ L glucose and sodium bicarbonate) with 20% FCS, 1% L-glutamine, 1% non-essential amino acid (NEAA, Gibco), 1% penicillin-streptomycin and incubated at 37 °C with 5% CO_2 in an incubator in T-75 culture flask. Cells were harvested and detached with trypsin-EDTA. The enzymatic reaction was stopped with DMEM media containing 20% FCS. Cells were centrifuged (1000 rpm, 5 min at 4 °C) and resuspended in 5 ml DMEM media. Cells were counted

with trypan blue and 0.5×10^6 viable cells were resuspended in 100 µl MEM medium (without supplements) for transplantation into the flank of NMRI mice. For the diabetic experiment, ADMSC (0.5×10^6 cells/ 100 µl/ injection) were transplanted by the intravenous route (IVR) and directly into the pancreas (IPR). In the control group, DMEM (100 µl/ injection) was injected by the intravenous route (IVR) without supplements.

2.2.5.4 MIN6 cells

MIN6 cells are a pancreatic β-cell line derived from mouse insulinoma 6, subclone. MIN6 cells were cultured in DMEM (4.5 g/ L D-glucose, Gibco) with 20% FCS, 1% penicillin-streptomycin, 50 µM β-mercaptoethanol in a T-75 flask in an incubator at 37 °C with 5% CO_2. Every two days, the media was changed. Cells were detached with trypsin-EDTA. The enzymatic reaction was stopped with DMEM media containing 20% FCS. Cells were centrifuged (1000 rpm, 5 min at 4 °C) and resuspended in 5 ml DMEM media. Afterwards, the cells were split into three new T-75 flasks.

2.2.6 Insulin measurement

2.2.6.1 Pancreatic insulin

After eight and thirty days of different experimental groups, the residual pancreas was retrieved. The pancreas was grinded and homogenized mechanically with mortar-pestle in 5 ml acid-methanol solution [76 ml (96% Ethanol) + 8 ml (1 M Phosphoric acid) + 4 ml (distilled water)]. Homogenized pancreas was transferred into a 15 ml tube and incubated overnight at 4 °C on a shaker. Next day, the tube was centrifuged at 300 rpm for 10 min. Protein concentration was measured with Bio-Rad Protein Assay and 50 µl of supernatant was diluted with 1 ml of immunoreactive insulin (IRI) buffer [Na_2HPO_4 (4.7 g), NaCl (6 g), BSA (3 g), NaN_3 (0.2 g), distilled water (1L)] and stored at -20 °C. Next day all the samples were diluted 1:25 but in case of normal mice (whole pancreas) or sham control, 1:40 dilution was taken. Insulin ELISA (DRG, Germany) was performed to measure insulin content in the residual pancreas. This ELISA kit was a solid phase two-side sandwich-based ELISA. After the addition of the sample, insulin present in the sample reacted with peroxidase-conjugated mouse monoclonal anti-insulin antibody attached to the coated plate. The washing step removed excess unbound enzyme of the labelled antibody and the bound conjugated antibody was detected with 200 µl of 3,3', 5-5'-tetramethylbenzidine

(TMB). This reaction was stopped by adding 50 µl acid (0.5 M H_2SO_4) provided with the kit and readings were captured at 450 nm with a spectrophotometer.

The absorbance value of each set of standards or calibrator (standard 0=0 µg/ L, standard 1=0.20 µg/ L, standard 2=0.50 µg/ L, standard 3=1.5 µg/ L, standard 4=3.0 µg/ L, standard 5=6.5 µg/ L), negative control (only water) and pancreatic samples were taken at 450 nm. A standard curve was prepared with the mean absorbance from every standard absorbance concentration value on the Y-axis (vertical) and concentration on the X-axis (horizontal). Optical density (OD) values were included in the equation generated from the regression analysis. Later the insulin content (µg/ L converted to µg/ ml) was divided by protein concentration (mg/ ml) to calculate µg insulin/ mg of protein and further converted into ng insulin/ mg of protein.

2.2.6.2 Serum insulin:

Mice were euthanized, according to the respective schedule of experiments and blood was collected by cardiac puncture. Blood was allowed to clot at RT for 30-45 min and serum was separated by centrifugation (1300 rpm for 15 min). The insulin ELISA kit was utilized as mentioned above. No dilution was required for the serum sample.

2.2.7 Real-Time PCR

2.2.7.1 RNA Isolation
2.2.7.1.1 Tissue

After euthanization, the pancreas was carefully and quickly retrieved from NMRI mice within one min. Total RNA was isolated by combining peqGOLD TrifastTM reagent and RNeasy Mini Kit (Qiagen). The isolated pancreas was homogenized in 1ml of peqGOLD TrifastTM reagent. 200 µl/ ml of chloroform was added and mixed properly. After centrifugation (12000 rpm at 4 °C for 30 min), the upper aqueous layer was transferred into a separate tube. Isopropanol (1.5 volume) was added to the upper aqueous layer and transferred to the column of the RNeasy Mini Kit (Qiagen). RNA was acquired by following the RNeasy Mini Kit instruction as per manufacturer's protocol.

2.2.7.1.2 Cell

Total RNA from MIN6 cells and hTERT-MSC was acquired by RNeasy Micro Kit (Qiagen) instruction as per manufacturer's protocol.

2.2.7.2 Quantification of RNA concentration

The RNA concentration was quantified with NanoDrop 1000 Spectrophotometer (NanoDrop, Wilmington). Pure RNA samples showed an optical density ratio (260/ 280 absorbance) relatively around 2. The RNA concentration was measured by NanoDrop 1000 Spectrophotometer in ng/ µl, depends on its absorbance at 260 nm.

2.2.7.3 DNase treatment

To exclude the possibility of genomic DNA contamination, DNase treatment was performed for above isolated RNA samples. 1000 ng of isolated RNA was treated with 1 µl DNase I, 1 µl DNA reaction buffer (10X) and molecular grade water free from RNase/ DNase in a tube. This tube was incubated for 14 min at 37 °C. To eliminate DNase from the samples, 1 µl of 25 mM EDTA was mixed in the tube and incubated at 65 °C for 15 min.

2.2.7.4 cDNA synthesis

In the above DNase treated tube, reverse transcription was executed to obtain cDNA synthesis. This step was performed by preparing a master mix consisting of 4 µl (5X first strand buffer), 2 µl (0.1 M DTT), 1 µl (0.5 µg Oligo (dT)20), 1 µl (SuperScript III RT (200 U)), 1 µl (10 mM dNTPs). 9 µl from the master mix was added to the tube to 20 µl final volume. Next, the tube was incubated for 50 min at 42 °C followed by 15 min at 70 °C. Afterwards, 180 µl RNase-free water was given to the tube to have 1:10 dilution.

2.2.7.5 Real-Time PCR

1:10 diluted cDNA samples were quantified for specific target sequence with the StepOne Plus real-time PCR system. Following steps were performed with the mixture of SYBR Green, water, specific primer and cDNA.

All the primers were designed with primer3 and BLAST. Primer3 and BLAST provided the specific primer-template sequence search in the database. All the primers were ordered from Thermo Fisher and diluted with RNase free water.

Steps	Temperature	Time	No. of cycles
Enzyme activation	95 °C	15 min	1 cycle
Denaturation	95 °C	15 sec	40 cycles

Annealing	60 °C	30 sec	
Extension	72 °C	30 sec	

To examine the specificity of the product, the melting curve quantification was accomplished by the following steps

Steps	Temperature	Time	No. of cycles
Denaturation	95 °C	30 sec	1 cycle
Starting Temp.	60 °C	30 sec	1 cycle
Melting step	60 °C	10 sec	1 cycle

All samples were run in triplicate and results were analyzed by the ΔΔCT method.

2.2.8 Western blotting

2.2.8.1 Sample preparation

2.2.8.1.1 Tissue
The pancreas was grinded and homogenized with mortar-pestle in liquid nitrogen. Afterwards, cells were lysed with Tissue PE LBTM (G-Biosciences) containing Protease ArrestTM (G-Biosciences) for protease inhibition activity. Protein lysate was kept on ice for five min and centrifuged at 12000 g for 30 min at 4 °C. The supernatant was collected and stored at -80 °C.

2.2.8.1.2 Cell
2×10^6 cells were lysed with 200 µl RIPA buffer (1X) containing protease inhibitors. Cells were vortexed for 20 sec and maintained on the ice for 20 min. Afterwards, there was a centrifugation step at 12,000 g for 20 min at 4 °C. The upper part was collected and stored at -80 °C.

2.2.8.2 Protein concentration
BSA standard (2mg/ ml) was diluted 1:1 with distilled water and different concentration of standards were prepared (0 mg/ ml, 0.1 mg/ ml, 0.3 mg/ ml, 0.4 mg/ ml, 0.5 mg/ ml, 0.6 mg/ ml, 0.7 mg/ ml, 0.8 mg/ ml, 1 mg/ ml). Afterwards, appropriate dilution for tissue lysate (1:20) and cell lysate (1:5) was prepared. A volume of 10 µl was added in duplicate to a 96 well plate from standards and protein samples (tissue and cell lysate) followed by 200 µl of Bio-Rad Protein Assay (1:5 dilution with distilled water). Bio-Rad Protein Assay is a dye-binding method. It analyzed the

binding of the protein with Coomassie Brilliant Blue G-250 dye. This dye combined with aromatic amino acid residues like arginine and provided absorbance at 465 nm. Similarly, when combined with protein, it shifted its absorbance to 595 nm. This absorbance was measured by Mithras LB 940 Multimode Microplate Reader. Thereafter, protein concentration was measured by comparing known values with a BSA standard curve.

2.2.8.3 SDS-PAGE

Protein separation was performed with sodium dodecyl sulfate-polyacrylamide gel electrophoresis (SDS-PAGE) based on size. There were two gels: stacking gel (pH 6.8) having a higher porosity, facilitates free migration of the protein without smearing in running buffer (72 g Glycine, 15 g Tris-base, 5 g SDS, pH 8.3) whereas separating gel (pH 8.8) divides the protein based on its molecular size in running buffer (pH 8.3). Gels were prepared as follows:

Reagents	Separating gel (10%)	Stacking gel (5%)
Acrylamide-Bis (30%)	5 ml	0.83 ml
1.5 M Tris/ HCl (pH 8.8)	3.75 ml	0
1 M Tris/ HCl (pH 6.8)	0	0.63 ml
H_2O (RO)	5.93 ml	3.4 ml
APS (10%)	150 μl	50 μl
SDS (10%)	150 μl	50 μl
TEMED	15 μl	5 μl

2.2.8.4 Denaturation of protein

All the proteins (30 μg) from different samples were denatured with 1X Roti-load (4X) and boiled at 95 °C for 5 min. This step resulted in more unfolded proteins and provided access to antibodies to find more binding sites. Afterwards, different samples were centrifuged and the equivalent amount of protein was loaded onto the gels along with a protein marker in the first lane. The vertical gel electrophoretic apparatus with running buffer (1X) was used for the electrophoresis. After completion, gels were washed thrice (15 min) with transfer buffer (5.8 g Tris-base, 2.9 g Glycine, 0.37 g SDS, 200 ml methanol).

2.2.8.5 Blotting procedure

After washing with transfer buffer, gels were arranged in a sandwich pattern; first four filter papers, followed by activated polyvinylidene fluoride (PVDF) membrane and gel onto it. On the top again four filter papers. This was put in a semi-dry blotting chamber (Bio-Rad) and run for 48 min. This transfer chamber transferred the protein from a gel to PVDF membrane. Thereafter, wash the membrane with TBST (1X; TBS containing 0.1% Tween 20) and continue with blocking (milk powder; 5% or BSA) at RT for 1 hr. Afterwards, the membrane was incubated with a specific antibody in milk powder (5%) or BSA overnight at 4 °C. Next day, the membrane was washed thrice (15 min) with TBST and incubated with secondary antibodies at RT for 1 hr. The membrane was washed again thrice (15 min) with TBST and developed with an enhanced chemiluminescence system (ECL).

2.2.9 Immunohistochemistry

2.2.9.1 Fixation and embedding

The pancreas was removed at the end of the experiment and fixed for four to six hr in 5 ml of formalin (3.5-3.7%). Afterwards, washed with 70% ethanol for five hr (change 70% ethanol every hr) on a shaker at RT and kept overnight at 4 °C in 70% ethanol for washing. Next day, tissues samples were dehydrated as follows:

Substance	Time
Ethanol (80%)	30 min
Ethanol (96%)	45 min
Ethanol (100%)	45 min
EBE 1 (EBE: Ethanol=1:2)	1 hr
EBE 2 (EBE: Ethanol=1:1)	1 hr
EBE 3 (EBE: Ethanol=2:1)	30 min
EBE 4 (EBE: 100%)	30 min
Paraffin (46- 48) at 50 ℃	Overnight
Paraffin (60 ℃)	2 hr

Afterwards, all the pancreatic samples were embedded in paraffin wax and kept on a cool surface to harden the material. Post this step, store the paraffin blocks at RT.

2.2.9.2 Section cutting

Subsequent sections of 5-7 µm thickness were cut with a microtome (Reichtert Jung 2030, Germany) and brought on the slides in a 37 °C warm water bath. Dry them overnight at RT. Later mark each subsequent slide and stored at RT.

2.2.9.3 Insulin and BrdU staining

Slides were kept

- 2X 10 min in Rotihistol
- 2X 5 min in 100% ethanol
- 2X 5 min in 96% ethanol
- 2X 5 min in 70% ethanol
- 5 min with distilled water
- Cooked for 3X 5 min at 480 Watt in the microwave for antigen retrieval
- Cooled for 30 min at RT
- Washed with TRIS 2X (5 min)
- Blocked with 1% goat serum for 20 min in TRIS
- Incubated with specific primary antibody (polyclonal guinea pig anti-insulin; DAKO, Germany) in TRIS/ BSA 0.1% and kept overnight at 4 °C in a wet chamber.
- Washed 3X (5 min) with TRIS
- Incubated with an antibody (Alkaline phosphate conjugated affinity purified anti-guinea pig; Biomol, Germany) with 5% mouse serum in TRIS for 1 hr at RT.
- Washed 2X 5 min with TRIS buffer and developed blue color with vector blue substrate kit (Vector Laboratory). Color developed within 60 sec.
- Afterwards, sections were washed and treated with 1 M NaOH (1:11 dilution with distilled water) for permeabilization of the nuclear membrane for 3 min.
- Wash 3X 5 min with TRIS
- Next, rodent blocker (BIOCARE MEDICAL, Germany) was applied for 30 min and stained with anti-BrdU antibody (monoclonal mouse anti-BrdU antibody, DAKO, Germany) in TRIS/ BSA overnight at 4 °C in a wet chamber.
- Subsequent day the sections were washed 2X 5 min with TRIS and subjected to mouse-on-mouse HRP polymer (BIOCARE MEDICAL, Germany) for 45 min and later developed

with the red color with HRP (ImmPACT™ AMEC Red Substrate). Color developed within 90 sec. Later, the mounting medium (Dako) was applied.

- Images were captured with a light microscope (Leica microsystem, ICC50 HD) and evaluated with the Image J software.

2.2.9.4 FoxO1 staining

Immunohistochemistry was also performed with anti-FoxO1 (Abcam) antibody. Pancreatic tissues were fixed with 4% paraformaldehyde for four to six hr and embedded in paraffin. Afterwards, the 5-7 μm pancreatic tissue section was deparaffinized and permeabilized as described above. Sections were stained with primary (FoxO1; Rabbit Anti-FoxO1A antibody, Abcam) and secondary antibody (Goat anti Rabbit Alkaline phosphate, Dianova) as mentioned above. Later, the red color was developed with Fuchsin kit (Dako, Germany) and images were captured with light microscopy (Leica microsystem, ICC50 HD).

2.3.1 Identification of human Alu sequence/ human DNA.

To find out the transplanted hTERT-MSC and ADMSC in the NMRI mice, different organs such as liver, lung, kidney, spleen, pancreas and heart were isolated to find out genomic DNA. All the organs were weighed and incubated in 1.5 ml of lysis buffer (20 mM Tris-Cl, 5 mM EDTA, 400 mM NaCl and 1% SDS) containing 20 µl of Proteinase K (0.2 mg/ ml) at 56 °C for eight to ten hr. Thereafter, the phenol/ chloroform separation was performed. DNA was precipitated with ethanol and diluted with RNase/ DNase free water. The DNA concentration was measured with NanoDrop spectrophotometer. 1000 ng DNA was considered for PCR and products were analyzed on 1.5% agarose gel.

2.3.2 Flow cytometer

ADMSC and hTERT-MSC were characterized based on cell surface markers. Cells were grown in a T-25 flask and detached by the enzymatic reaction of trypsin-EDTA (Gibco, 25300-054). The reaction was stopped by adding DMEM containing 20% FCS. Cells were centrifuged (1000 rpm, 5 min at 4 °C) and resuspended in 5 ml PBS. Cells were counted with trypan blue. 1×10^6 cells were stained with 5 µl of CD90 (FITC; 1:20), 5 µl CD44 (PE; 1:20), 5 µl CD105 (PerCP-Cy5.5; 1:20) and 5 µl CD73 (APC; 1:20) in 100 µl of cell suspension. Tubes were incubated for 30 min on ice. Further, cells were washed twice with BD Pharmingen^{TM} Buffer (BD, 554656) and resuspended in 400 to 500 µl of BD Pharmingen^{TM} Buffer. Before analyzing, samples were mixed

properly or pass through a cell strainer (70 µM) to avoid clumping of the cells. Samples were run in BD FACSCANTO II (BD, Germany) within one hr and analyzed with BD FACS DIVA software (BD, Germany).

2.3.3 Model of direct and indirect co-culture

Direct co-culture means physical contact between MIN6 cells and hTERT-MSC whereas indirect contact or confrontation culture means they are separated by a semipermeable membrane which grants the exchange of the secretory product within the transwell as shown below.
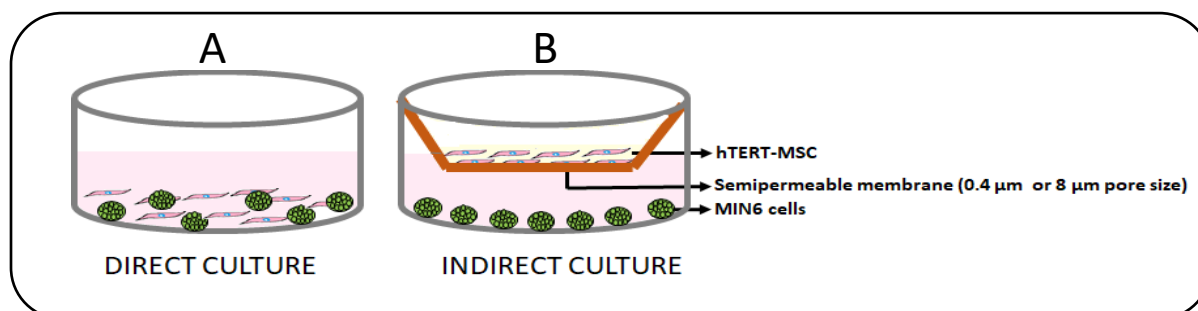
Figure 2.3.3: Systematic representation of direct co-culture and the indirect co-culture system. (A) Direct co-culture system provides physical contact between hTERT-MSC and MIN6 cells. However, in the indirect co-culture system, MIN6 cells were seeded on an adherent culture dish and hTERT-MSC on transwell. Cells were separated by a semipermeable membrane.

2.3.3.1 Viability

For direct co-culture condition, 5000 MIN6 cells/ well were grown in a 96-well plate. Next day, cells were challenged with different concentrations of STZ (0.5 mM, 1 mM or 2 mM) for 24 hr. Thereafter, 2000 hTERT-MSC were directly seeded onto the MIN6 cells. For indirect co-culture condition, 5000 MIN6 cells/ well were grown in a 96-well plate (HTS Transwell™ 96-Well Permeable Support System, Corning™) overnight, challenged with STZ (0.5 mM, 1 mM or 2 mM) for 24 hr and 2000 hTERT-MSC were seeded on the transwell (0.4 µm) for 24 hr. Afterwards insert was removed from the indirect co-culture plate (figure: 2.3.3 B). 50 µl of MTT solution (2 mg/ ml, Sigma) was added and incubated at 37 °C for 4 hr in dark. The medium was discarded and 200 µl of DMSO was added to disrupt the cells, which dissolved the purple formazan crystal. DMSO was also added to the blank without cells. Cells were incubated at RT for 1 hr. Absorbance was measured at 590 nm and 620 nm (reference filter) with Mithras LB 940 Multimode Microplate Reader.

2.3.3.2 Migration

For indirect co-culture condition, 0.3×10^6 MIN6 cells were grown in a 24-well plate overnight, followed by STZ challenge (0.5 mM, 1 mM or 2 mM). Next day, 2×10^4 hTERT-MSC were placed in the insert with 8 µm pore size for 24 hr. Inserts were removed and the inner part was swapped by cotton, followed by two washes with PBS. Thereafter, stained with the FDA for 15 min at 37 °C. Pictures were captured and migrated cells were counted with the Image J software. Arbitrary background migration of cells was performed with an equal concentration of the FCS (20%) in the lower well and insert.

2.3.3.3 RNA and Western blotting samples

Both direct and indirect culture, 0.5×10^6 MIN6 cells were grown in a six-well plate overnight. Next day, MIN6 cells were challenged with STZ (1 mM) for 24 hr. Afterwards, in direct co-culture, 0.2×10^6 hTERT-MSC were added directly onto the MIN6 cells to attain physical contact whereas, in indirect co-culture, 0.2×10^6 hTERT-MSC were grown on the semipermeable membrane of the transwell insert (0.4 µm). Samples were prepared for PCR and Western blotting as mentioned above.

2.3.4. Statistics

2.3.4.1 Statistical analysis was accomplished with Prism 8 (GraphPad, USA) employing several methods dependent upon various experimental groups. Data were represented as the mean ± SEM (otherwise mentioned in the respective figure). The normal distribution of the data was reviewed with the Shapiro-Wilk normality test. In the case of the normal distribution, to compare two groups unpaired t-test or one-way ANOVA was employed. Two-way ANOVA was practised for distinct diabetic effect having several time points. Post ANOVA mean significance, Tukey's post-hoc test was conducted among different groups. In the case of non-significant difference, a Kruskal-Wallis test with Dunn's post-hoc comparison was applied. Compression was conducted with the control. Values considered significant $*p< 0.05$, $**p< 0.01$, $***p< 0.001$.

2.3.4.2 Analysis of immunohistochemistry data

For calculating islets, one islet was considered when having more than six cells inside it. To neglect the possibility of biases in calculating the number of islets and number and BrdU cells, the blinded external examiner was provided with stained sections and independent assessment was performed. Six or seven mice were utilized in every group. From one mouse four sections were considered.

These four sections were picked with an interval of five sections. To compare the different groups, One-way ANOVA with Tukey's post-hoc test was applied. Insulin area was evaluated with Image J software and further statistics were performed with Prism 8 as mentioned above. All the images were captured with a light microscope (Leica microsystem, ICC50 HD).

2.3.4.3 Processing of real-time qPCR data with 2^-ΔΔCt method:

The relative quantification method was applied and expression fold change of target gene was calculated with $2^{\wedge}$-ΔΔCt. For instance, the control sample (CS) with Ct=15 of the target gene was compared with the treated sample (TS) having Ct=13 of the target gene along with selected housekeeping gene; control (HCS; Ct=16) and treated (HTS: Ct=15.5).

2.3.4.3.1 Normalize Ct values of CS and TS

Ct values of CS and TS were normalized with regard to selected housekeeping control sample (HCS) target gene.

ΔCt (Control sample) = ΔCt (CS) - ΔCt (HCS)/ 15 – 16 = -1

ΔCt (Treated sample) = ΔCt (TS) - ΔCt (HTS)/ 13 – 15.5 = -2.5

2.3.4.3.2 Normalize ΔCt of the TS to ΔCt of the CS

ΔΔCt = ΔCt (Treated sample) - ΔCt (Control sample)/ -2.5 – (-1) = -1.5

2.3.4.3.3 Calculate fold change in the expression

$2^{\wedge}$-ΔΔCt = $2^{\wedge}$- (-1.5) = 2.8

The treated sample showed 2.8-fold higher expression than the control sample.

3. RESULTS

3.1 Characterization and safety efficacy of MSC

3.1.1 Characterization of mesenchymal stem cells (MSC)

3.1.1.1 Morphology

Mesenchymal stem cells (MSC) were characterized based on morphology and cell surface marker profiling. According to the guidelines of the International Society for Cellular Therapy (ISCT) [173], hTERT-MSC and ADMSC were examined for plastic adherence property and fibroblast-like structure as illustrated in figure 3.1.1.1 A and 3.1.1.1 B.
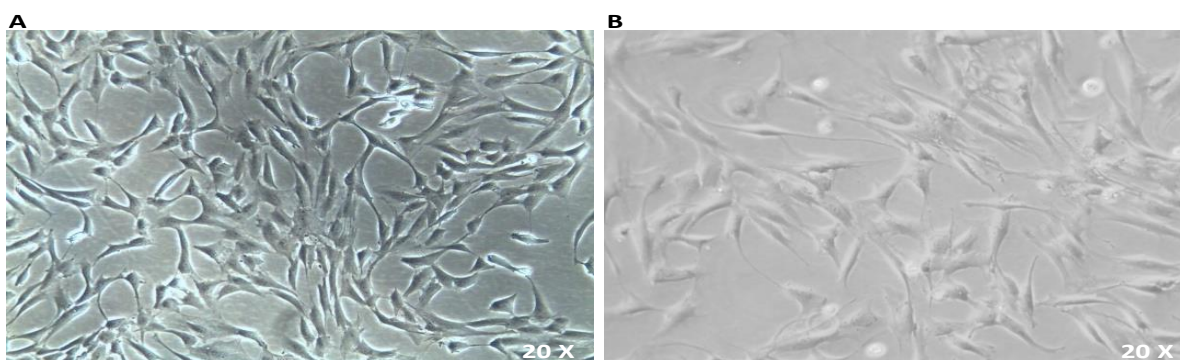
Figure 3.1.1.1: Morphology of MSC; (A) hTERT-MSC and (B) ADMSC. hTERT-MSC (human telomerase reverse transcriptase mesenchymal stem cells) and ADMSC (adipose derived mesenchymal stem cells).

3.1.1.2 Flow cytometry

Next, hTERT-MSC and ADMSC were analyzed for $CD90^+$, $CD44^+$, $CD105^+$, $CD73^+$ markers by a flow cytometer. In the upper control panel of figure 3.1.1.2 A and B, the graph was plotted for side scattered (SSC) versus forward scattered (FSC) unstained population. This unstained population of cells was further gated for the double positive for PerCP-Cy5.5-A channel ($CD105^+$) and PE channel ($CD44^+$), FITC channel ($CD90^+$) and PE channel ($CD44^+$), APC channel ($CD73^+$) and PE channel ($CD44^+$) resulted in the unstained population of the cells in the lower part.

Further, hTERT-MSC (figure 3.1.1.2 A; lower panel) were stained for $CD90^+$, $CD44^+$, $CD105^+$, $CD73^+$ markers. This stained population of the cells were analyzed for double positive cells: $CD105^+ + CD44^+$ population (99.3%), $CD90^+ + CD44^+$ population (99.1%) and $CD73^+ + CD44^+$ population (98.5%) in the same setting as mentioned above.

Similarly, ADMSC were also characterized (figure 3.1.1.2 B). Upper panel served as the control for the respective markers and lower plots were double positive for $CD105^+ + CD44^+$ (98.7%), $CD90^+ + CD44^+$ (98.9%) and $CD73^+ + CD44^+$ population (97.8%).
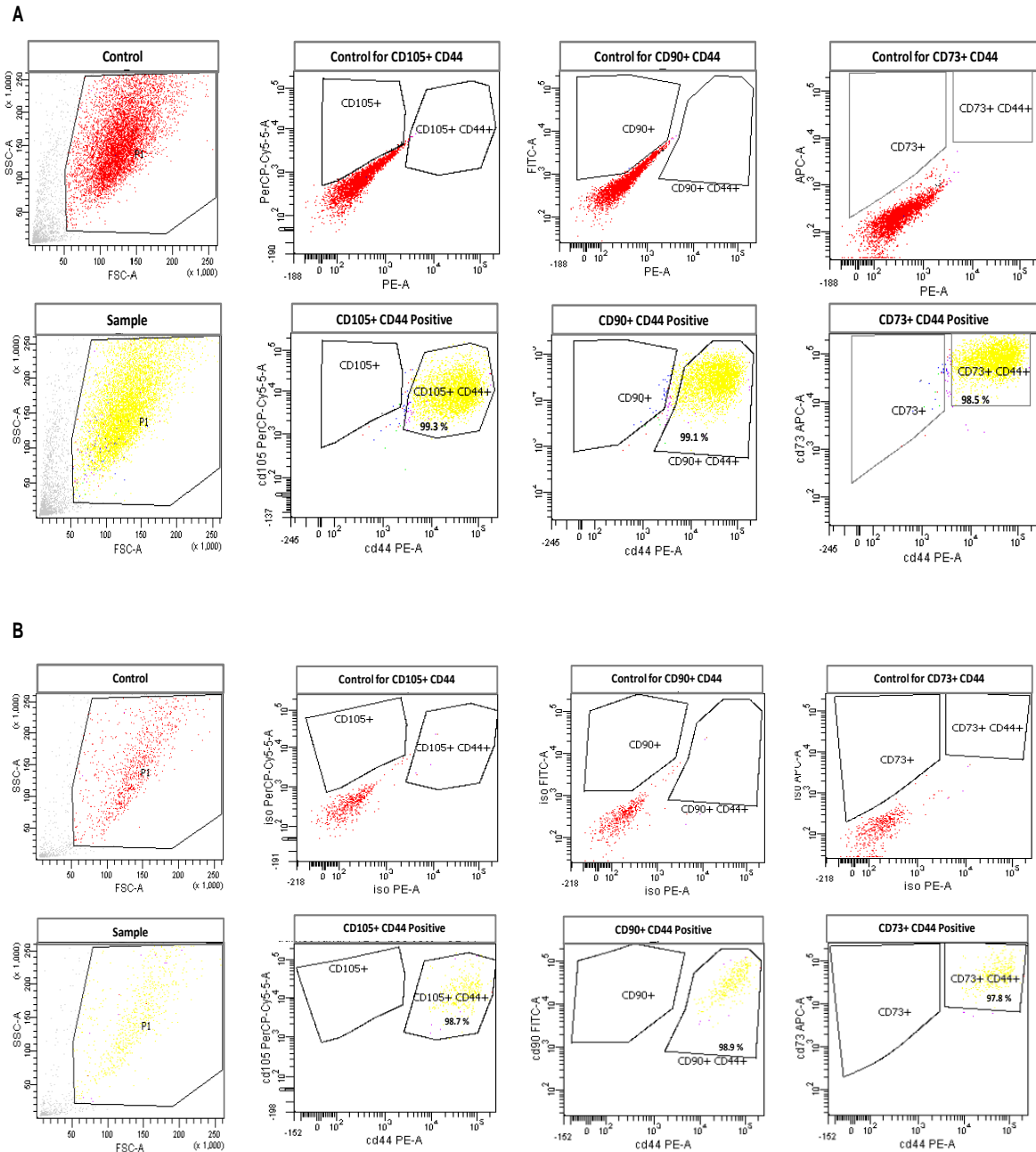
Figure 3.1.1.2: Flow cytometry evaluation of cell surface marker of MSC. Panel (A) represents the positive expression of $CD90^+$, $CD44^+$, $CD105^+$, $CD73^+$ of hTERT-MSC. Panel (B) demonstrates the flow cytometry

plot of specific cell surface markers of ADMSC. hTERT-MSC (human telomerase reverse transcriptase mesenchymal stem cells) and ADMSC (adipose derived mesenchymal stem cells).

These cells were also negative for the hematopoietic lineage such as CD34, CD79a, CD14 or CD11b, CD45 and HLA-DR which is not presented in the panel. It is important to confirm the expression of these characteristic cellular membrane-bound molecules after several passages. We used an immortalized hTERT-MSC line with a stable surface marker profile at subsequent passages. But primary ADMSC displayed spontaneous multipotency at regular culture conditions. After eight to ten passages, ADMSC showed a slower proliferative rate, the cells became wider and structurally looked different from the earlier passages.

3.1.2 Safety efficacy of MSC in diabetic therapy

MSC are at low risk of tumor formation, but different sources such as cell lines are always controversial in this respect. It is important to exclude this possibility for any stem cell therapy. We investigated the tumorigenicity potential of MSC from two different sources; hTERT-MSC (a cell line derived from bone marrow) and ADMSC (MSC isolated from adipose tissue of a single person).
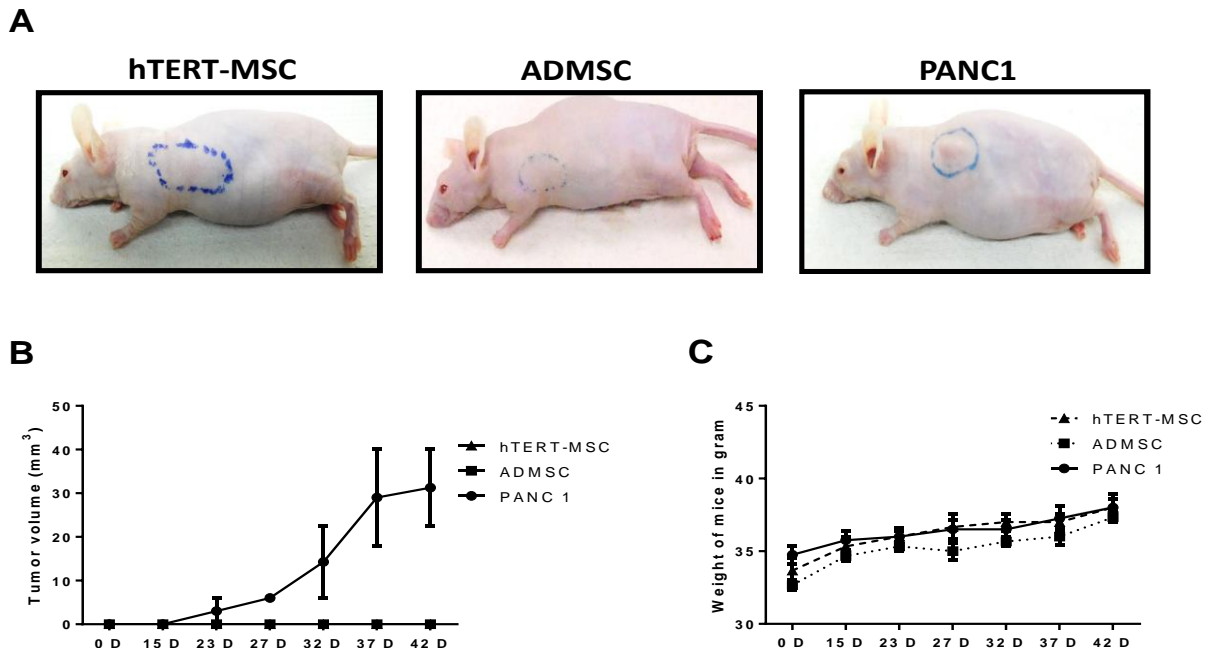
Figure 3.1.2: Tumor formation in NMRI nude mice. (A) Sample images of tumor formation after 42 days; No tumor observed in hTERT-MSC and ADMSC but PANC1 group showed the tumor after 15 days. (B)

47

and (C) represents the tumor volume and body weight. hTERT-MSC (human telomerase reverse transcriptase mesenchymal stem cells) and ADMSC (adipose derived mesenchymal stem cells). Data represent the mean ± SEM, n=4.

0.5×10^6 cells were administered subcutaneously (s.c) and the tumor was measured with Vernier caliper thrice a week in NMRI nude mice. There was no tumor observed with 0.5×10^6 hTERT-MSC and 0.5×10^6 ADMSC up to 42 days, but with 0.5×10^6 PANC1 (positive control) tumor was observed (figure 3.1.2 A). In PANC1 group, tumor formed after 15 days and had an incrementing pattern up to 42 days as shown in figure 3.1.2 B. This experiment was terminated at >15mm/ 42 days considering the duration of a human tumor trial. Figure 3.1.2 C represented the body weight of different groups. No significant difference was observed in body weight between the groups.

3.2. Regeneration of the pancreas after pancreatectomy

3.2.1 Blood glucose level and body weight

The effect of transplanted hTERT-MSC by different routes on the regeneration of pancreas was studied in 50% partially pancreatectomized mice. In literature, ranging from 0.5×10^6 to 1×10^7 MSC were reported for the treatment of murine diabetes [174-177]. Therefore, minimum cell number (0.5×10^6) that exerts a maximum curative effect was applied to ward off the pulmonary embolism in the mice. Hence, 0.5×10^6 hTERT-MSC were transplanted by two different routes; intravenous route (IVR) and intrapancreatic route (IPR). After eight days of 0.5×10^6 hTERT-MSC transplantation, the blood glucose level was measured in control injected i.v. with a culture medium only, IVR and IPR group. The blood glucose level in control (13.6 ± 0.73 mmol/ L) was higher as compared to IVR (12.7 ± 0.74 mmol/ L) and IPR (11.5 ± 0.63 mmol/ L) group. There was a decrease in blood glucose levels in the IVR group and even further in the IPR group, but no significant difference was observed as shown in figure 3.2.1 A.

After surgery, as per German animal welfare act, the health condition of mice was scrupulously assessed based on a unique scoring scheme (specifically designed for abdominal surgery, refer to table 1). More than score two required treatment while score zero indicated that mice were in a healthy condition. In comparison with control mice, the IPR group revived faster at the fourth day onwards ($p< 0.01$) whereas in the IVR group, recovery was observed on the seventh day ($p< 0.01$).

After eight days, the IPR group (p< 0.0001) had fully revived from surgical stress followed by IVR (p< 0.01) and control group (figure 3.2.1 B).

Body weights of the mice were monitored daily. No significant difference was noticed among the three experimental groups during the period of eight days, but it seemed, the groups receiving MSC recovered and gained weight faster than sham-transplanted control (figure 3.2.1 C). In accordance with figure 3.2.1 D survival percentage was highest (93%) in the IPR group, second in IVR (86%) and lowest in the control group (71%) but without any statistical difference.
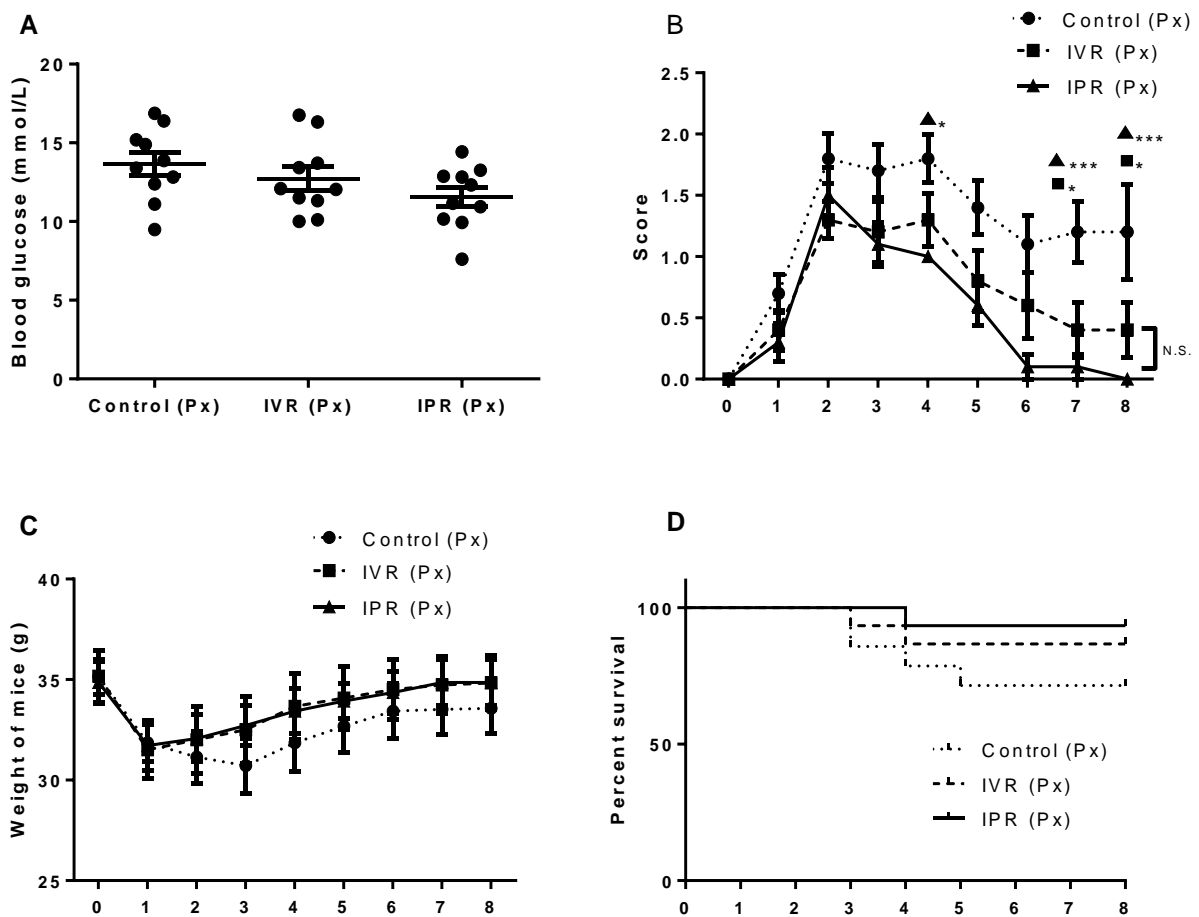
Figure 3.2.1: (A) Represents the blood glucose level eight days after partial pancreatectomy. The IPR-MSC administration showed the lowest mean blood glucose level. (B) Represents health scoring system. (C) Body weight up to eight days. (D) Demonstrates the survival rate in control, intravenous route (IVR) and intrapancreatic route (IPR). Data represent the mean ± SEM, n=10, *p< 0.05, **p< 0.01, ***p< 0.001.

3.2.2 Organ weights after partial pancreatectomy

To examine the potential organ damage as a consequence of partial pancreatectomy; kidney, heart, spleen, lung and pancreas were inspected and weighed. No statistical difference was observed in the weight of the kidney, heart, spleen, lung and pancreas of different groups as shown in figure 3.2.2 A, B, C, D and E.
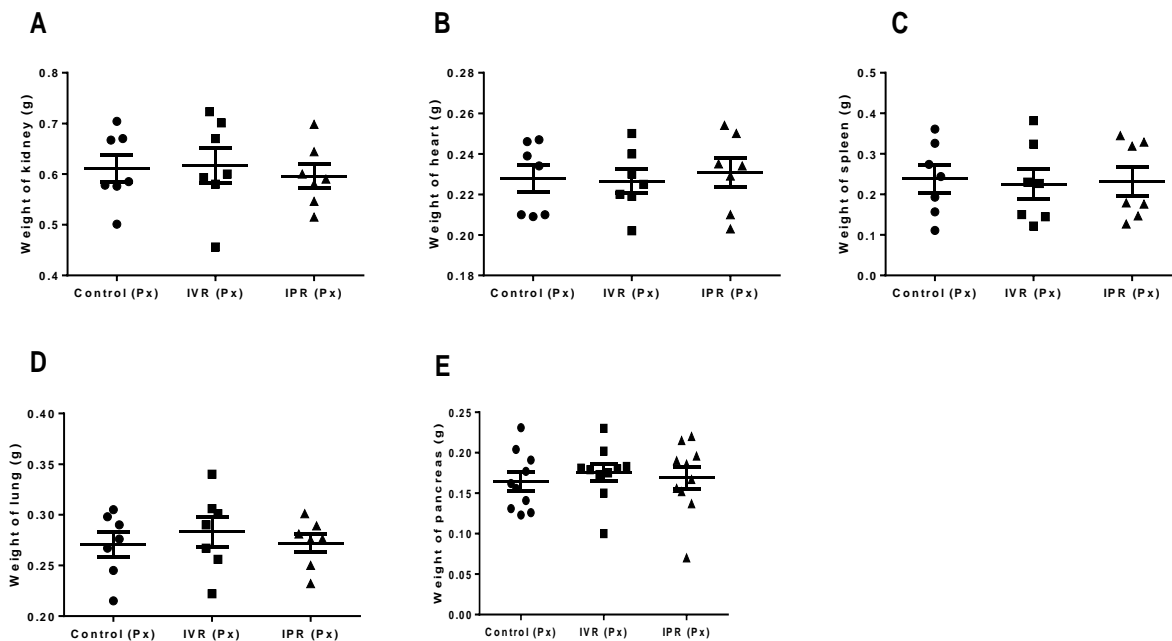
Figure 3.2.2: Weight of different organs after partial pancreatectomy. (A) The weights of individual values of the mouse kidney, (B) heart, (C) spleen, (D) lung and (E) pancreas in different groups were evaluated. Intravenous route (IVR) and intrapancreatic route (IPR). Data represent the mean ± SEM, n=8. *p< 0.05.

3.2.3 Detection of human Alu sequence/ human DNA

After eight days of pancreatectomy, we searched for the retention of injected 0.5×10^6 hTERT-MSC in mouse organs using human Alu sequence. Human Alu sequences were detected in the lungs in four out of eight (4/8) specimen and one pancreas (1/8) within the IVR group. However, human sequences remained undiscovered in the liver, spleen, kidney and heart (figure 3.2.3). In this group, most of the cells were captured in the lungs (filter organ) and only a few reached to the damaged pancreas.

In the IPR group, the human Alu sequence was mainly located in the pancreas (5/8) and remained undiscovered in other organs. As expected, no human Alu sequence was found in the sham-injected control group. A most remarkable observation was the absence of hTERT-MSC in

undamaged tissue (figure 3.2.3). Human DNA was retrieved in the damaged pancreas of five out of eight (5/8) mice in the IPR group whereas in the IVR group only one pancreas was identified to carry human DNA.

	Organ	Control (Px)	IVR (Px)	IPR (Px)
1	Lung	0/8	4/8	0/8
2	Liver	0/8	0/8	0/8
3	Spleen	0/8	0/8	0/8
4	Kidney	0/8	0/8	0/8
5	Heart	0/8	0/8	0/8
6	Pancreas	0/7	1/8	5/8
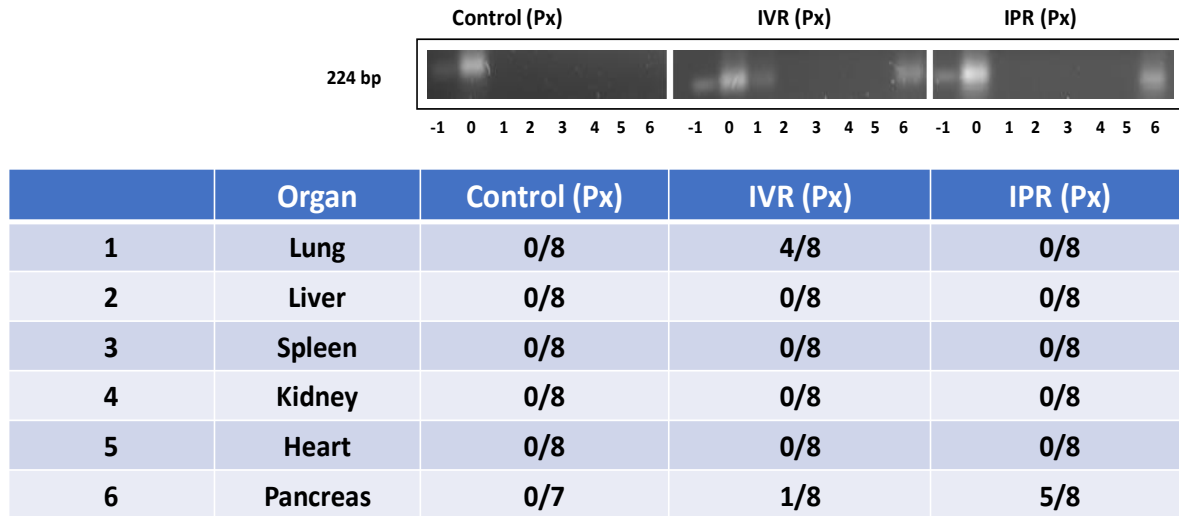
Figure 3.2.3: Localization of hTERT-MSC by the human Alu sequence. 0.5×10^6 hTERT-MSC were transplanted in IVR, IPR and the control group with MEM media post pancreatectomy. After eight days, all mice were sacrificed and investigated for human Alu sequence in different organs. The figure represents the gel showing human Alu sequence in different organs followed by the frequency in different tissues. Ladder (-1), positive control; human DNA (0), lung (1), liver (2), spleen (3), kidney (4), heart (5), pancreas (6). Intravenous route (IVR) and intrapancreatic route (IPR), n=7/8.

3.2.4 Pancreatic β-cell proliferation

In this experiment, proliferating pancreatic β-cells were labelled with bromodeoxyuridine (BrdU) by injecting three times in three consecutive days before the retrieval of the organ. In figure 3.2.4 A, brown spot within the islets represented the BrdU-labelled newly formed β-cell nucleus. The higher number of proliferating pancreatic β-cells (stained in brown) within the islets (stained in blue) in the IPR (9.6 ± 0.85) group were observed as compared to control (5.0 ± 1.16; $p < 0.0044$) and systemic route of transplantation (7.9 ± 0.97; $p < 0.0117$); figure 3.2.4 B. The number of BrdU positive cells was almost double in the IPR group compared to control. We did not find a difference between the IVR and IPR groups (figure 3.2.4 B). An increasing trend in the islet area was also observed from control ($604 \pm 58.57 \ \mu m^2$) to IVR ($711 \pm 68.12 \ \mu m^2$) and IPR ($826 \pm 76.30 \ \mu m^2$) but without any significance, as shown in figure 3.2.4 C. Along with the

BrdU positive cells and islet area, the number of islet per field in a section was also statistically significant in IPR (9.2 ± 0.55) compared to control (5.53 ± 0.71; $p< 0.0034$) and IVR (8.7 ± 0.61; $p< 0.86$); figure 3.2.4 D.

A
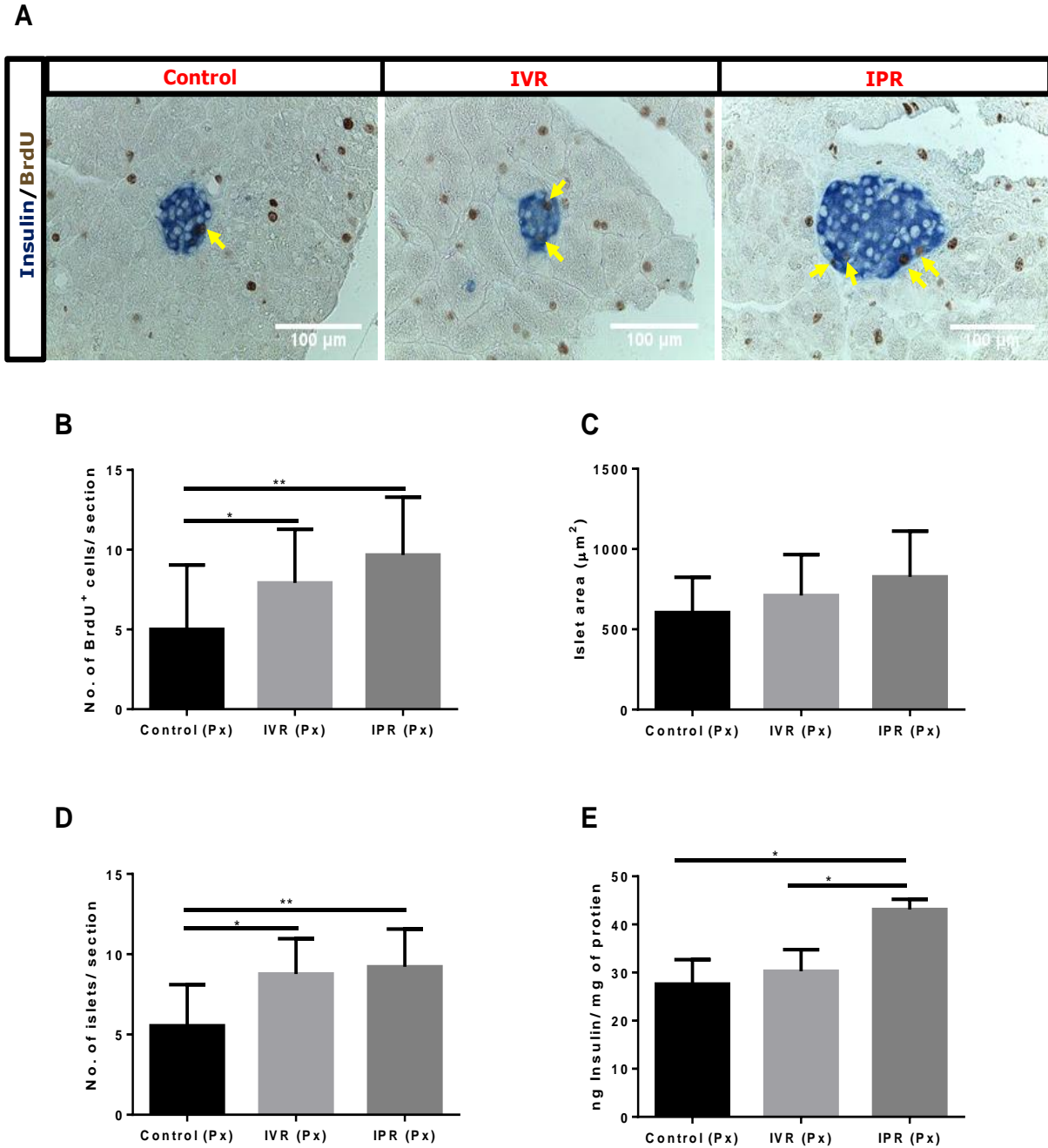
Figure 3.2.4: MSC associated pancreatic β-cell proliferation after pancreatectomy in control, IVR and IPR group. (A) Represents the light microscopic pictures of proliferating pancreatic β-cells within the islets. (B) Demonstrates the total number of BrdU^{+} cells within the islets per section and (C) islet area.

(D) Islets per section. (E) Insulin quantification of pancreatectomized mice with ELISA after eight days. Data represent the mean ± SEM with four sections from each mouse. The four sections were picked with an interval of five sections (5-7 µm thickness each). To avoid bias in counting, an independent evaluation was performed by the blinded examiner (G.H.). Intravenous route (IVR), intrapancreatic route (IPR) and bromodeoxyuridine (BrdU), n=7, *p< 0.05, **p< 0.01.

Further, we measured the total insulin content in the remnant pancreas subsequent to partial pancreatectomy and transplantation of hTERT-MSC. It was significantly increased in the IPR group as opposed to the control group (p< 0.0140) and IVR group (p< 0.023); figure 3.2.4 E. No difference was observed between IPR and IVR group. It was notable that the capacity of insulin-storage and synthesis depended upon the route of administration of hTERT-MSC.

3.2.5 Induction of growth factors and anti-inflammatory effect of MSC

Since BrdU incorporation in β-cells was higher after hTERT-MSC administration, growth factors EGF and IGF-1 were evaluated. A significant difference was noticed between IPR and control (p< 0.002). At the protein level, there was also an increase in IVR compared to control (p< 0.03) as shown in figure 3.2.5 A. Indeed, both results were confirmed at the transcriptional level by RT-PCR. EGF gene expression increased in the IVR group (p< 0.0092) and further escalated in IPR (p< 0.001) as opposed to control. Significantly different variances were observed comparing routes of hTERT-MSC administration (p< 0.0321) as shown in figure 3.2.5 B. Taken together, route-dependent EGF expression was discovered both at protein and mRNA level in the MSC treated groups.

Likewise, IGF-1 also resulted in a higher expression, but independent upon the route of administration. No significant difference was measured between IPR and IVR (p< 0.2), but a higher expression of both systemic (p< 0.023) and local route (p< 0.01) compared to control was found (see figure 3.2.5 B).

Further, differences in the expression of GLUT-2 were detected. GLUT-2 expression was ~3.3-fold higher in IPR compared to control and ~2-fold over IVR. However, no significant variance was observed between IPR and IVR (figure 3.2.5 C). In addition, Ins1 and Ins2 gene expression were also measured in the residual pancreas to confirm the enhanced insulin concentration measured in figure 3.2.4 E. Higher expression of Ins2 gene was observed in IVR (p< 0.004) and

IPR (p< 0.0002) groups as opposed to control. Similarly, a difference was monitored in Ins1 gene expression between the control and IPR group (p< 0.02); figure 3.2.5 C.

After partial pancreatectomy, local cells within the pancreas were reported to produce inflammatory cytokines [178]. Therefore, inflammatory molecules IFN-γ and TNF-α were assessed in the remnant pancreas. hTERT-MSC administration downregulated the gene expression of IFN-γ in the IVR group (p< 0.001) and IPR group (p< 0.001) than control (figure 3.2.5 D). Similarly, TNF-α also showed a reduction in the IVR group (p< 0.0009) and IPR (p< 0.0006) compared to control after hTERT-MSC administration (figure 3.2.5 D). However, no variance was observed between the IPR and IVR group.
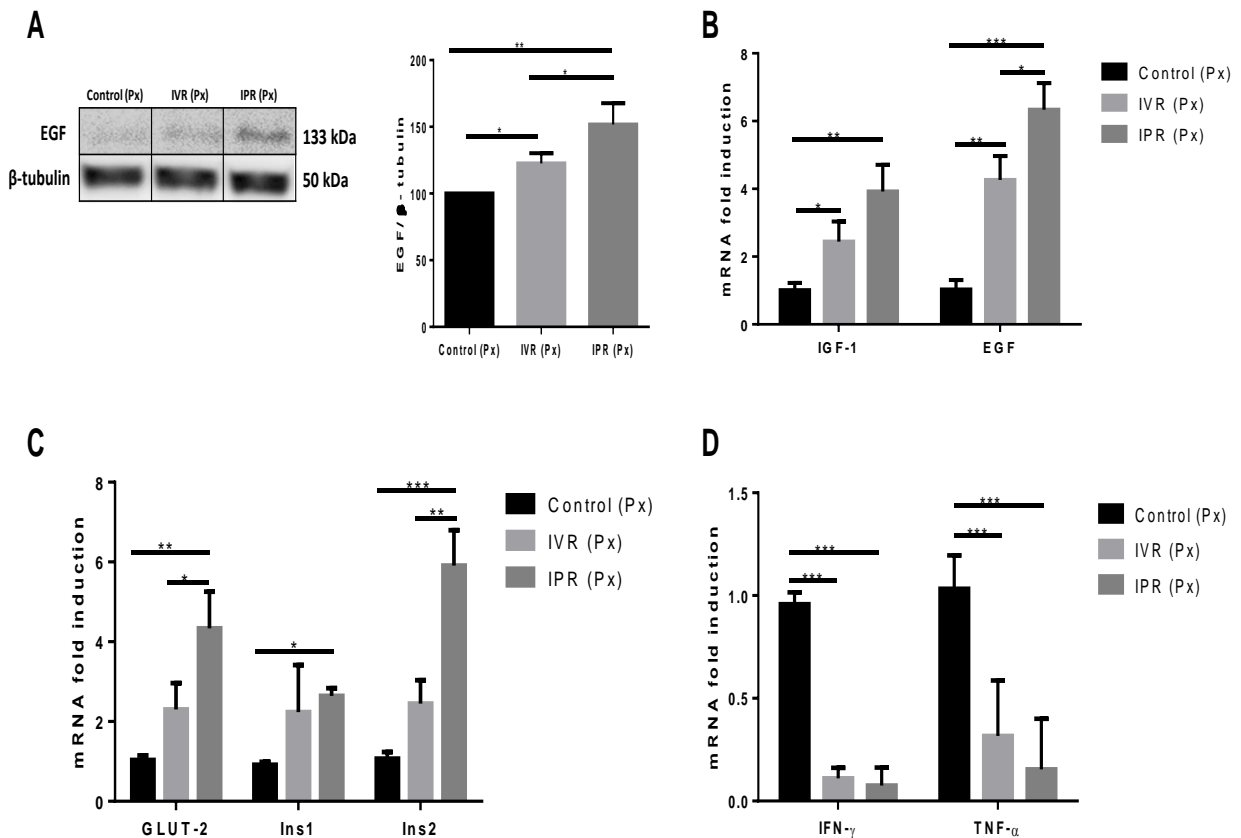
Figure 3.2.5: Increase of growth and reduction of inflammatory factors eight days after administration of hTERT-MSC in the pancreas of partially pancreatectomized mice. Panel (A) represents the EGF expression at the protein level by Western blot. (B) Gene expression of EGF and IGF-1 at mRNA level by RT-PCR. (C) Change in GLUT-2, Ins1 and Ins2 gene expression. (D) Demonstrates immunomodulatory properties

of hTERT-MSC reducing IFN-γ and TNF-α murine mRNA levels. Intravenous route (IVR), intrapancreatic route (IPR), epidermal growth factor (EGF), insulin-like growth factor-1 (IGF-1), glucose transporter 2 (GLUT-2), preproinsulin 1 (Ins1) and preproinsulin 2 (Ins2). Data represent the mean ± SEM. n=4, *$p<$ 0.05, **$p<$ 0.01, ***$p<$ 0.001, comparisons done with the control.

3.2.6 MSC infusion-initiated expression of pancreatic progenitor markers

To investigate the activation of PI3K/ AKT/ FOXA2/ PDX1 signaling cascade post hTERT-MSC administration, Western blot was performed to check the phosphorylation of AKT protein (P-AKT). A significant increase of P-AKT expression was noticed at the protein level between IPR and control ($p<$ 0.03). At the transcription level, AKT gene was found increased as well in the IPR versus IVR ($p<$ 0.01) and control ($p<$ 0.001) as shown in figure 3.2.6 A. Moreover, PI3K transcription which acts as an upstream modulator of P-AKT was also activated after hTERT-MSC administration. Similar results were obtained when the IPR group was compared with IVR ($p<$ 0.01) and control ($p<$ 0.001).
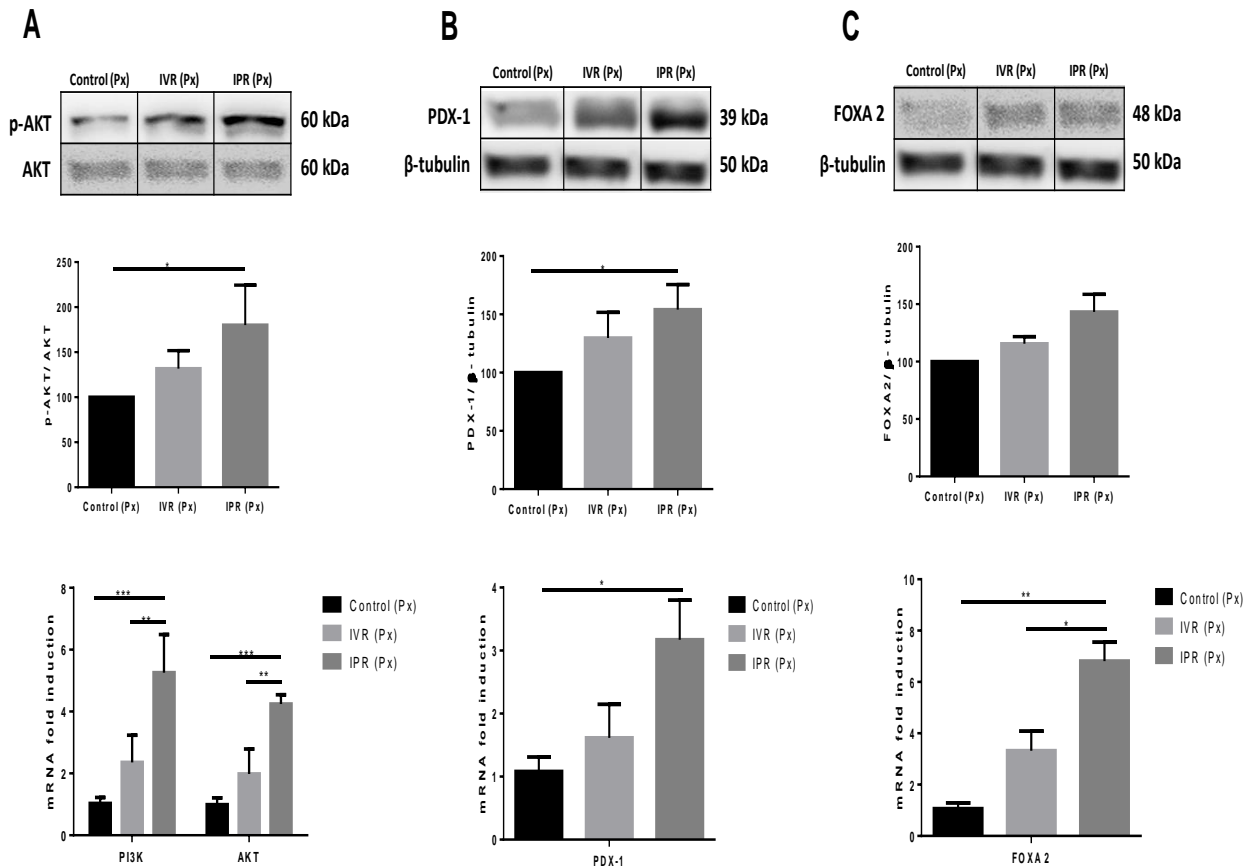
Figure 3.2.6: hTERT-MSC activated murine endocrine pancreatic progenitor markers FOXA2 and PDX-1 through phosphorylation of AKT (P-AKT) post hTERT-MSC administration in partially pancreatectomized mice. (A) Demonstrates the phosphorylation of AKT band at the protein level with Western blot (upper and middle row) followed by mRNA expression of PI3K and AKT gene (lower row). (B) Pancreatic and duodenal homeobox 1 expression at protein and transcription level. (C) Expression of FOXA2 protein remained insignificant at the protein level but showed significance at the transcription level. Intravenous route (IVR), intrapancreatic route (IPR), PI3K (Phosphatidylinositol-4, 5-bisphosphate 3-kinase), AKT (Protein kinase B), Forkhead box A2 (FOXA2*)*, pancreatic and duodenal homeobox 1 (PDX-1). The data represent the mean ± SEM. n=4, *p< 0.05, **p< 0.01, ***p< 0.001, comparisons done with the control.

PDX-1 induction in the pancreas is known to reflect pancreatic β-cell regeneration. Therefore, PDX-1 was measured and a statistical difference was observed at the protein level (p< 0.02) with Western blot and at mRNA level (p< 0.017) compared to control after hTERT-MSC transplanted locally in the pancreas as shown in the figure 3.2.6 B. No variance was monitored between the IVR and the control group.

Similarly, post hTERT-MSC administration in partially pancreatectomized mice, when pancreatic β-cell proliferation was supposed to be maximal, insignificant variance was observed in FOXA2 at protein level between the groups but ~2-fold higher gene expression was measured in the IVR (p< 0.04) and ~6 fold (p< 0.009) in IPR than control with real-time PCR as shown in figure 3.2.6 C.

3.2.7 FoxO1 expression downregulated by MSC

The transcription factor, FoxO1 has the potential to activate progenitor markers and regulate pancreatic β-cell proliferation. In proliferative and regenerative microenvironment of partial pancreatectomy, FoxO1 protein was significantly reduced in the IPR group (p< 0.01) in the Western blot samples as shown in figure 3.2.7 A. Similarly, downregulation of FoxO1 gene expression was monitored in the IPR (p< 0.0024) and IVR group (p< 0.0283) compared to control (figure 3.2.7 B). To further validate its expression, islets were stained with FoxO1 antibody. A moderate downregulating pattern of FoxO1 (only within the islets) was observed in the IVR which further reduced in IPR group (figure 3.2.7 C).
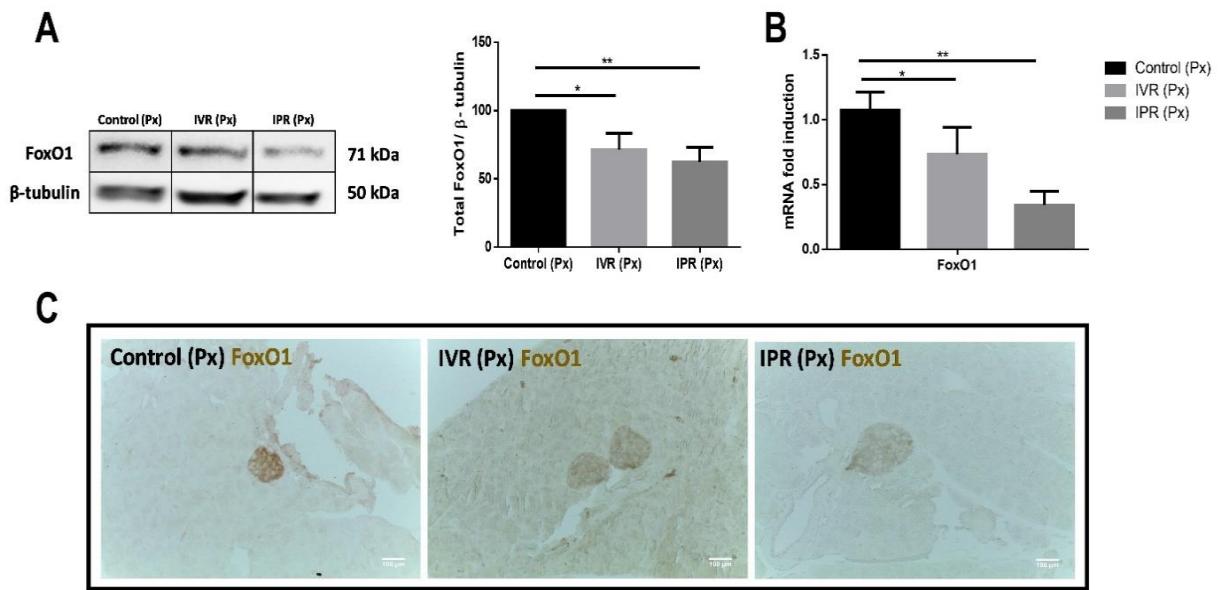
Figure 3.2.7: Downregulation of FoxO1 expression post-hTERT-MSC administration. (A) At the end of the experiment, MSC route dependent reduction in FoxO1 protein was observed after partial pancreatectomy. (B) Real-time PCR revealed the downregulation of FoxO1 at the mRNA level. (C) Immunohistochemistry was performed to stain FoxO1 within the islets of all the groups. Intravenous route (IVR), intrapancreatic route (IPR), Forkhead box 1 (FoxO1). The data represent the mean ± SEM, n=4, *p< 0.05, **p< 0.01, ***p< 0.001, comparisons done with the control.

3.3 Antidiabetic effect of MSC

3.3.1 Comparison of IVR and IPR in the diabetic mouse model

In the diabetic experiment, IPR and IVR routes of ADMSC effects were compared in terms of blood glucose level, body weight, health scoring system and survival rate in mice administered three low doses of STZ. Prior to administration of STZ, the mean non-fasting blood glucose concentration was 8.7 ± 1.8 mmol/ L. Five days after first STZ injection, blood glucose climbed to 11.5 ± 2.3 mmol/ L and further to 19.5 ± 5.3 mmol/ L on day ten. However, injection of MSC on day seven via IPR resulted in significantly lower mean blood glucose level on day ten (11.5 ± 4.1 mmol/ L) when compared with IVR (18.4 ± 5.4 mmol/ L, p< 0.003) and STZ only (19.5 ± 4.3 mmol/ L, p< 0.0162) (figure 3.3.1 A). This effect persisted until the end of the experiment (30 days) with respective blood glucose concentration in the IPR (12 ± 4.4 mmol/ L) showing a

significant difference to IVR (18.8 ± 8.1 mmol/ L; p< 0.0373), STZ alone (21.4 ± 8.2 mmol/ L, p< 0.0238) and to non-diabetic control (6.6 ± 1.3 mmol/ L, p< 0.0426) as depicted in figure 3.3.1 A.
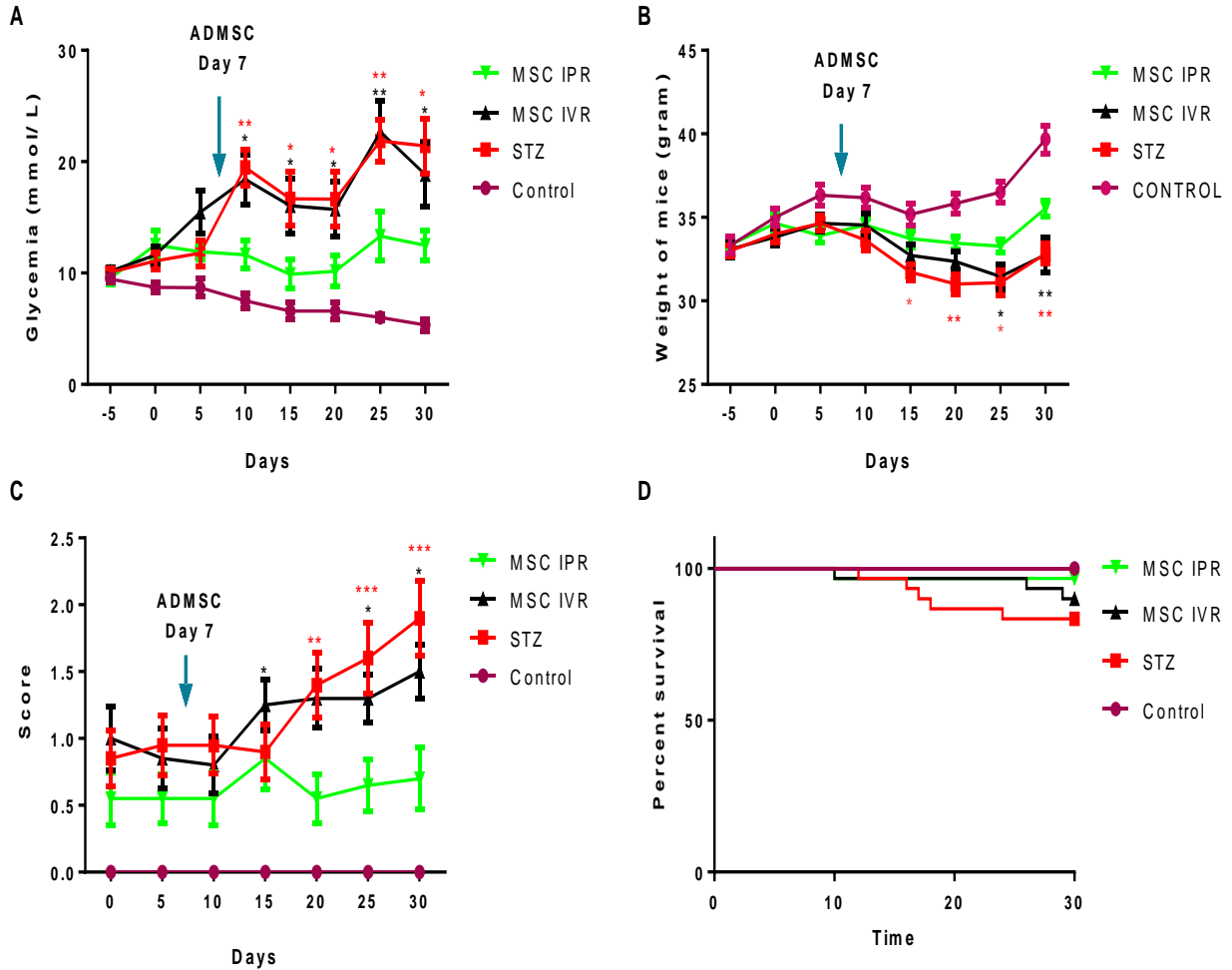
Figure 3.3.1: A beneficial effect of ADMSC in STZ-induced diabetic mice. Panel (A) represents the mean blood glucose concentrations subsequent to ADMSC administration on day seven up to day 30. (B) Change in body weight of diabetic mice. (C) Health scores and (D) survival rates in control, STZ, IVR and IPR groups after 30 days of ADMSC administration. Intravenous route (IVR) and intrapancreatic route (IPR), streptozotocin (STZ) only, control=No STZ and no MSC administration. The data represent the mean ± SEM, n=11, *p< 0.05, **p< 0.01, ***p< 0.001.

Similarly, mean body weight on day minus five was 33.7 ± 1.2 g, which changed on day 15 in IPR (33.7 ± 1.6 g), IVR (32 ± 2.1 g), STZ (31 ± 1.6 g) and non-diabetic control group (35 ± 1.7 g). At the end of the experiment (day 30), a significant difference of IPR (35 ± 1.57 g) compared with

IVR (32.75 ± 2.91 g, $p < 0.005$), STZ (32.8 ± 1.99 g, $p < 0.0024$) and control (39 ± 2.06 g, $p < 0.001$) was observed (figure 3.3.1 B). Indeed, the health scoring system (refer table 2) also reflected the same trend as body weight. Day 15 onwards, IPR started reviving from diabetic stress and at the end of the experiment significant difference versus IVR ($p < 0.014$) and STZ ($p < 0.001$) was monitored (figure 3.3.1 C). After 30 days of the experiment, the survival rate was highest in non-diabetic control (100%), followed by diabetic mice treated with MSC through IPR (96.6%), IVR (90%) or STZ-alone (83.3%) but without any statistical difference (figure 3.3.1 D).

3.3.2 Effect of diabetes on different organs

For safety of the procedure and to cover potential systemic effects of STZ and MSC, weights of several lung, spleen, kidney and heart were measured at the end of the experiment. No statistical difference was observed (figure 3.3.2 A, B, C and D). Interestingly, within the span of 30 days, pancreatic weight varied depending on the treatment with or without MSC. Mean pancreas weight in IPR (204 ± 3.92 mg) was increased as opposed to IVR (183 ± 4.76 mg, $p < 0.047$) and STZ-only group (163 ± 5.18 mg, $p < 0.0012$), respectively, but not compared with the non-diabetic control group (215 ± 7.37 mg, $p < 0.50$) as shown in figure 3.3.2 E.
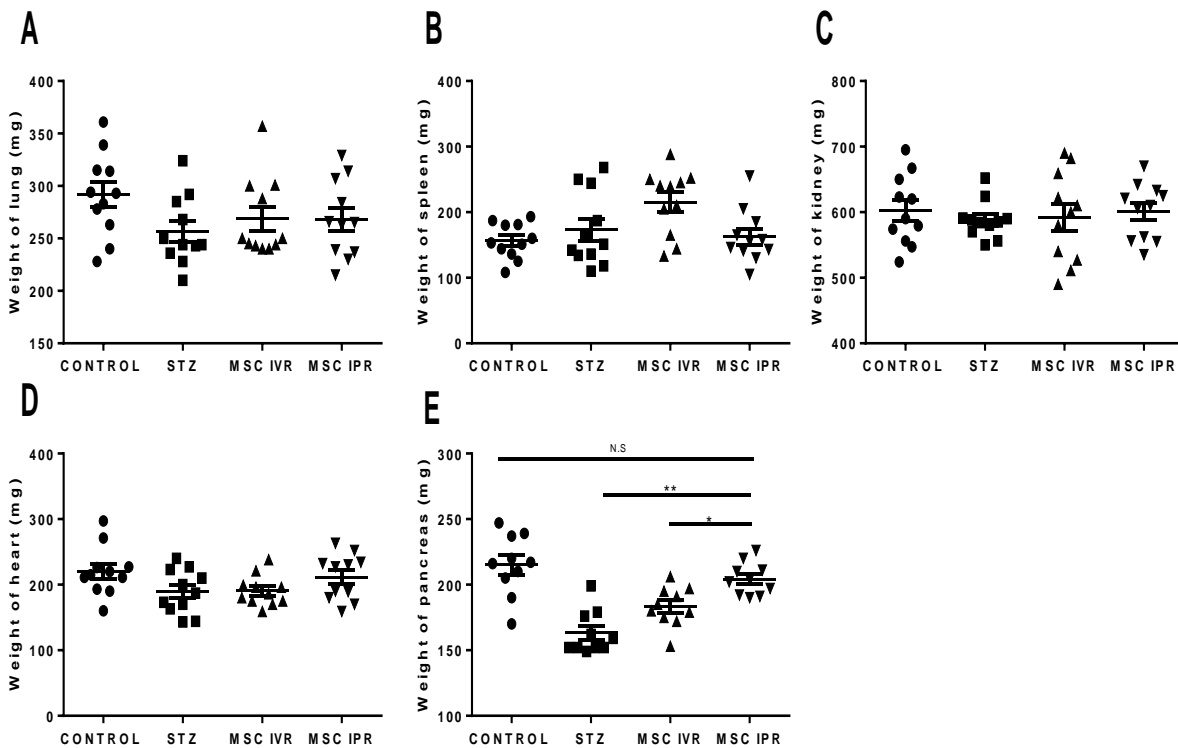
Figure 3.3.2: Weight of organs after ADMSC administration through IPR and IVR in STZ-induced diabetic mice: (A) Weight of individual value of the mouse lung, (B) spleen, (C) kidney, (D) heart and (E) pancreas in different groups were evaluated. Intravenous route (IVR), intrapancreatic route (IPR) and streptozotocin (STZ), not significant (N.S). Data represent the mean ± SEM, n=11. *p< 0.05, **p< 0.01.

3.3.3 Distribution and engraftment of ADMSC after IVR and IPR injection

After 30 days of 0.5×10^6 ADMSC infusion in diabetic mice, the human Alu sequence was screened in lung, liver, spleen, kidney, heart and pancreas. In the IVR group, human DNA was detected in one out of ten lungs, a kidney and a pancreas (Figure 3.3.3). In the IPR group, the human Alu sequence was observed in two pancreases and remained undetected in the other organs. No human Alu sequence was detected in the untreated groups (non-diabetic control and STZ).

	Organ	Control	MSC IVR	MSC IPR
1	Liver	0/5	0/10	0/10
2	Lung	0/5	1/10	0/10
3	Spleen	0/5	0/10	0/10
4	Kidney	0/5	1/10	0/10
5	Heart	0/5	0/10	0/10
6	Pancreas	0/5	1/10	2/10
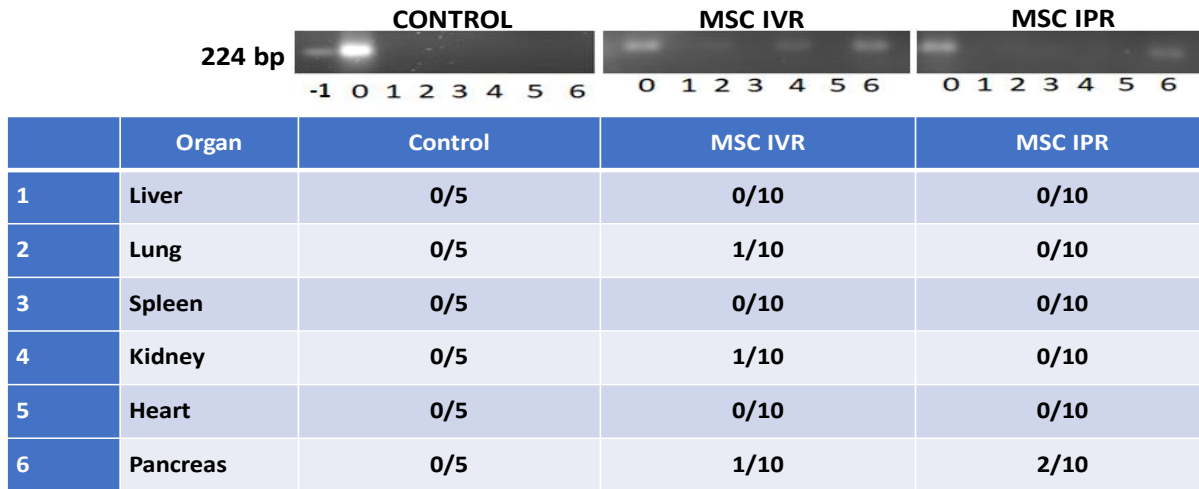
Figure 3.3.3: Detection of human DNA in diabetic pancreas after 30 days of ADMSC administration. 0.5×10^6 ADMSC were injected in IPR, IVR and investigated for human Alu sequence in several organs. In control and STZ, no MSC were administered and none of the human Alu sequences was detected. In IVR, Alu sequence was observed in lung, kidney and pancreas, whereas in IPR detected only in the pancreas. Ladder (-1), positive control; human DNA (0), liver (1), lung (2), spleen (3), kidney (4), heart (5) and pancreas (6). Intravenous route (IVR) and intrapancreatic route (IPR), streptozotocin (STZ), n= 5 or 10.

3.3.4 Proliferative effect of ADMSC on endogenous β-cells

We investigated the endogenous β-cell proliferation with BrdU after ADMSC administration. BrdU was injected three times before the retrieval of the organ in three consecutive days and the number of proliferating β-cells (brown spot) within the islets (blue color) was investigated in non-diabetic control, STZ, IVR and IPR as shown in figure 3.3.4 A.
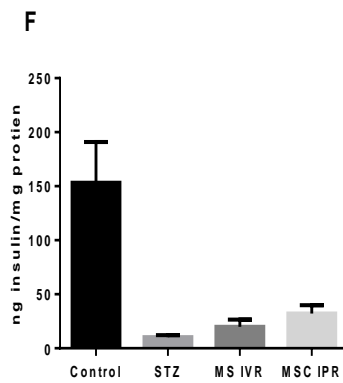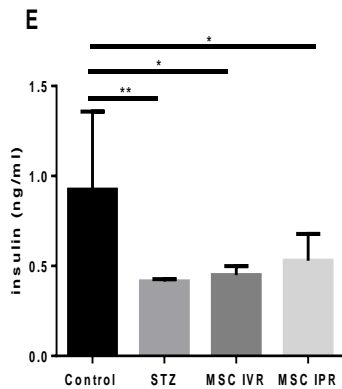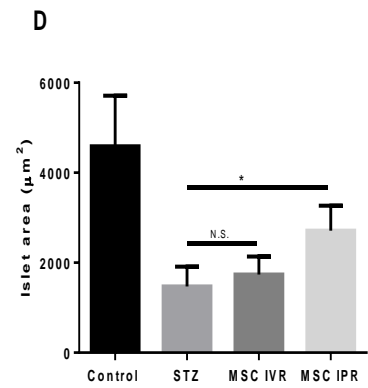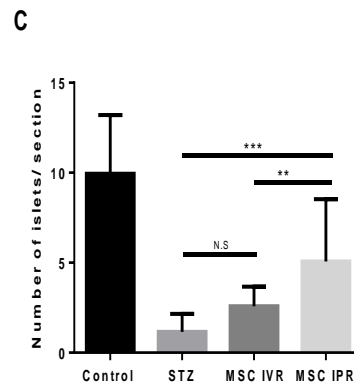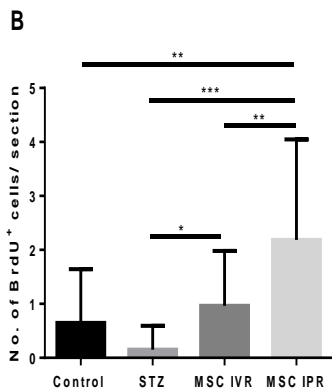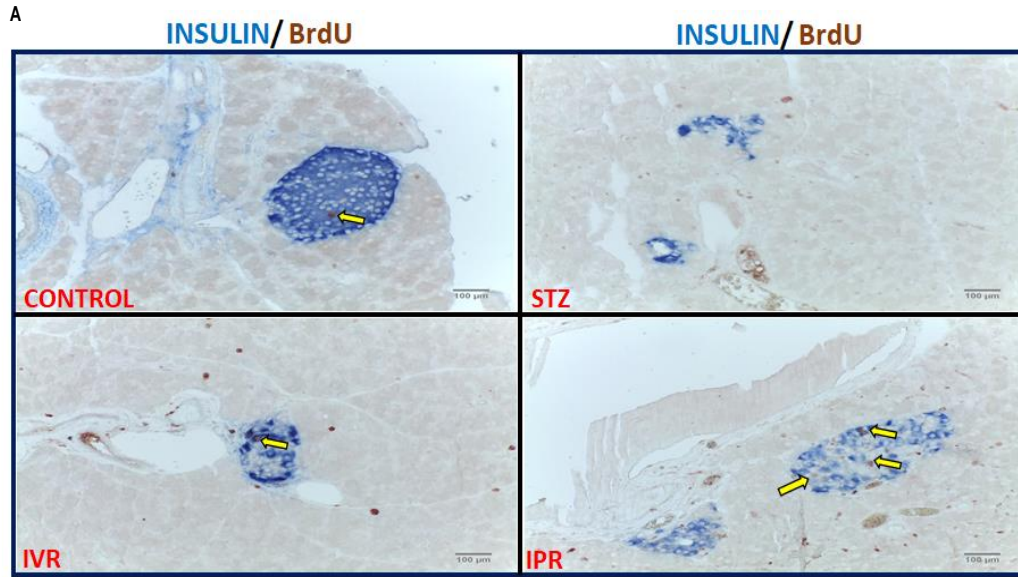
Figure 3.3.4: Proliferative effect of ADMSC administration on pancreatic β-cells after 30 days of diabetes induced by subsequent three low doses of STZ in diabetic mice. (A) Light microscopic pictures of

proliferating pancreatic β-cells within the islets of control, STZ, IVR and IPR. (B) Number of BrdU positive cells was calculated as described in the M&M section with insulin and BrdU immunostaining. Panel (C) demonstrates the number of islets per section, (D) islets area, (E) and (F) insulin content in the blood and pancreas, respectively. Insulin concentrations were determined by mouse ELISA. Intravenous route (IVR), intrapancreatic route (IPR), streptozotocin (STZ), bromodeoxyuridine (BrdU) and not significant (N.S). The data represent the mean ± SEM of four sections from each mouse. All the four sections were picked with an interval of five sections (each section 5-7 µm in thickness). To avoid bias in the counting, an independent evaluation was performed with blinded investigator (G.H.), n= 6 *p< 0.05, **p< 0.01, ***p< 0.001.

Interestingly, BrdU positive cellular nuclei initiating cell division by chromatin remodelling were also observed in the control. However, the number of BrdU positive β-cells were superior in the IPR (2.18 ± 1.86) compared with IVR (0.96 ± 1.01, p< 0.01), STZ (0.15 ± 0.44, p< 0.001) and control (0.647 ± 0.99, p< 0.01) as shown in figure 3.3.4 B. Proliferating β-cells might give rise to newly formed islets. Therefore, the number of islets per section was also calculated. Significant difference was monitored between IPR (5.07 ± 3.4), IVR (2.5 ± 1.08, p< 0.007) and STZ (1.15 ± 1.03, p< 0.001); figure 3.3.4 C.

Route-dependent islet area was also monitored in IPR (2710.5 ± 184.9 µm^2), IVR (1737.5 ± 132.5 µm^2), STZ (1471.8 ± 146.5 µm^2) and non-diabetic control (4586.6 ± 375.2 µm^2) as shown in figure 3.3.4 D. Further, the insulin concentration of blood and pancreas was investigated after 30 days of ADMSC administration in all four groups. With this parameter, we did not find a statistical difference between IPR and IVR (figure 3.3.4 E and 3.3.4 F).

3.3.5 Effect of ADMSC through growth factors and immune modulation.

Mesenchymal stem cells can secrete a wide range of trophic factors or growth factors *in-vivo* and *in-vitro* to protect damaged tissue [179]. In this study murine growth factor, EGF significantly increased after local transplantation (IPR) as compared to IVR (p< 0.0019), STZ (p< 0.023) and non-diabetic control (p< 0.042) as shown in figure 3.3.5 A. We did not find any significant difference in Ins1, Ins2 and IGF-1 gene expressions (figure 3.3.5 A).

MSC are also known for immunomodulatory properties [180]. Hence, pro-inflammatory and anti-inflammatory molecules were investigated in the pancreas. Among different assessed molecules, pro-inflammatory molecules (IL-1β and TNF-α) were downregulated in the IPR group

compared to STZ (IL-1β; p< 0.020 and TNF-α; p< 0.036) and anti-inflammatory molecule such as IL-10 upregulated in the IPR versus control (p< 0.019) as shown in figure 3.3.5 B. Further, the gene expression ratio of BAX (apoptotic) versus BCL-2 (anti-apoptotic) was also increased in locally administrated MSC compared to STZ-only (p< 0.013); figure 3.3.5 C.

To elucidate the role of different signaling pathways, pancreatic gene expression of DLK1, ERK and FoxO1 were investigated in ADMSC treated mice with RT-PCR. Interestingly, the DLK1 gene was activated and significantly increased in the IPR compared to IVR (p< 0.001), STZ (p< 0.001) and non-diabetic control (p< 0.001). Likewise, locally administered ADMSC also upregulated ERK expression in the IPR group compared to control (p< 0.041). Further FoxO1 was investigated and downregulation was noticed in the ADMSC treated group with a significant difference between IPR and the untreated control group (p< 0.034) as shown in figure 3.3.5 D.
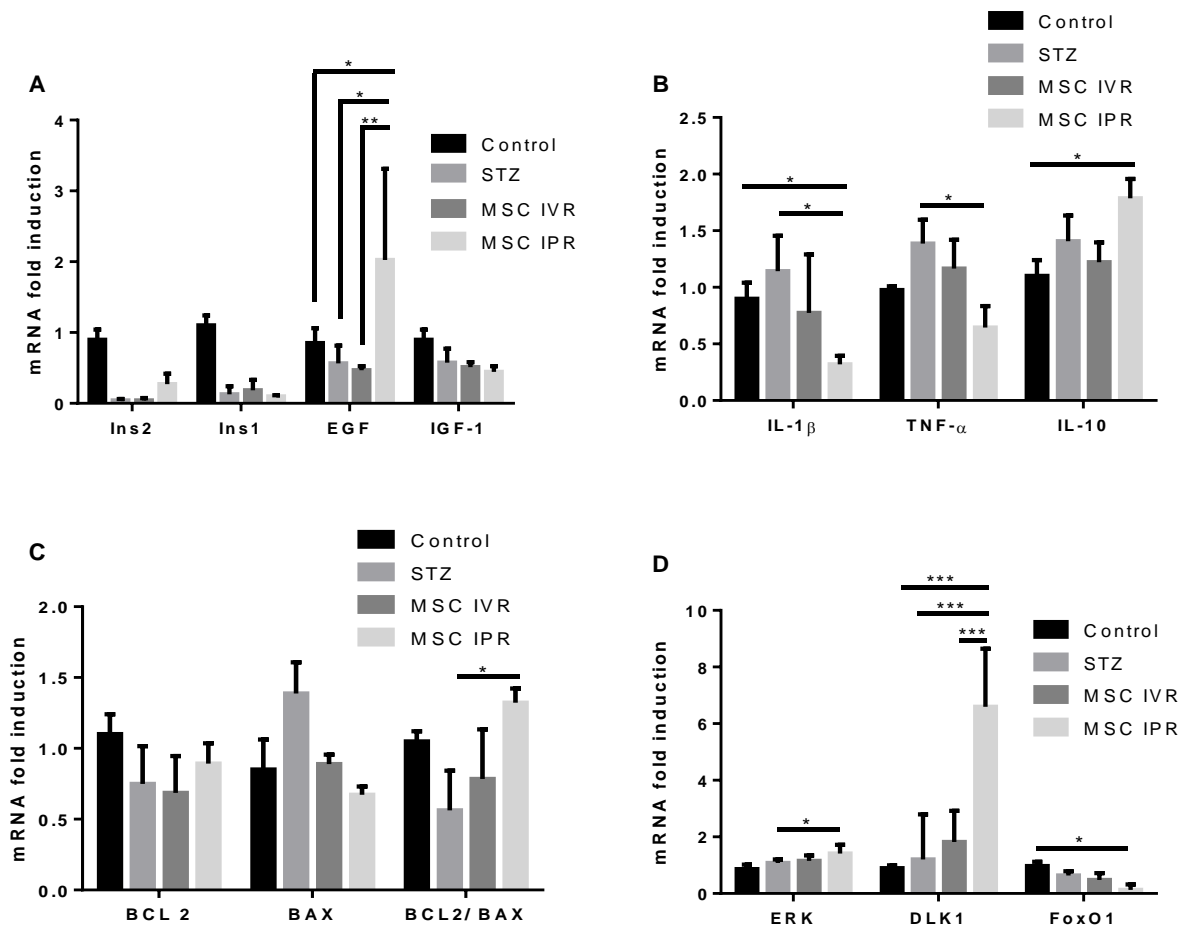
Figure 3.3.5: Effect of ADMSC on murine pancreatic growth factors, immunomodulatory molecules and DLK1/ ERK/ FoxO1signaling pathway. (A) Endogenous growth factors (EGF and IGF-1) were secreted by the pancreas after ADMSC administration. (B) ADMSC restored Th1/ Th2 balance in diabetic mice by downregulating IL-1β, TNF-α and upregulating IL-10. (C) MSC decreased apoptosis via anti-apoptotic (BCL-2) and BAX (apoptotic) molecules. (D) Activation of DLK1/ ERK/ FoxO1 pathway post-ADMSC administration. Intravenous route (IVR), intrapancreatic route (IPR), epidermal growth factor (EGF), insulin-like growth factor-1 (IGF-1), preproinsulin 1 (Ins1), preproinsulin 2 (Ins2), interleukin 1 beta (IL-1β), tumor necrosis factor alpha (TNF-α), interleukin-10 (IL-10), BCL-2-associated X protein (BAX), B-cell lymphoma 2 (BCL-2), extracellular signal-regulated kinases (ERK), Delta like non canonical notch ligand 1 (DLK1), Forkhead box 1 (FoxO1). The data represent the mean ± SEM, n=3 or 4. *p< 0.05, **p< 0.01, ***p< 0.001.

3.3.6 Direct and indirect co-culture system of MSC with MIN6 cells

MSC's preventive impact on pancreatic β-cell damage was investigated in STZ-injured MIN6 cells through direct co-culture (DC; physical contact between MSC and MIN6) and indirect co-culture system (IDC; MSC and MIN6 were separated by a semipermeable membrane). In indirect co-culture system, hTERT-MSC enhanced the viability of the MIN6 cells in the presence of low STZ concentrations (0.5 mM; p< 0.032 and 1 mM; p< 0.01) but failed to maintain a similar response at high STZ concentration (2 mM); p< 0.578 (figure 3.3.6 A). On the other hand, direct co-culture system increased the viability of MIN6 cells at 0.5 mM (p< 0.01), 1 mM (p< 0.001) and even at 2 mM STZ concentration (p< 0.001) as shown in figure 3.3.6 B.

In figure 3.2.3 and 3.3.3, analysis of the human Alu sequence was highly specific but poorly sensitive for human MSC migration into the damaged murine pancreas. Therefore, the migration of MSC towards STZ-injured MIN6 cells was investigated with an indirect culture system. Significant migration of hTERT-MSC was observed even at a low dose of STZ (0.5 mM; p< 0.01) compared to MIN6 cells cultured in the absence of STZ. Migration further increased at 1 mM (p< 0.001) but not at 2 mM (p< 0.039) STZ; figure 3.3.6 C. In order to determine the mechanisms of MSC chemotaxis, factors known to facilitate migration were assessed. Among them, murine SDF-1 gene expression was enhanced under both DC (p< 0.041) and IDC (p< 0.026) conditions in MIN6 cells. On the other hand, human CXCR4 gene was increased in hTERT-MSC under DC (p< 0.001) and IDC (p< 0.001) condition compared to control at 1 mM concentration of STZ (figure 3.3.6 D).
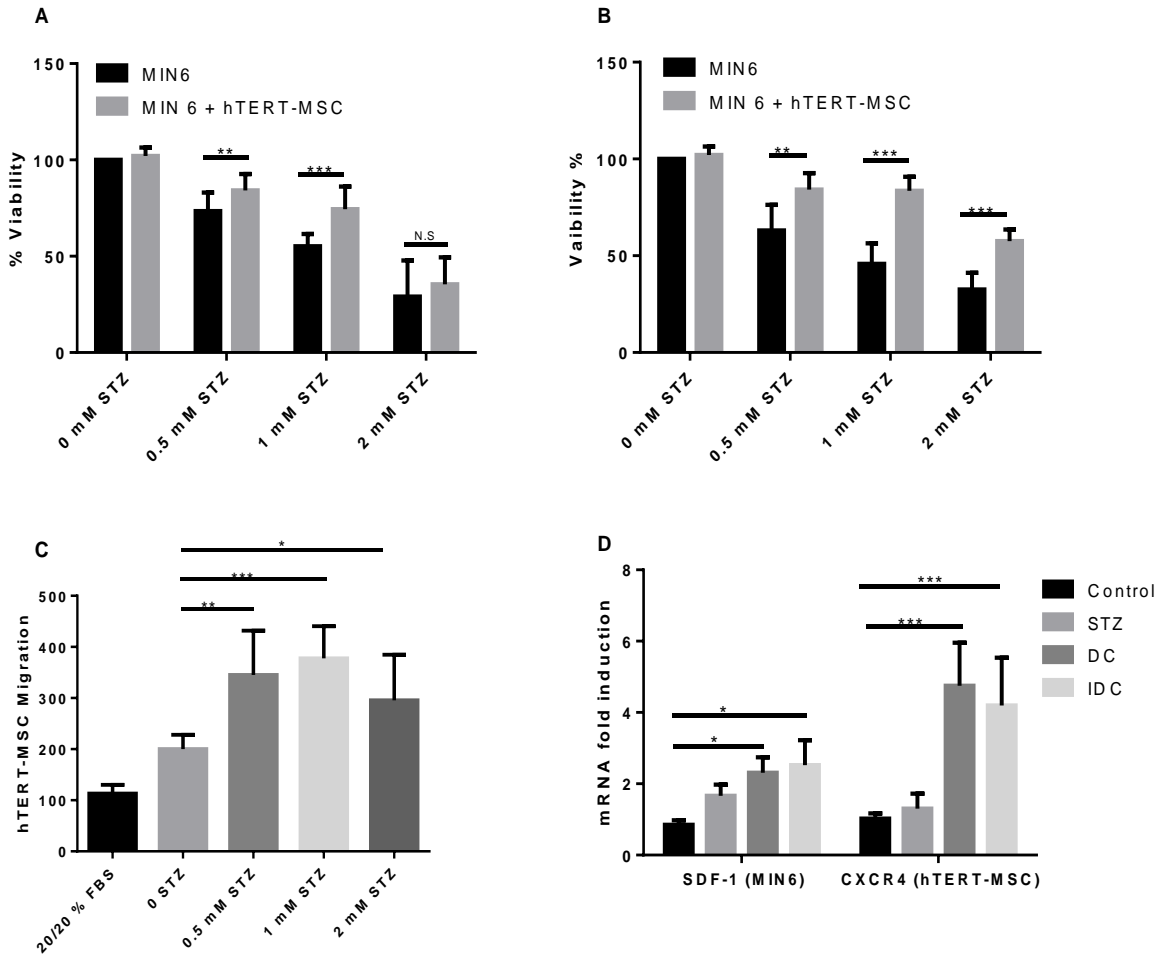
Figure 3.3.6: MSC preserved MIN6 viability and migration towards STZ-injured MIN6 cells. (A) In indirect co-culture system (IDC), hTERT-MSC enhanced viability of damaged MIN6 at increasing concentrations of STZ (0.5 mM, 1 mM). Panel (B) demonstrates the augmented viability of STZ-injured MIN6 cells in direct co-culture (DC). The viability of MIN6 in the absence and presence hTERT-MSC determined by MTT assay and given as the percentage of controls without STZ. (C) hTERT-MSC migrated to STZ-injured MIN6 cells in IDC. To correct for unspecific background mobility or base level migration of hTERT-MSC toward MIN6 cells, 20% fetal calf serum was filled in the lower well and in the insert of the transwell. (D) SDF-1 gene expression was monitored in MIN6 cells and CXCR4 in hTERT-MSC at DC and IDC with RT-PCR. The data represent the mean ± SEM, n=3 or 4. *p< 0.05, **p< 0.01, ***p< 0.001.

3.3.7 hTERT-MSC enhanced murine AKT and ERK pathway

In figure 3.2.4, hTERT-MSC administration to pancreatectomized mice enhanced the insulin content of the residual pancreas. Therefore, several immunomodulatory molecules such as TIMP-1, IDO1, HFG, EGF, b-FGF and VEGF were investigated in hTERT-MSC challenged by STZ-

injured MIN6 cells. Among them, TIMP-1 was upregulated in IDC (p< 0.068) and significantly increased in DC (p< 0.049) compared to control. In fact, IDO1 followed the same pattern. VEGF was also significantly increased in the hTERT-MSC when cultured in direct contact (p< 0.01) and indirect contact (p< 0.035) with STZ-injured MIN6 cells as shown in figure 3.3.7 A. The results suggest that hTERT-MSC reacted to putative soluble messenger molecules from damaged cells in their vicinity and restored the Ins1 and Ins2 gene expression in MIN6 cells (figure 3.3.7 B).
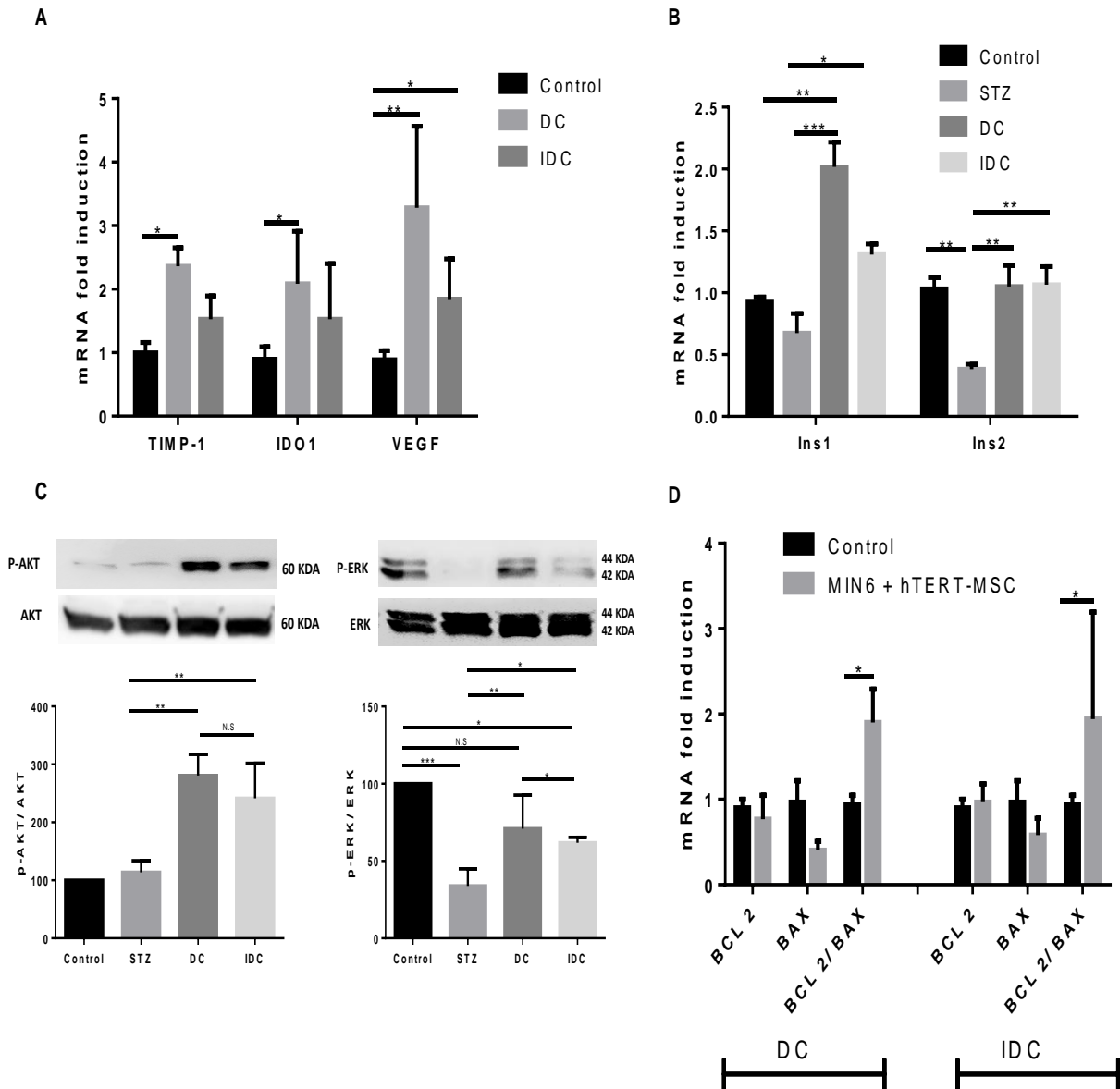
Figure 3.3.7: MSC protected STZ-injured MIN6 cells through the activation of the AKT/ ERK signaling pathway. (A) MSC produced VEGF and other immunomodulatory molecules (IDO1 and TIMP-1) after

interacting with STZ-injured MIN6 cells. (B) MSC restored and maintained the Ins1 and Ins2 gene expression in MIN6 cells after STZ destruction. (C) MSC activated the phosphorylation of AKT and ERK protein in STZ-injured MIN6 cells as demonstrated by Western blot. (D) AKT/ ERK activated the BCL-2 and BAX signaling pathway to protect STZ-injured MIN6 cells in both DC and IDC. TIMP metallopeptidase inhibitor 1 (TIMP-1), indoleamine 2,3-dioxygenase 1 (IDO1), vascular endothelial growth factor (VEGF), preproinsulin 1 (Ins1), preproinsulin 2 (Ins2), AKT (Protein kinase B), extracellular signal-regulated kinases (ERK), BCL-2-associated X protein, (BAX), B-cell lymphoma 2 (BCL-2). The data represent the mean ± SEM, n=3 or 4. *p< 0.05, **p< 0.01, ***p< 0.001.

Further, AKT and ERK signaling pathways were investigated by the Western blot. In the presence of 1 mM STZ, reduction of P-AKT and P-ERK proteins was observed which was subsequently restored by the addition of hTERT-MSC in both DC and IDC as shown in figure 3.3.7 C. In AKT signaling pathway, a significant difference was observed between DC (p< 0.0023) and IDC (p< 0.0064) compared to STZ alone. However, both IDC and DC activated the phosphorylation of AKT in STZ-injured MIN6 cells. Similarly, the ERK pathway showed more phosphorylation in the case of DC (p< 0.01) than IDC (p< 0.0258) when compared with STZ (figure 3.3.7 C). Activated phosphorylated forms of ERK and AKT could reduce MIN6 mitochondrial-dependent apoptosis through BCL-2 and BAX. Therefore, the ratio of BCL-2 versus BAX was investigated. In both DC (p< 0.0389) and IDC (p< 0.0428), BCL-2 versus BAX ratio was higher compared to control as shown in figure 3.3.7 D.

4. DISCUSSION AND CONCLUSION

4.1 Discussion

MSC based type 1 diabetic therapy has been considered as an alternative treatment and already displayed a beneficial effect on hyperglycemia in animal models [176, 181]. Hess et al. demonstrated, systemically administered MSC reversed hyperinsulinemia and hyperglycemia in STZ-induced diabetic mice and migrated to the damaged tissue [177]. The intravenous or intra-arterial route of transplantation was preferred in preclinical and clinical studies [152-154]. However, the therapeutic effectiveness of MSC depends upon its route of administration [150]. Systemic route of transplantation misguided MSC to lung barrier, resulting in microvasculature entrapment and reduced overall potential. Therefore, we have investigated more closely the administration of human MSC by the systemic route (MSC injected into the murine tail vein) and local route (directly transferred to pancreatic tissue or intrapancreatic injection) in NMRI nude mice. First, this model was studied for safety efficacy of MSC derived from two distinct sources; bone marrow-derived hTERT-MSC cell line and primary adipose derived MSC from a diabetic patient. Second, the regeneration potential of pancreatic β-cells after MSC administration in partial pancreatectomized mice was investigated. Third, the antidiabetic effect and sustainability of administered MSC were examined in STZ-induced diabetic mice through the intravenous route (IVR) and intrapancreatic route (IPR).

4.1.1 Safety efficacy of characterized MSC

hTERT-MSC and ADMSC were first confirmed to have plastic adherence property and fibroblast-like structure. In conformity with the International Society for Cellular Therapy (ISCT) [173], MSC from both sources were confirmed for their cellular membrane-bound markers such as $CD90^+$, $CD44^+$, $CD105^+$, $CD73^+$ and negative for hematopoietic lineage. hTERT-MSC showed a stable cell surface marker profiling with subsequent passages, but ADMSC displayed spontaneous multipotency after several passages. However, after passage eight to twelve, ADMSC showed morphological abnormalities and proliferation arrest due to replicative senescence [182]. Therefore, ADMSC were used up to eight passages.

MSC are at minimal risk of tumor formation and have been successfully applied in clinical and preclinical trials [183]. However, genetically unaltered MSC showed a malignant tumor after transplantation *in-vivo* [184]. For every single cell line including pancreatic progenitors derived from primary cells, this safety issue needs to be addressed, if the *in-vivo* application is considered.

Therefore, we designed an experiment to evaluate the tumor formation ability of hTERT-MSC and ADMSC in NMRI nude mice. We did not observe any tumor from the two different sources of stem cells after transplantation.

4.1.2 MSC promoted β-cell regeneration after partial pancreatectomy

Partial pancreatectomy is an established model for β-cell regeneration [185] but not yet in context with MSC. The primary purpose of this experiment was to first find out whether MSC modulate the regenerative potential of pancreatic β-cells and second whether there is a difference in MSC effect with different routes (IVR and IPR). After partial pancreatectomy, fluctuating blood glucose and body weight was observed in control, IVR and IPR groups. However, surgical stress assessment for abdominal surgery showed superior beneficial effects of the IPR group.

The therapeutic effect is assumed to depend upon the migration of MSC toward the inflamed residual pancreas within the first hours and days following pancreatectomy. The human Alu sequence was used to track the transplanted cells in the animal model with quantitative real-time PCR [186, 187]. Accordingly, migration of transplanted MSC was monitored in different organs, eight days subsequent to pancreatectomy. A majority of hTERT-MSC injected intravenously were expected to move towards lung microvasculature. In correspondence, half of the lung specimens were positive for human Alu sequence (4/8) and only one pancreas. In contrast with the IPR group, most of the human DNA as an indicator for the administered MSC were detected within the pancreas (5/8). The human Alu sequence was not detected in non-operative organs (kidney, spleen, heart and liver) which supported the assumption of an active locomotor response towards the inflamed site. After eight days of partial pancreatectomy, human DNA was clearly found in the pancreas and indicated that MSC were present and possibly exerted beneficial effects on the surroundings of the cellular microenvironment.

Pancreatectomy model of regeneration does not induce severe diabetes as it provides a strong proliferative signal to β-cells. Experimental evidence suggested that pancreatic β-cells proliferate from pre-existing cells rather than the progenitors residing within the pancreas [61, 185]. In the present study, pancreatic cells undergoing chromatin remodelling in cell cycle progression were labelled with BrdU. The number of BrdU and insulin doubly labelled cells was approximately two-fold in the IPR group as compared to control and IVR. In addition, the number of islets per pancreatic cross section and the insulin content of the residual pancreas was highest in the IPR

and thus provided evidence of a superior proliferative effect on pancreatic β-cells as opposed to IVR. In this study, murine growth factors (HGF, b-FGF, IGF-1, VEGF and EGF) were probed because treatment with a combination of EGF and ciliary neurotrophic factor (CNTF) was reported to induce β-cell proliferation in mice [188, 189]. Similarly, EGF along with gastrin also maintained β-cell mass in diabetes [190]. Among different growth factors examined in the experiments provided here, EGF and IGF-1 transcripts were significantly upregulated. Murine EGF gene expression was route dependent as an intrapancreatic injection induced highest EGF expression in the residual pancreas. EGF expression in the pancreatic β-cells was reported to enhance GLUT-2 gene expression which controls insulin secretion [191]. In accordance, we observed enhanced GLUT-2 expression in the IPR group.

MSC are acknowledged for immune modulation and anti-inflammatory effect in the damaged organ [192, 193]. A reduction in IFN-γ and TNF-α expression in damaged tissue was reported after MSC transplantation [194]. In the present experiment, MSC administered through either systemic route or local route, downregulated the expression of IFN-γ and TNF-α. MSC migration towards injured tissue could be enhanced by iron oxide nanoparticles labelling [195]. In this study, MSC were not labelled *in-vivo*. The factors determining the fraction of MSC's homing to the injured organ rather than being entrapped in the microvasculature of the lung are still under debate.

After partial pancreatectomy, FOXA2 and PDX-1 (pancreatic progenitor transcription factors) were addressed for the proliferation of pre-existing β-cells. [55, 59, 106, 107, 196]. In pancreatic β-cells, the definitive endoderm marker FOXA2 controlled the expression of PDX-1 and acted as an upstream regulator [75]. Similarly, in accordance with the literature, activation and upregulation of FOXA2 and PDX-1 were observed.

Further, signaling pathways such as PI3K/ AKT, ERK and TGF-β were evaluated. Liu C et al. recently demonstrated the activation of AKT and ERK1/ 2 pathway in rat insulinoma-derived INS-1E β-cells through hTERT-MSC *in-vitro* [197]. Similarly, in this study, phosphorylation of AKT protein was detected at protein and mRNA level after hTERT-MSC administration in the IPR group, confirming Liu C et al. data *in-vivo*. Activation of IRS2-AKT signaling pathways through FoxO1 downregulation was reported in pancreatic β-cell proliferation after partial pancreatectomy [55]. In this experiment, IRS2 expression post hTERT-MSC administration was not observed.

ERK and TGF-β gene expression were highly upregulated by pancreatectomy but irrespective of the route of hTERT-MSC treatment.

Further, PI3K/ AKT/ FoxO1 molecular interaction was inspected. After ablation of FoxO1 in gut epithelium, a normal blood glucose level was restored in a diabetic mice model [198]. In another investigation, conservation and proliferation of β-cells was reported via G type Iα/p-AKT/p-FoxO1 signaling pathway [199]. Likewise, in this study, downregulation of FoxO1 was noticed in IVR and a further reduction in the IPR group. Again, route dependent downregulation pattern of FoxO1 was observed after hTERT-MSC administration.

4.1.3 Superior antidiabetic effect of MSC through IPR

Mesenchymal stem cells have the potential to secrete cytokines, growth factors, anti-apoptotic and immunomodulatory molecules, which make them prominent candidates for the treatment of autoimmune diseases, such as TID [154]. MSC route of transplantation in preclinical diabetic studies is debatable. The most efficient route should deliver the highest regeneration and lowest side effect [200]. Yaochite JN et al. reported on the superior effect of MSC administered through intrasplenic over the intrapancreatic route [162]. In another study, intravenously administrated human umbilical cord-derived MSC had a greater beneficial effect than the intrapancreatic injection [163]. However, a recent investigation concluded, the intrapancreatic route of MSC strictly controlled the blood glucose level and had a dominant influence over the intravenous route [164]. In pancreatectomy study, after observing the advantage of MSC injected locally in the pancreas, the curative effectiveness of MSC transplanted through various routes (IVR and IPR) in the TID model was analyzed.

After 10-15 days of ADMSC administration in the IPR group, reduced blood glucose and increased body weight in STZ-induced diabetic mice was observed whereas these parameters were not changed in the IVR and STZ group. Likewise, the mouse-health-score-sheet confirmed a cure from diabetic symptoms and an improved survival rate in the IPR group. Moreover, a higher pancreatic wet weight was associated with faster recovery from diabetes in the IPR group. Within a 30 day window, other organs remained comparatively unaltered in regard to weight.

In our study, the IPR group displayed higher retention of ADMSC in the pancreas (20%) compared to IVR (10%). Survival and localization of MSC are the most important aspects of transplantation therapy. In a myocardial infarction model, after intracoronary injection of labelled MSC, only 5%

were detected in the heart after the initial two hours and further reduced to 1% at 18 hr [201]. However, in another myocardial infarction study, a reduction in the injected MSC from 34-80% (0 hr) to 0.03-3.5% (6 weeks) was observed after MSC were administered locally [202].

In past, MSC were traced with different methods [203]. Tracking with 3.0 T MRI non-invasive scanner revealed that intramyocardial transplanted MSC were present in the mouse heart up to four weeks [204]. Lee S et al. demonstrated the presence of MSC combined with matrigel in the pancreas seven and 28 days after intrapancreatic injection applying bioluminescence imaging [205]. Further, they searched for human Alu sequence in myocardial infarction model demonstrating that most of the transplanted MSC were trapped in the lungs and approximately 1,500 cells out of 1×10^6 actually reached to the infarcted heart [144].

In the diabetic scenario, PKH-26 and NIR815 (fluorescent dye) labelled MSC transplanted intravenously showed maximum signal in the chest on day seven and disappeared after eleven days onwards [164]. In another study human Alu sequence method was utilized, after intraperitoneal injection of human umbilical cord Wharton jelly cells in STZ-induced diabetic mice, the majority of the cells were observed in the liver (15.72%), followed by kidney (2.94%), pancreas (1.75%), spleen (0.09%) and 79.51% cells remained unidentified [206].

Likewise, in this study, the human Alu sequence was also detected in the lung probably due to cell entrapment in the microvasculature and kidney, the latter potentially because of adverse effects of high blood glucose levels or STZ damage to the glomerular microvessels and the proximal tubular system. However, we did not investigate the kidney and lung further in this regard.

Intrapancreatic injection is an invasive procedure adopted in this study and could be translated to the human for TID in future. This route was previously employed for treating cystic tumor of the pancreas with endoscopic ultrasound-guided ethanol lavage and paclitaxel injection in patients [207, 208]. Moreover, autologous bone marrow or umbilical cord blood cells were infused in the pancreas of T2D patients resulting in improved insulin secretion and blood glucose regulation [209-211].

In the present study, we demonstrated recovery of reduced insulin release through proliferating β-cells after 30 days of MSC transplantation in diabetic mice. Some experimental evidence was reported that an immature β-cell population persisted in the pancreatic niche as a source of

functional β-cells throughout life [212]. Rare proliferating β-cells were observed in the control group without STZ and MSC. In the treated groups, IPR showed higher proliferating β-cells per cross section compared with IVR and control. No proliferation was determined in the STZ only group. Likewise, the calculated section areas stained with anti-insulin antibody also adhered to the same pattern. We found a rising tendency in both serum and pancreatic insulin in the IPR group but with an insignificant variation. Still, after MSC injection into the pancreas, blood glucose levels and diabetic symptoms were comparatively lower than in the other groups.

MSC rescued the pancreas from diabetic stress by inducing the secretion of growth factors with anti-apoptotic effects on β-cells. Furthermore, they were reported to turn pro- to anti-inflammatory microenvironment [213, 214]. Accordingly, after ADMSC administration, pro-inflammatory pancreatic cytokines such as IL-1β and TNF-α were downregulated and anti-inflammatory IL-10 was upregulated in this study, only in the IPR group. These immunomodulatory properties of MSC were in conformity with the literature, after ADMSC administration, modulation of IL-1β, TNF-α and IL-10 were described as well [215-217]. Similarly, only in the IPR group higher BCL-2 versus BAX ratio which indicates anti-apoptotic outweighing apoptotic mechanism was observed.

EGF expression in transgenic mice increased β-cell proliferation [218]. In the present study, significantly higher murine EGF expression was recognized, particularly in the IPR group. Beneficial effects of MSC administration in autoimmune diabetic condition were reported, but the underlying molecular mechanisms in β-cell is still under debate [219, 220]. Therefore, MSC potential cellular pathways were investigated. This study resulted in experimental evidence that ERK and MAPK were predominantly activated in the IPR group. ERK was suggested to modulate the FoxO1 nuclear export in β-cells [221, 222]. Likewise, the results of the present study confirmed the downregulation of FoxO1 expression in the IPR group alone. We have further looked at the activation of DLK1 associated with MSC injection locally into the pancreas. In literature, DLK1 was informed to inhibit adipogenic differentiation [223]. DLK1 was also identified as a critical factor for MSC differentiation [224] because its overexpression regulated the ERK and FoxO1 pathways [74]. This is the first report to show the activation of DLK1/ EGF/ ERK/ FoxO1 signaling pathway is linked to MSC administration in low dose STZ-induced diabetes. Administration of STZ in multiple low doses was established as a model of type 1 diabetes by researchers. By

contrast, a single high dose of STZ inflicts acute chemical injury without activation of the immune system. Therefore, in this study low dose administration of STZ was utilized.

MSC infused intravenously were described to relieve from diabetic symptoms [176, 225, 226], however, in direct comparison with IPR, smaller effects were observed in the IVR group in the present report. To further address this issue, *in-vivo* conditions were translated into an *in-vitro* model. Thereby paracrine effects or indirect co-culture (IDC) conditions were established between MSC and STZ-injured MIN6 cells separated by a semipermeable membrane which reflected the intravenous route. On the other hand, physical contact or direct co-culture (DC) condition represented the intrapancreatic route. Our study confirmed the higher viability of STZ-injured MIN6 cells when co-cultured in physical contact (DC). At 2mM STZ concentration, viability significantly lowered in IDC, but the DC protective effect prevailed. We further modelled the *in-vivo* migration of MSC after transplantation (IVR) and *in-vitro* with IDC using Boyden chamber. After infusion, MSC recruited to the damaged pancreas, which is an essential prerequisite of stem cell therapy for injured tissue. In the acute pancreatitis mice model, a high level of SDF-1 expression was measured up to seven days [148]. Moreover, chemoattractant SDF-1 (CXCL12) was increased in MIN6 cells after being damaged by STZ which could attract MSC through the CXCR4 receptor. Concomitantly, abundant expression of CXCR4 was measured in MSC in both the DC and IDC system and proposed that migration of MSC towards MIN6 cells was mediated through SDF-1/ CXCR4 interaction.

Activation of murine EGF was noticed after the intrapancreatic injection of MSC in STZ-induced diabetic mice, but we did not find growth factors specific for human. Therefore, human growth factors excreted by MSC after interaction with STZ-injured MIN6 cells in both DC and IDC were examined. *In-vitro*, neither human nor murine EGF expression was detected. Interestingly, other factors released from MSC such as TIMP-1, IDO1 and VEGF were found at higher concentrations in DC which restored Ins1 and Ins2 insulin transcripts in MIN6 cells. In literature, TIMP-1, IDO1 and VEGF were discussed to retain the structural integrity of an inflamed microenvironment [144, 171]. Further, mitogen-activated protein kinases (MAPK)/ extracellular-signal-regulated kinase (ERK) pathway was upregulated *in-vivo*. Therefore, ERK protein was measured by Western blot after co-culturing MSC with STZ-injured MIN6 cells in DC and IDC. Higher expression of phosphorylated ERK protein was observed in DC rather than IDC. Similarly, phosphorylated AKT

also upregulated in STZ-injured MIN6 cells. In this study, we confirmed the upregulation of ERK protein after intrapancreatic injection *in-vivo* and in the *in-vitro* DC system. Further, the ratio of BCL-2 versus BAX was measured in both the DC and IDC systems. The *in-vivo* study resulted in higher BCL-2 versus BAX expression in IPR compared to the IVR group. The *in-vitro* condition showed that the BCL-2/ BAX ratio was significantly increased in both DC and IDC.

4.2 Conclusion

4.2.1 The present data confirmed that the intrapancreatic transplantation of hTERT-MSC (IPR) had a superior regenerative effect as opposed to intravenous administration (IVR) or systemic transplantation in partially pancreatectomized NMRI nude mice. hTERT-MSC administration was associated with reduction of pro-inflammatory cytokines (IFN-γ, TNF-α) and augmented release of growth factors EGF and IGF-1 from the pancreas. The secreted growth factors provided a proliferative stimulus to newly established β-cells through the activation of the AKT/ FOXA2/ PDX-1/ FoxO1 signaling pathway.
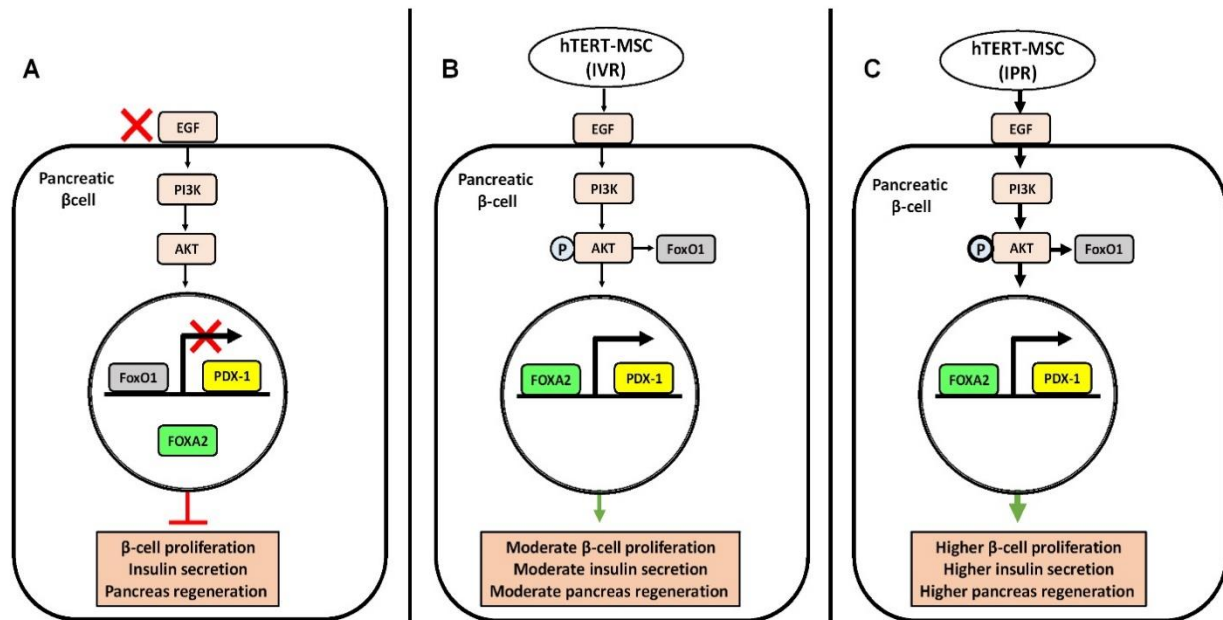
Figure 4.2.1: Mechanism of pancreatic β-cell proliferation after hTERT-MSC administration in the partially pancreatectomized NMRI mouse model. (A) Demonstrates the control group (B) hTERT-MSC administration through the intravenous route (IVR) and (C) intrapancreatic route (IPR).

This signaling cascade prompted the recovery of the resected pancreas to reconstitute islet structure. Local injection of MSC through the intrapancreatic route (IPR) had a stronger

regenerative outcome, verified by higher β-cell proliferation and insulin secretion than intravenous route (IVR) and could be employed in the prevention of diabetes mellitus or surgical pancreatic injury as illustrated in figure 4.2.1.

4.2.2 In T1D study, we provide evidence that intrapancreatic (IPR) or local route of ADMSC administration exerted a higher antidiabetic effect compared to intravenous (IVR) or systemic route of transplantation in STZ-induced diabetic NMRI nude mice. ADMSC administered through intrapancreatic injection prevented hyperglycemia, improved body weight with enhanced survival and displayed higher retention in the pancreas (20%) compared to IVR (10%). Indeed, BrdU positive cells, islets number and area were significantly increased in IPR. This antidiabetic effect was attributed by the downregulation of pro-inflammatory molecules IL-1β and TNF-α, releasing growth factor (EGF) and upregulation of anti-inflammatory molecule IL-10. DLK1 induced ERK activation, which finally downregulated the FoxO1 expression and provided protection through a BCL-2/ BAX signaling cascade. To this end, this report is the first to describe the antidiabetic effect of MSC via the DLK1/ EGF/ ERK/ FoxO1 signaling pathway after IPR administration as shown in 4.2.2.
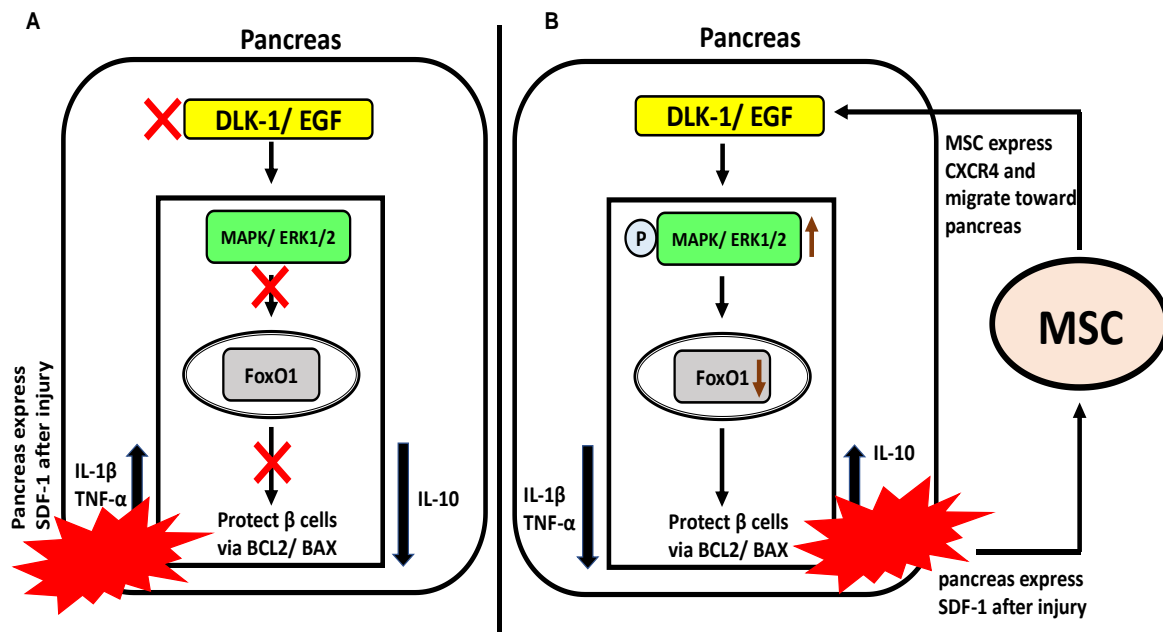
Figure 4.2.2: Proposed mechanism of MSC protection in STZ-induced diabetic mice. (A) Demonstrates the pancreas in the absence of MSC. (B) MSC administration into the pancreas activates DLK1/ ERK/ FoxO1 signaling pathway.

REFERENCES

1.   Burn, P., *Type 1 diabetes.* Nature Reviews Drug Discovery, 2010. **9**(3): p. 187-188.

2.   Polonsky, K.S., *The past 200 years in diabetes.* N Engl J Med, 2012. **367**(14): p. 1332-40.

3.   Ahmed, A.M., *History of diabetes mellitus.* Saudi Med J, 2002. **23**(4): p. 373-8.

4.   Banting, F.G., et al., *Pancreatic Extracts in the Treatment of Diabetes Mellitus.* Can Med Assoc J, 1922. **12**(3): p. 141-6.

5.   Bliss, M., *The discovery of insulin: the inside story.* Publ Am Inst Hist Pharm, 1997. **16**: p. 93-9.

6.   American Diabetes, A., *Diagnosis and classification of diabetes mellitus.* Diabetes Care, 2011. **34 Suppl 1**: p. S62-9.

7.   Alfadhli, E.M., *Gestational diabetes mellitus.* Saudi Med J, 2015. **36**(4): p. 399-406.

8.   Resmini, E., et al., *Secondary diabetes associated with principal endocrinopathies: the impact of new treatment modalities.* Acta Diabetol, 2009. **46**(2): p. 85-95.

9.   Wong, C.W., et al., *Kidney and eye diseases: common risk factors, etiological mechanisms, and pathways.* Kidney Int, 2014. **85**(6): p. 1290-302.

10.   Rodriguez-Poncelas, A., et al., *Chronic Kidney Disease and Diabetic Retinopathy in Patients with Type 2 Diabetes.* PLoS One, 2016. **11**(2): p. e0149448.

11.   Marwick, T.H., *Diabetic heart disease.* Heart, 2006. **92**(3): p. 296-300.

12.   Ogurtsova, K., et al., *IDF Diabetes Atlas: Global estimates for the prevalence of diabetes for 2015 and 2040.* Diabetes Res Clin Pract, 2017. **128**: p. 40-50.

13.   Tripathy, J.P., et al., *Prevalence and risk factors of diabetes in a large community-based study in North India: results from a STEPS survey in Punjab, India.* Diabetol Metab Syndr, 2017. **9**: p. 8.

14.   Benjamin Goffrier, M.S., Jörg Bätzing-Feigenbaum, *Administrative prevalence and incidence of diabetes mellitus in Germany, 2009-2015.* Versorgungsatlas Report No. 17/03. Berlin 2017, 2017. **Berlin 2017**

15.   *Variation and trends in incidence of childhood diabetes in Europe. EURODIAB ACE Study Group.* Lancet, 2000. **355**(9207): p. 873-6.

16.   American Diabetes, A., *(2) Classification and diagnosis of diabetes.* Diabetes Care, 2015. **38 Suppl**: p. S8-S16.

17.   Katsarou, A., et al., *Type 1 diabetes mellitus.* Nat Rev Dis Primers, 2017. **3**: p. 17016.

18.   Krischer, J.P., et al., *The 6 year incidence of diabetes-associated autoantibodies in genetically at-risk children: the TEDDY study.* Diabetologia, 2015. **58**(5): p. 980-7.

19.   Wallberg, M. and A. Cooke, *Immune mechanisms in type 1 diabetes.* Trends Immunol, 2013. **34**(12): p. 583-91.

20.   Kuhn, C., et al., *Regulatory mechanisms of immune tolerance in type 1 diabetes and their failures.* J Autoimmun, 2016. **71**: p. 69-77.

21.   Willcox, A., et al., *Analysis of islet inflammation in human type 1 diabetes.* Clin Exp Immunol, 2009. **155**(2): p. 173-81.

22.   Calderon, B. and E.R. Unanue, *Antigen presentation events in autoimmune diabetes.* Current Opinion in Immunology, 2012. **24**(1): p. 119-128.

23.   Ferris, S.T., J.A. Carrero, and E.R. Unanue, *Antigen presentation events during the initiation of autoimmune diabetes in the NOD mouse.* Journal of Autoimmunity, 2016. **71**: p. 19-25.

24.   O'Brien, B.A., et al., *A deficiency in the in vivo clearance of apoptotic cells is a feature of the NOD mouse.* Journal of Autoimmunity, 2006. **26**(2): p. 104-115.

25.   Flodstrom, M., et al., *Target cell defense prevents the development of diabetes after viral infection.* Nat Immunol, 2002. **3**(4): p. 373-82.

26.   Sitrin, J., et al., *Regulatory T cells control NK cells in an insulitic lesion by depriving them of IL-2.* Journal of Experimental Medicine, 2013. **210**(6): p. 1153-1165.

27.   DeFronzo, R.A., et al., *Type 2 diabetes mellitus.* Nat Rev Dis Primers, 2015. **1**: p. 15019.

28.   King, A.J., *The use of animal models in diabetes research.* Br J Pharmacol, 2012. **166**(3): p. 877-94.

29.   Rees, D.A. and J.C. Alcolado, *Animal models of diabetes mellitus.* Diabet Med, 2005. **22**(4): p. 359-70.

30.   Sandler, S. and I. Swenne, *Streptozotocin, but not alloxan, induces DNA repair synthesis in mouse pancreatic islets in vitro.* Diabetologia, 1983. **25**(5): p. 444-7.

31.   Sandler, S., M. Welsh, and A. Andersson, *Streptozotocin-induced impairment of islet B-cell metabolism and its prevention by a hydroxyl radical scavenger and inhibitors of poly(ADP-ribose) synthetase.* Acta Pharmacol Toxicol (Copenh), 1983. **53**(5): p. 392-400.

32.   Linn, T., et al., *Spontaneous glucose intolerance in the progeny of low dose streptozotocin-induced diabetic mice.* Diabetologia, 1993. **36**(12): p. 1245-51.

33. McEvoy, R.C., et al., *Multiple low-dose streptozotocin-induced diabetes in the mouse. Evidence for stimulation of a cytotoxic cellular immune response against an insulin-producing beta cell line.* J Clin Invest, 1984. **74**(3): p. 715-22.

34. Fogh, J. and B.C. Giovanella, *The Nude mouse in experimental and clinical research.* 1978, New York: Academic Press. v. <1 >.

35. Khatri, R., et al., *Intraportal Transplantation of Pancreatic Islets in Mouse Model.* J Vis Exp, 2018(135).

36. Dolensek, J., M.S. Rupnik, and A. Stozer, *Structural similarities and differences between the human and the mouse pancreas.* Islets, 2015. **7**(1): p. e1024405.

37. Sakula, A., *Paul Langerhans (1847-1888): a centenary tribute.* J R Soc Med, 1988. **81**(7): p. 414-5.

38. Weir, G.C. and S. Bonner-Weir, *Islets of Langerhans: the puzzle of intraislet interactions and their relevance to diabetes.* J Clin Invest, 1990. **85**(4): p. 983-7.

39. Kallman, F. and C. Grobstein, *Fine Structure of Differentiating Mouse Pancreatic Exocrine Cells in Transfilter Culture.* J Cell Biol, 1964. **20**: p. 399-413.

40. Munger, B.L., *A light and electron microscopic study of cellular differentiation in the pancreatic islets of the mouse.* Am J Anat, 1958. **103**(2): p. 275-311.

41. Pictet, R.L., et al., *An ultrastructural analysis of the developing embryonic pancreas.* Dev Biol, 1972. **29**(4): p. 436-67.

42. Wessells, N.K. and J.H. Cohen, *Early Pancreas Organogenesis: Morphogenesis, Tissue Interactions, and Mass Effects.* Dev Biol, 1967. **15**(3): p. 237-70.

43. Gittes, G.K., *Developmental biology of the pancreas: a comprehensive review.* Dev Biol, 2009. **326**(1): p. 4-35.

44. Ellis, C., A. Ramzy, and T.J. Kieffer, *Regenerative medicine and cell-based approaches to restore pancreatic function.* Nat Rev Gastroenterol Hepatol, 2017. **14**(10): p. 612-628.

45. Clark, W.R. and W.J. Rutter, *Synthesis and accumulation of insulin in the fetal rat pancreas.* Dev Biol, 1972. **29**(4): p. 468-81.

46. Granger, A. and J.A. Kushner, *Cellular origins of beta-cell regeneration: a legacy view of historical controversies.* J Intern Med, 2009. **266**(4): p. 325-38.

47. Weaver, C.V. and D.J. Garry, *Regenerative biology: a historical perspective and modern applications.* Regen Med, 2008. **3**(1): p. 63-82.

48. Watanabe, H., et al., *Aging is associated with decreased pancreatic acinar cell regeneration and phosphatidylinositol 3-kinase/Akt activation.* Gastroenterology, 2005. **128**(5): p. 1391-404.

49. Tanigawa, K., et al., *Effect of aging on B-cell function and replication in rat pancreas after 90% pancreatectomy.* Pancreas, 1997. **15**(1): p. 53-9.

50. Morel, P., et al., *Total pancreatectomy in the pig for islet transplantation. Technical alternatives.* Transplantation, 1991. **52**(1): p. 11-5.

51. Fisher, S.J., et al., *Low-dose IGF-I has no selective advantage over insulin in regulating glucose metabolism in hyperglycemic depancreatized dogs.* J Endocrinol, 2001. **168**(1): p. 49-58.

52. He, S., et al., *Treatment and risk factor analysis of hypoglycemia in diabetic rhesus monkeys.* Exp Biol Med (Maywood), 2011. **236**(2): p. 212-8.

53. Socorro, M.a.E., Farzad, *Pancreatic Regeneration: Models, Mechanisms, and Inconsistencies.* Pancreapedia: Exocrine Pancreas Knowledge Base, 2014.

54. Togashi, Y., et al., *beta-Cell proliferation after a partial pancreatectomy is independent of IRS-2 in mice.* Endocrinology, 2014. **155**(5): p. 1643-52.

55. Peshavaria, M., et al., *Regulation of pancreatic beta-cell regeneration in the normoglycemic 60% partial-pancreatectomy mouse.* Diabetes, 2006. **55**(12): p. 3289-98.

56. Sharma, A., et al., *The homeodomain protein IDX-1 increases after an early burst of proliferation during pancreatic regeneration.* Diabetes, 1999. **48**(3): p. 507-13.

57. Watanabe, H., et al., *Activation of phosphatidylinositol-3 kinase regulates pancreatic duodenal homeobox-1 in duct cells during pancreatic regeneration.* Pancreas, 2008. **36**(2): p. 153-9.

58. Desai, B.M., et al., *Preexisting pancreatic acinar cells contribute to acinar cell, but not islet beta cell, regeneration.* J Clin Invest, 2007. **117**(4): p. 971-7.

59. Dor, Y., et al., *Adult pancreatic beta-cells are formed by self-duplication rather than stem-cell differentiation.* Nature, 2004. **429**(6987): p. 41-6.

60. Li, W.C., et al., *Activation of pancreatic-duct-derived progenitor cells during pancreas regeneration in adult rats.* J Cell Sci, 2010. **123**(Pt 16): p. 2792-802.

61. Xiao, X., et al., *No evidence for beta cell neogenesis in murine adult pancreas.* J Clin Invest, 2013. **123**(5): p. 2207-17.

62. Lee, C.S., et al., *Regeneration of pancreatic islets after partial pancreatectomy in mice does not involve the reactivation of neurogenin-3.* Diabetes, 2006. **55**(2): p. 269-72.

63. Murtaugh, L.C. and M.D. Keefe, *Regeneration and repair of the exocrine pancreas.* Annu Rev Physiol, 2015. **77**: p. 229-49.

64. Lerch, M.M. and F.S. Gorelick, *Models of acute and chronic pancreatitis.* Gastroenterology, 2013. **144**(6): p. 1180-93.

65. Konturek, J.W., et al., *Secretion of protein and epidermal growth factor (EGF) by transplanted human pancreas.* Int J Pancreatol, 1992. **12**(1): p. 23-9.

66. Jaworek, J. and S.J. Konturek, *Distribution, release, and secretory activity of epidermal growth factor in the pancreas.* Int J Pancreatol, 1990. **6**(3): p. 189-205.

67. Suarez-Pinzon, W.L., et al., *Combination therapy with epidermal growth factor and gastrin increases beta-cell mass and reverses hyperglycemia in diabetic NOD mice.* Diabetes, 2005. **54**(9): p. 2596-601.

68. Song, I., et al., *Beta Cell Mass Restoration in Alloxan-Diabetic Mice Treated with EGF and Gastrin.* PLoS One, 2015. **10**(10): p. e0140148.

69. Solar, M., et al., *Pancreatic exocrine duct cells give rise to insulin-producing beta cells during embryogenesis but not after birth.* Dev Cell, 2009. **17**(6): p. 849-60.

70. Smas, C.M. and H.S. Sul, *Pref-1, a protein containing EGF-like repeats, inhibits adipocyte differentiation.* Cell, 1993. **73**(4): p. 725-34.

71. Wang, Y. and H.S. Sul, *Pref-1 regulates mesenchymal cell commitment and differentiation through Sox9.* Cell Metab, 2009. **9**(3): p. 287-302.

72. Tanimizu, N., et al., *Isolation of hepatoblasts based on the expression of Dlk/Pref-1.* J Cell Sci, 2003. **116**(Pt 9): p. 1775-86.

73. Carlsson, C., et al., *Growth hormone and prolactin stimulate the expression of rat preadipocyte factor-1/delta-like protein in pancreatic islets: molecular cloning and expression pattern during development and growth of the endocrine pancreas.* Endocrinology, 1997. **138**(9): p. 3940-8.

74. Rhee, M., et al., *Preadipocyte factor 1 induces pancreatic ductal cell differentiation into insulin-producing cells.* Sci Rep, 2016. **6**: p. 23960.

75. Lee, C.S., et al., *Foxa2 controls Pdx1 gene expression in pancreatic beta-cells in vivo.* Diabetes, 2002. **51**(8): p. 2546-51.

76. Pagliuca, F.W. and D.A. Melton, *How to make a functional beta-cell.* Development, 2013. **140**(12): p. 2472-83.

77. Jensen, J., et al., *Independent development of pancreatic alpha- and beta-cells from neurogenin3-expressing precursors: a role for the notch pathway in repression of premature differentiation.* Diabetes, 2000. **49**(2): p. 163-76.

78. Marshak, S., et al., *Purification of the beta-cell glucose-sensitive factor that transactivates the insulin gene differentially in normal and transformed islet cells.* Proc Natl Acad Sci U S A, 1996. **93**(26): p. 15057-62.

79. Jonsson, J., et al., *Insulin-promoter-factor 1 is required for pancreas development in mice.* Nature, 1994. **371**(6498): p. 606-9.

80. Stoffers, D.A., et al., *Pancreatic agenesis attributable to a single nucleotide deletion in the human IPF1 gene coding sequence.* Nat Genet, 1997. **15**(1): p. 106-10.

81. Stoffers, D.A., et al., *Early-onset type-II diabetes mellitus (MODY4) linked to IPF1.* Nat Genet, 1997. **17**(2): p. 138-9.

82. Zhang, T., et al., *FoxO1 Plays an Important Role in Regulating beta-Cell Compensation for Insulin Resistance in Male Mice.* Endocrinology, 2016. **157**(3): p. 1055-70.

83. Mussig, K., et al., *Association of common genetic variation in the FOXO1 gene with beta-cell dysfunction, impaired glucose tolerance, and type 2 diabetes.* J Clin Endocrinol Metab, 2009. **94**(4): p. 1353-60.

84. Kim-Muller, J.Y., et al., *Metabolic inflexibility impairs insulin secretion and results in MODY-like diabetes in triple FoxO-deficient mice.* Cell Metab, 2014. **20**(4): p. 593-602.

85. Kawamori, D., et al., *The forkhead transcription factor Foxo1 bridges the JNK pathway and the transcription factor PDX-1 through its intracellular translocation.* J Biol Chem, 2006. **281**(2): p. 1091-8.

86. Kitamura, T., et al., *The forkhead transcription factor Foxo1 links insulin signaling to Pdx1 regulation of pancreatic beta cell growth.* J Clin Invest, 2002. **110**(12): p. 1839-47.

87. Czech, M.P., *Insulin's expanding control of forkheads.* Proc Natl Acad Sci U S A, 2003. **100**(20): p. 11198-200.

88. Nakae, J., et al., *The forkhead transcription factor Foxo1 regulates adipocyte differentiation.* Dev Cell, 2003. **4**(1): p. 119-29.

89.   Del Guerra, S., et al., *Functional and molecular defects of pancreatic islets in human type 2 diabetes.* Diabetes, 2005. **54**(3): p. 727-35.

90.   Kitamura, T., *The role of FOXO1 in beta-cell failure and type 2 diabetes mellitus.* Nat Rev Endocrinol, 2013. **9**(10): p. 615-23.

91.   Tonne, J.M., et al., *Global gene expression profiling of pancreatic islets in mice during streptozotocin-induced beta-cell damage and pancreatic Glp-1 gene therapy.* Dis Model Mech, 2013. **6**(5): p. 1236-45.

92.   Van Assche, F.A., L. Aerts, and F. De Prins, *A morphological study of the endocrine pancreas in human pregnancy.* Br J Obstet Gynaecol, 1978. **85**(11): p. 818-20.

93.   Saisho, Y., et al., *beta-cell mass and turnover in humans: effects of obesity and aging.* Diabetes Care, 2013. **36**(1): p. 111-7.

94.   Thorel, F., et al., *Conversion of adult pancreatic alpha-cells to beta-cells after extreme beta-cell loss.* Nature, 2010. **464**(7292): p. 1149-54.

95.   Chera, S., et al., *Diabetes recovery by age-dependent conversion of pancreatic delta-cells into insulin producers.* Nature, 2014. **514**(7523): p. 503-7.

96.   Collombat, P., et al., *Opposing actions of Arx and Pax4 in endocrine pancreas development.* Genes Dev, 2003. **17**(20): p. 2591-603.

97.   Babiker, N.E., et al., *The progress of Stem cells in the treatment of diabetes mellitus type 1.* Progress in Stem Cell, 2017(01): p. 175-188%V 4.

98.   McCall, M. and A.M. Shapiro, *Update on islet transplantation.* Cold Spring Harb Perspect Med, 2012. **2**(7): p. a007823.

99.   Shapiro, A.M., et al., *Islet transplantation in seven patients with type 1 diabetes mellitus using a glucocorticoid-free immunosuppressive regimen.* N Engl J Med, 2000. **343**(4): p. 230-8.

100.   Cantarelli, E., et al., *Bone marrow as an alternative site for islet transplantation.* Blood, 2009. **114**(20): p. 4566-74.

101.   Echeverri, G.J., et al., *Endoscopic gastric submucosal transplantation of islets (ENDO-STI): technique and initial results in diabetic pigs.* Am J Transplant, 2009. **9**(11): p. 2485-96.

102.   Korsgren, O., et al., *Optimising islet engraftment is critical for successful clinical islet transplantation.* Diabetologia, 2008. **51**(2): p. 227-32.

103. Merani, S., et al., *Optimal implantation site for pancreatic islet transplantation.* Br J Surg, 2008. **95**(12): p. 1449-61.

104. Aguayo-Mazzucato, C. and S. Bonner-Weir, *Stem cell therapy for type 1 diabetes mellitus.* Nat Rev Endocrinol, 2010. **6**(3): p. 139-48.

105. Naujok, O., et al., *A new experimental protocol for preferential differentiation of mouse embryonic stem cells into insulin-producing cells.* Cell Transplant, 2008. **17**(10-11): p. 1231-42.

106. D'Amour, K.A., et al., *Production of pancreatic hormone-expressing endocrine cells from human embryonic stem cells.* Nat Biotechnol, 2006. **24**(11): p. 1392-401.

107. D'Amour, K.A., et al., *Efficient differentiation of human embryonic stem cells to definitive endoderm.* Nat Biotechnol, 2005. **23**(12): p. 1534-41.

108. Tada, S., et al., *Characterization of mesendoderm: a diverging point of the definitive endoderm and mesoderm in embryonic stem cell differentiation culture.* Development, 2005. **132**(19): p. 4363-74.

109. Rezania, A., et al., *Reversal of diabetes with insulin-producing cells derived in vitro from human pluripotent stem cells.* Nat Biotechnol, 2014. **32**(11): p. 1121-33.

110. Benthuysen, J.R., A.C. Carrano, and M. Sander, *Advances in beta cell replacement and regeneration strategies for treating diabetes.* J Clin Invest, 2016. **126**(10): p. 3651-3660.

111. Takahashi, K. and S. Yamanaka, *Induction of pluripotent stem cells from mouse embryonic and adult fibroblast cultures by defined factors.* Cell, 2006. **126**(4): p. 663-76.

112. Stadtfeld, M., et al., *Induced pluripotent stem cells generated without viral integration.* Science, 2008. **322**(5903): p. 945-9.

113. Jang, J., et al., *Disease-specific induced pluripotent stem cells: a platform for human disease modeling and drug discovery.* Exp Mol Med, 2012. **44**(3): p. 202-13.

114. Zhang, D., et al., *Highly efficient differentiation of human ES cells and iPS cells into mature pancreatic insulin-producing cells.* Cell Res, 2009. **19**(4): p. 429-38.

115. Teo, A.K., et al., *Derivation of human induced pluripotent stem cells from patients with maturity onset diabetes of the young.* J Biol Chem, 2013. **288**(8): p. 5353-6.

116. Raikwar, S.P., et al., *Human iPS cell-derived insulin producing cells form vascularized organoids under the kidney capsules of diabetic mice.* PLoS One, 2015. **10**(1): p. e0116582.

117. Calafiore, R. and G. Basta, *Stem cells for the cell and molecular therapy of type 1 diabetes mellitus (T1D): the gap between dream and reality.* Am J Stem Cells, 2015. **4**(1): p. 22-31.

118. Friedenstein, A.J., R.K. Chailakhjan, and K.S. Lalykina, *The development of fibroblast colonies in monolayer cultures of guinea-pig bone marrow and spleen cells.* Cell Tissue Kinet, 1970. **3**(4): p. 393-403.

119. Friedenstein, A.J., J.F. Gorskaja, and N.N. Kulagina, *Fibroblast precursors in normal and irradiated mouse hematopoietic organs.* Exp Hematol, 1976. **4**(5): p. 267-74.

120. Friedenstein, A.J., et al., *Stromal cells responsible for transferring the microenvironment of the hemopoietic tissues. Cloning in vitro and retransplantation in vivo.* Transplantation, 1974. **17**(4): p. 331-40.

121. Caplan, A.I., *Mesenchymal stem cells.* J Orthop Res, 1991. **9**(5): p. 641-50.

122. Rekittke, N.E., et al., *Regenerative Therapy of Type 1 Diabetes Mellitus: From Pancreatic Islet Transplantation to Mesenchymal Stem Cells.* Stem Cells Int, 2016. **2016**: p. 3764681.

123. Timper, K., et al., *Human adipose tissue-derived mesenchymal stem cells differentiate into insulin, somatostatin, and glucagon expressing cells.* Biochem Biophys Res Commun, 2006. **341**(4): p. 1135-40.

124. Pittenger, M.F., et al., *Multilineage potential of adult human mesenchymal stem cells.* Science, 1999. **284**(5411): p. 143-7.

125. Cianfarani, F., et al., *Diabetes impairs adipose tissue-derived stem cell function and efficiency in promoting wound healing.* Wound Repair Regen, 2013. **21**(4): p. 545-53.

126. Tobita, M., S. Tajima, and H. Mizuno, *Adipose tissue-derived mesenchymal stem cells and platelet-rich plasma: stem cell transplantation methods that enhance stemness.* Stem Cell Res Ther, 2015. **6**: p. 215.

127. Wang, Y., et al., *Plasticity of mesenchymal stem cells in immunomodulation: pathological and therapeutic implications.* Nat Immunol, 2014. **15**(11): p. 1009-16.

128. Phadnis, S.M., et al., *Mesenchymal stem cells derived from bone marrow of diabetic patients portrait unique markers influenced by the diabetic microenvironment.* Rev Diabet Stud, 2009. **6**(4): p. 260-70.

129. Atoui, R. and R.C. Chiu, *Concise review: immunomodulatory properties of mesenchymal stem cells in cellular transplantation: update, controversies, and unknowns.* Stem Cells Transl Med, 2012. **1**(3): p. 200-5.

130.   Squillaro, T., G. Peluso, and U. Galderisi, *Clinical Trials With Mesenchymal Stem Cells: An Update.* Cell Transplant, 2016. **25**(5): p. 829-48.

131.   Wu, H. and R.I. Mahato, *Mesenchymal stem cell-based therapy for type 1 diabetes.* Discov Med, 2014. **17**(93): p. 139-43.

132.   Chandra, V., et al., *Islet-like cell aggregates generated from human adipose tissue derived stem cells ameliorate experimental diabetes in mice.* PLoS One, 2011. **6**(6): p. e20615.

133.   Dang, L.T.-T., et al., *Production of islet-like insulin-producing cell clusters in vitro from adiposederived stem cells.* Biomedical Research and Therapy, 2015. **2**(1): p. 3.

134.   Hashemian, S.J., M. Kouhnavard, and E. Nasli-Esfahani, *Mesenchymal Stem Cells: Rising Concerns over Their Application in Treatment of Type One Diabetes Mellitus.* J Diabetes Res, 2015. **2015**: p. 675103.

135.   Piper, S.L., et al., *Inducible immortality in hTERT-human mesenchymal stem cells.* J Orthop Res, 2012. **30**(12): p. 1879-85.

136.   Ikbale el, A., et al., *Effects of hTERT immortalization on osteogenic and adipogenic differentiation of dental pulp stem cells.* Data Brief, 2016. **6**: p. 696-9.

137.   Krysko, D.V., et al., *Macrophages use different internalization mechanisms to clear apoptotic and necrotic cells.* Cell Death Differ, 2006. **13**(12): p. 2011-22.

138.   Ma, S., et al., *Immunobiology of mesenchymal stem cells.* Cell Death Differ, 2014. **21**(2): p. 216-25.

139.   Ma, X.L., et al., *Human mesenchymal stem cells increases expression of alpha-tubulin and angiopoietin 1 and 2 in focal cerebral ischemia and reperfusion.* Curr Neurovasc Res, 2013. **10**(2): p. 103-11.

140.   Shi, Y., et al., *How mesenchymal stem cells interact with tissue immune responses.* Trends Immunol, 2012. **33**(3): p. 136-43.

141.   Svobodova, E., et al., *The role of mouse mesenchymal stem cells in differentiation of naive T-cells into anti-inflammatory regulatory T-cell or proinflammatory helper T-cell 17 population.* Stem Cells Dev, 2012. **21**(6): p. 901-10.

142.   Mougiakakos, D., et al., *The impact of inflammatory licensing on heme oxygenase-1-mediated induction of regulatory T cells by human mesenchymal stem cells.* Blood, 2011. **117**(18): p. 4826-35.

143. Ren, G., et al., *Mesenchymal stem cell-mediated immunosuppression occurs via concerted action of chemokines and nitric oxide.* Cell Stem Cell, 2008. **2**(2): p. 141-50.

144. Lee, R.H., et al., *Intravenous hMSCs improve myocardial infarction in mice because cells embolized in lung are activated to secrete the anti-inflammatory protein TSG-6.* Cell Stem Cell, 2009. **5**(1): p. 54-63.

145. Gu, Y.Z., et al., *Different roles of PD-L1 and FasL in immunomodulation mediated by human placenta-derived mesenchymal stem cells.* Hum Immunol, 2013. **74**(3): p. 267-76.

146. Ley, K., et al., *Getting to the site of inflammation: the leukocyte adhesion cascade updated.* Nat Rev Immunol, 2007. **7**(9): p. 678-89.

147. Steingen, C., et al., *Characterization of key mechanisms in transmigration and invasion of mesenchymal stem cells.* J Mol Cell Cardiol, 2008. **44**(6): p. 1072-84.

148. Gong, J., et al., *The SDF-1/CXCR4 axis regulates migration of transplanted bone marrow mesenchymal stem cells towards the pancreas in rats with acute pancreatitis.* Mol Med Rep, 2014. **9**(5): p. 1575-82.

149. Sordi, V., et al., *Bone marrow mesenchymal stem cells express a restricted set of functionally active chemokine receptors capable of promoting migration to pancreatic islets.* Blood, 2005. **106**(2): p. 419-27.

150. Gao, J., et al., *The dynamic in vivo distribution of bone marrow-derived mesenchymal stem cells after infusion.* Cells Tissues Organs, 2001. **169**(1): p. 12-20.

151. Lee, R.H., et al., *Multipotent stromal cells from human marrow home to and promote repair of pancreatic islets and renal glomeruli in diabetic NOD/scid mice.* Proc Natl Acad Sci U S A, 2006. **103**(46): p. 17438-43.

152. Carlsson, P.O., et al., *Preserved beta-cell function in type 1 diabetes by mesenchymal stromal cells.* Diabetes, 2015. **64**(2): p. 587-92.

153. Dang, L.T., et al., *Intravenous Infusion of Human Adipose Tissue-Derived Mesenchymal Stem Cells to Treat Type 1 Diabetic Mellitus in Mice: An Evaluation of Grafted Cell Doses.* Adv Exp Med Biol, 2018.

154. Li, L., et al., *Infusion with Human Bone Marrow-derived Mesenchymal Stem Cells Improves beta-cell Function in Patients and Non-obese Mice with Severe Diabetes.* Sci Rep, 2016. **6**: p. 37894.

155. Schrepfer, S., et al., *Stem cell transplantation: the lung barrier.* Transplant Proc, 2007. **39**(2): p. 573-6.

156. Toma, C., et al., *Fate of culture-expanded mesenchymal stem cells in the microvasculature: in vivo observations of cell kinetics.* Circ Res, 2009. **104**(3): p. 398-402.

157. Furlani, D., et al., *Is the intravascular administration of mesenchymal stem cells safe? Mesenchymal stem cells and intravital microscopy.* Microvasc Res, 2009. **77**(3): p. 370-6.

158. Aguilar, S., et al., *Murine but not human mesenchymal stem cells generate osteosarcoma-like lesions in the lung.* Stem Cells, 2007. **25**(6): p. 1586-94.

159. Lundberg, J., et al., *Targeted intra-arterial transplantation of stem cells to the injured CNS is more effective than intravenous administration: engraftment is dependent on cell type and adhesion molecule expression.* Cell Transplant, 2012. **21**(1): p. 333-43.

160. Zhang, X., et al., *Local delivery of mesenchymal stem cells with poly-lactic-co-glycolic acid nano-fiber scaffold suppress arthritis in rats.* PLoS One, 2014. **9**(12): p. e114621.

161. Wang, M., et al., *Intraperitoneal injection (IP), Intravenous injection (IV) or anal injection (AI)? Best way for mesenchymal stem cells transplantation for colitis.* Sci Rep, 2016. **6**: p. 30696.

162. Yaochite, J.N., et al., *Therapeutic efficacy and biodistribution of allogeneic mesenchymal stem cells delivered by intrasplenic and intrapancreatic routes in streptozotocin-induced diabetic mice.* Stem Cell Res Ther, 2015. **6**: p. 31.

163. Phan, N.K., et al., *Preliminary evaluation of intravenous infusion and intrapancreatic injection of human umbilical cord blood-derived mesenchymal stem cells for the treatment of diabetic mice.* Biomedical Research and Therapy, 2014. **1**(3): p. 16.

164. Murai, N., et al., *Intrapancreatic injection of human bone marrow-derived mesenchymal stem/stromal cells alleviates hyperglycemia and modulates the macrophage state in streptozotocin-induced type 1 diabetic mice.* PLoS One, 2017. **12**(10): p. e0186637.

165. Park, K.S., et al., *Trophic molecules derived from human mesenchymal stem cells enhance survival, function, and angiogenesis of isolated islets after transplantation.* Transplantation, 2010. **89**(5): p. 509-17.

166. de Souza, B.M., et al., *Effect of co-culture of mesenchymal stem/stromal cells with pancreatic islets on viability and function outcomes: a systematic review and meta-analysis.* Islets, 2017. **9**(2): p. 30-42.

167. Liu, C., et al., *Mesenchymal stem cell (MSC)-mediated survival of insulin producing pancreatic beta-cells during cellular stress involves signalling via Akt and ERK1/2.* Mol Cell Endocrinol, 2018. **473**: p. 235-244.

168. Rackham, C.L., et al., *Preculturing Islets With Adipose-Derived Mesenchymal Stromal Cells Is an Effective Strategy for Improving Transplantation Efficiency at the Clinically Preferred Intraportal Site.* Cell Med, 2014. **7**(1): p. 37-47.

169. Karaoz, E., et al., *Bone marrow-derived mesenchymal stem cells co-cultured with pancreatic islets display beta cell plasticity.* J Tissue Eng Regen Med, 2011. **5**(6): p. 491-500.

170. Lin, P., et al., *Dynamic analysis of bone marrow mesenchymal stem cells migrating to pancreatic islets using coculture microfluidic chips: An accelerated migrating rate and better survival of pancreatic islets were revealed.* Neuro Endocrinol Lett, 2009. **30**(2): p. 204-8.

171. Jung, E.J., et al., *Bone marrow-derived mesenchymal stromal cells support rat pancreatic islet survival and insulin secretory function in vitro.* Cytotherapy, 2011. **13**(1): p. 19-29.

172. Papaccio, G., C. Strate, and T. Linn, *Pancreatic duct infiltration in the low-dose streptozocin-treated mouse.* Histol Histopathol, 1994. **9**(3): p. 529-34.

173. Galipeau, J., et al., *International Society for Cellular Therapy perspective on immune functional assays for mesenchymal stromal cells as potency release criterion for advanced phase clinical trials.* Cytotherapy, 2016. **18**(2): p. 151-9.

174. Ezquer, F.E., et al., *Systemic administration of multipotent mesenchymal stromal cells reverts hyperglycemia and prevents nephropathy in type 1 diabetic mice.* Biol Blood Marrow Transplant, 2008. **14**(6): p. 631-40.

175. Ezquer, F., et al., *The antidiabetic effect of MSCs is not impaired by insulin prophylaxis and is not improved by a second dose of cells.* PLoS One, 2011. **6**(1): p. e16566.

176. Ho, J.H., et al., *Multiple intravenous transplantations of mesenchymal stem cells effectively restore long-term blood glucose homeostasis by hepatic engraftment and beta-cell differentiation in streptozocin-induced diabetic mice.* Cell Transplant, 2012. **21**(5): p. 997-1009.

177. Hess, D., et al., *Bone marrow-derived stem cells initiate pancreatic regeneration.* Nat Biotechnol, 2003. **21**(7): p. 763-70.

178. Kim, K.J., et al., *Pancreatic Diabetes after Distal Pancreatectomy: Incidence Rate and Risk Factors.* Korean J Hepatobiliary Pancreat Surg, 2011. **15**(2): p. 123-7.

179. Hofer, H.R. and R.S. Tuan, *Secreted trophic factors of mesenchymal stem cells support neurovascular and musculoskeletal therapies.* Stem Cell Res Ther, 2016. **7**(1): p. 131.

180. Nauta, A.J. and W.E. Fibbe, *Immunomodulatory properties of mesenchymal stromal cells.* Blood, 2007. **110**(10): p. 3499-506.

181. Kota, D.J., et al., *TSG-6 produced by hMSCs delays the onset of autoimmune diabetes by suppressing Th1 development and enhancing tolerogenicity.* Diabetes, 2013. **62**(6): p. 2048-58.

182. Wagner, W., et al., *Replicative senescence of mesenchymal stem cells: a continuous and organized process.* PLoS One, 2008. **3**(5): p. e2213.

183. Dang, L.T.-T., N.K. Phan, and K.D. Truong, *Mesenchymal stem cells for diabetes mellitus treatment: new advances.* Biomedical Research and Therapy; Vol 4 No 1 (2017), 2017.

184. Jeong, J.O., et al., *Malignant tumor formation after transplantation of short-term cultured bone marrow mesenchymal stem cells in experimental myocardial infarction and diabetic neuropathy.* Circ Res, 2011. **108**(11): p. 1340-7.

185. Lee, S.H., E. Hao, and F. Levine, *beta-Cell replication and islet neogenesis following partial pancreatectomy.* Islets, 2011. **3**(4): p. 188-95.

186. McBride, C., D. Gaupp, and D.G. Phinney, *Quantifying levels of transplanted murine and human mesenchymal stem cells in vivo by real-time PCR.* Cytotherapy, 2003. **5**(1): p. 7-18.

187. Kim, Y.S., et al., *Tracking intravenous adipose-derived mesenchymal stem cells in a model of elastase-induced emphysema.* Tuberc Respir Dis (Seoul), 2014. **77**(3): p. 116-23.

188. Lemper, M., et al., *A combination of cytokines EGF and CNTF protects the functional beta cell mass in mice with short-term hyperglycaemia.* Diabetologia, 2016. **59**(9): p. 1948-58.

189. Baeyens, L., et al., *Transient cytokine treatment induces acinar cell reprogramming and regenerates functional beta cell mass in diabetic mice.* Nat Biotechnol, 2014. **32**(1): p. 76-83.

190. van Belle, T.L., K.T. Coppieters, and M.G. von Herrath, *Type 1 diabetes: etiology, immunology, and therapeutic strategies.* Physiol Rev, 2011. **91**(1): p. 79-118.

191. Miettinen, P.J., et al., *Downregulation of EGF receptor signaling in pancreatic islets causes diabetes due to impaired postnatal beta-cell growth.* Diabetes, 2006. **55**(12): p. 3299-308.

192. Yin, Y., et al., *Human umbilical cord-derived mesenchymal stem cells direct macrophage polarization to alleviate pancreatic islets dysfunction in type 2 diabetic mice.* Cell Death Dis, 2018. **9**(7): p. 760.

193. Ahmed, S.M., et al., *Mesenchymal Stromal Cell Therapy for Pancreatitis: A Systematic Review.* Oxid Med Cell Longev, 2018. **2018**: p. 3250864.

194. English, K., et al., *IFN-gamma and TNF-alpha differentially regulate immunomodulation by murine mesenchymal stem cells.* Immunol Lett, 2007. **110**(2): p. 91-100.

195. Li, X., et al., *Iron oxide nanoparticles promote the migration of mesenchymal stem cells to injury sites.* Int J Nanomedicine, 2019. **14**: p. 573-589.

196. Yasunaga, M., et al., *Induction and monitoring of definitive and visceral endoderm differentiation of mouse ES cells.* Nat Biotechnol, 2005. **23**(12): p. 1542-50.

197. Liu, C., et al., *Mesenchymal stem cell (MSC)-mediated survival of insulin producing pancreatic beta-cells during cellular stress involves signalling via Akt and ERK1/2.* Mol Cell Endocrinol, 2018.

198. Talchai, C., et al., *Generation of functional insulin-producing cells in the gut by Foxo1 ablation.* Nat Genet, 2012. **44**(4): p. 406-12, S1.

199. Wong, J.C., et al., *Pancreatic-beta-cell survival and proliferation are promoted by protein kinase G type Ialpha and downstream regulation of AKT/FOXO1.* Diab Vasc Dis Res, 2017. **14**(5): p. 434-449.

200. Kurtz, A., *Mesenchymal stem cell delivery routes and fate.* Int J Stem Cells, 2008. **1**(1): p. 1-7.

201. Penicka, M., et al., *Images in cardiovascular medicine. Early tissue distribution of bone marrow mononuclear cells after transcoronary transplantation in a patient with acute myocardial infarction.* Circulation, 2005. **112**(4): p. e63-5.

202. Muller-Ehmsen, J., et al., *Effective engraftment but poor mid-term persistence of mononuclear and mesenchymal bone marrow cells in acute and chronic rat myocardial infarction.* J Mol Cell Cardiol, 2006. **41**(5): p. 876-84.

203. Sohni, A. and C.M. Verfaillie, *Mesenchymal stem cells migration homing and tracking.* Stem Cells Int, 2013. **2013**: p. 130763.

204. Drey, F., et al., *Noninvasive in vivo tracking of mesenchymal stem cells and evaluation of cell therapeutic effects in a murine model using a clinical 3.0 T MRI.* Cell Transplant, 2013. **22**(11): p. 1971-80.

205. Lee, S., et al., *In vivo bioluminescence imaging of transplanted mesenchymal stem cells as a potential source for pancreatic regeneration.* Mol Imaging, 2014. **13**.

206. Maldonado, M., et al., *Human umbilical cord Wharton jelly cells promote extra-pancreatic insulin formation and repair of renal damage in STZ-induced diabetic mice.* Cell Commun Signal, 2017. **15**(1): p. 43.

207. Oh, H.C., et al., *New treatment for cystic tumors of the pancreas: EUS-guided ethanol lavage with paclitaxel injection.* Gastrointest Endosc, 2008. **67**(4): p. 636-42.

208. Karaca, C., et al., *Feasibility of EUS-guided injection of irinotecan-loaded microspheres into the swine pancreas.* Gastrointest Endosc, 2011. **73**(3): p. 603-6.

209. Tong, Q., et al., *Improved insulin secretion following intrapancreatic UCB transplantation in patients with T2DM.* J Clin Endocrinol Metab, 2013. **98**(9): p. E1501-4.

210. Wang, L., et al., *Autologous bone marrow stem cell transplantation for the treatment of type 2 diabetes mellitus.* Chin Med J (Engl), 2011. **124**(22): p. 3622-8.

211. Estrada, E.J., et al., *Combined treatment of intrapancreatic autologous bone marrow stem cells and hyperbaric oxygen in type 2 diabetes mellitus.* Cell Transplant, 2008. **17**(12): p. 1295-304.

212. van der Meulen, T., et al., *Virgin Beta Cells Persist throughout Life at a Neogenic Niche within Pancreatic Islets.* Cell Metab, 2017. **25**(4): p. 911-926 e6.

213. Suarez-Pinzon, W.L., et al., *Combination therapy with epidermal growth factor and gastrin induces neogenesis of human islet {beta}-cells from pancreatic duct cells and an increase in functional {beta}-cell mass.* J Clin Endocrinol Metab, 2005. **90**(6): p. 3401-9.

214. Ezquer, F., et al., *The antidiabetic effect of mesenchymal stem cells is unrelated to their transdifferentiation potential but to their capability to restore Th1/Th2 balance and to modify the pancreatic microenvironment.* Stem Cells, 2012. **30**(8): p. 1664-74.

215. Jurewicz, M., et al., *Congenic mesenchymal stem cell therapy reverses hyperglycemia in experimental type 1 diabetes.* Diabetes, 2010. **59**(12): p. 3139-47.

216. Moritani, M., et al., *Abrogation of autoimmune diabetes in nonobese diabetic mice and protection against effector lymphocytes by transgenic paracrine TGF-beta1*. J Clin Invest, 1998. **102**(3): p. 499-506.

217. Yoo, S.W., et al., *Immune following suppression mesenchymal stem cell transplantation in the ischemic brain is mediated by TGF-beta*. Neurobiol Dis, 2013. **58**: p. 249-57.

218. Krakowski, M.L., et al., *Transgenic expression of epidermal growth factor and keratinocyte growth factor in beta-cells results in substantial morphological changes*. J Endocrinol, 1999. **162**(2): p. 167-75.

219. Bassi, E.J., et al., *Immune regulatory properties of allogeneic adipose-derived mesenchymal stem cells in the treatment of experimental autoimmune diabetes*. Diabetes, 2012. **61**(10): p. 2534-45.

220. Boumaza, I., et al., *Autologous bone marrow-derived rat mesenchymal stem cells promote PDX-1 and insulin expression in the islets, alter T cell cytokine pattern and preserve regulatory T cells in the periphery and induce sustained normoglycemia*. J Autoimmun, 2009. **32**(1): p. 33-42.

221. Mezza, T., et al., *Nuclear Export of FoxO1 Is Associated with ERK Signaling in beta-Cells Lacking Insulin Receptors*. J Biol Chem, 2016. **291**(41): p. 21485-21495.

222. Asada, S., et al., *Mitogen-activated protein kinases, Erk and p38, phosphorylate and regulate Foxo1*. Cell Signal, 2007. **19**(3): p. 519-27.

223. Abdallah, B.M., et al., *Dlk1/FA1 is a novel endocrine regulator of bone and fat mass and its serum level is modulated by growth hormone*. Endocrinology, 2007. **148**(7): p. 3111-21.

224. Sul, H.S., *Minireview: Pref-1: role in adipogenesis and mesenchymal cell fate*. Mol Endocrinol, 2009. **23**(11): p. 1717-25.

225. Dang, L.T., et al., *Intravenous Infusion of Human Adipose Tissue-Derived Mesenchymal Stem Cells to Treat Type 1 Diabetic Mellitus in Mice: An Evaluation of Grafted Cell Doses*. Adv Exp Med Biol, 2018. **1083**: p. 145-156.

226. Gu, X., et al., *Efficacy and Safety of Autologous Bone Marrow Mesenchymal Stem Cell Transplantation in Patients with Diabetic Retinopathy*. Cell Physiol Biochem, 2018. **49**(1): p. 40-52.

Table 1: Score sheet for the regeneration experiment.

Mouse ID:	Date:								
	Time:								
1. Body Weight	Score								
Based on initial weight []									
Based on control group weight []									
Uninfluenced or rise	**0**								
Reduction, but <10%	**1**								
Reduction > 10%	**2**								
Reduction > 20%	**3**								
2. General condition									
Shiny eyes, body openings and skin clean	**0**								
Cloudy eyes, increased muscle tone, more visible breathing	**1**								
Eyes sunken dull, sticky body openings, increased breathing	**2**								
Abnormal posture, the animal feels cold, eyes closed, cramps, paralysis, breath sounds, bluish mucous membranes, diarrhoea	**3**								
3. Spontaneous behaviour									
Attentive, curious, straightening, quick movements	**0**								
Decreased reactions, movement reduced, restricted or excessive activity	**1**								
Partial separation from the group, movement reduced, pain when walking	**2**								
Apathetic, no reaction or aggressiveness in handling, severely restricted movement, isolation, drag forward.	**3**								
5. Other termination criteria									
Self-injury (e.g. in case of excessive itching)	**3**								
Total score									

Table 2: Score sheet for the diabetes experiment.

Mouse identification:	Date:									
	Time:									
1. Body weight	**Score**									
Based on starting weight []										
Based on the weight of the control group []										
Uninfluenced or rise	**0**									
Reduction, but < 10%	**1**									
Reduction > 10%	**2**									
Reduction > 20%	**3**									
2. General condition										
Shiny eyes, body openings and skin clean	**0**									
Cloudy eyes, increased muscle tone, more visible breathing	**1**									
Eyes sunken dull, sticky body openings, increased breathing	**2**									
Abnormal posture, animal feels cold, eyes closed, cramps, paralysis, breathing sounds, bluish mucous membranes, diarrhoea	**3**									
3. Spontaneous behaviour										
Attentive, curious, straightening, quick movements	**0**									
Decreased reactions, movement reduced, restricted or excessive activity	**1**									
Partial separation from the group, movement reduced, pain when walking	**2**									
Apathetic, no reaction or aggressiveness in handling, severely restricted movement, isolation, drag forward.	**3**									
4. Trial-specific criteria										
Blood sugar < 200mg/dl	**0**									
Blood sugar increased (> 200 mg/dl)	**1**									
Blood sugar increased (> 400 mg/dl)	**2**									
Blood sugar reduced (< 60 mg/dl) At the same time, weight loss	**3**									
5. Other termination criteria										
Self-injury (e.g. excessive itching)	**3**									
Total score										

Table 3: Score sheet for the tumor experiment.

Mouse identification:	Date:									
	Time:									
1. Body weight	Score									
Based on starting weight []										
Based on the weight of the control group []										
Unaffected or increase	**0**									
Reduction, but < 10%	**1**									
Reduction > 10%	**2**									
Reduction > 20%	**3**									
2. General condition										
Shiny eyes, body openings and skin clean	**0**									
Cloudy eyes, increased muscle tone, more visible breathing	**1**									
Eyes sunken dull, sticky body openings, increased breathing	**2**									
Abnormal posture, animal feels cold, eyes closed, cramps, paralysis, breathing sounds, bluish mucous membranes, diarrhoea	**3**									
3. Spontaneous behaviour										
Attentive, curious, straightening, quick movements	**0**									
Decreased reactions, movement reduced, restricted or excessive activity	**1**									
Partial separation from the group, movement reduced, pain when walking	**2**									
Apathetic, no reaction or aggressiveness in handling, severely restricted movement, isolation, drag forward.	**3**									
4. Trial-specific criteria										
No tumor	**0**									
Tumor < 10 mm	**1**									
Tumor >10 mm < 15mm	**2**									
Tumor > 15mm	**3**									
5. Other termination criteria										
Self-injury (e.g. excessive itching)	**3**									
Total score										

DECLARATION

I declare that I have completed this dissertation single-handedly without the unauthorized help of a second party and only with the assistance acknowledged therein. I have appropriately acknowledged and referenced all text passages that are derived literally from or are based on the content of published or unpublished work of others, and all information that relates to verbal communications. I have abided by the principles of good scientific conduct laid down in the charter of the Justus Liebig University of Giessen in carrying out the investigations described in the dissertation.

Giessen, _____   Rahul Khatri
                                                              _____

PUBLICATIONS

- **R Khatri**, Friedrich S, Linn T., **2020**. Intrapancreatic MSC transplantation facilitates β-cell regeneration (manuscript under review).

- **R Khatri**, Mazurek S, Friedrich S, Linn T., **2020**. Local transplantation of mesenchymal stem cells promotes beta-cell regeneration through activation of FoxO1 pathway following partial pancreatectomy (manuscript under review).

- Schröder C*, **Khatri R***, Friedrich S, Linn T., **2020**. Class I and II histone deacetylase inhibitor LBH589 promotes endocrine differentiation in bone marrow derived human mesenchymal stem cells and suppresses uncontrolled proliferation. Exp Clin Endocrinol Diabetes.

- Doering L*, **Khatri R***, Friedrich S, Sauer S, Howaldt HP, Linn T., **2019**. Regulation of somatostatin expression by vitamin D3 and valproic acid in human adipose-derived mesenchymal stem cells. Stem Cell Res Ther Aug 2019 6;10(1):240

- Saqib, M., **Khatri, R**., Singh, B., Gupta, A., Bhaskar, S., **2019**. Cell wall fraction of Mycobacterium indicus pranii shows potential Th1 adjuvant activity**.** Int Immunopharmacol. 70:408-416

- **Khatri, R**., Hussmann, B., Rawat, D., Gurol, A.O., Linn, T., **2018**. Intraportal Transplantation of Pancreatic Islets in Mouse Model. J Vis Exp.

- **Khatri, R**., Krishnan, S., Roy, S., Chattopadhyay, S., Kumar, V., Mukhopadhyay, A., **2016**. Reactive Oxygen Species Limit the Ability of Bone Marrow Stromal Cells to Support Hematopoietic Reconstitution in Aging Mice. Stem Cells Dev 25, 948-958**.**

- Rekittke, N.E., Ang, M., Rawat, D., **Khatri, R**., Linn, T., **2016**. Regenerative Therapy of Type 1 Diabetes Mellitus: From Pancreatic Islet Transplantation to Mesenchymal Stem Cells. Stem Cells Int 2016, 3764681.

- Saqib, M., **Khatri, R**., Singh, B., Gupta, A., Kumar, A., Bhaskar, S., **2016**. Mycobacterium indicus pranii as a booster vaccine enhances BCG induced immunity and confers higher protection in animal models of tuberculosis. Tuberculosis (Edinb) 101, 164-173.